

ARCADIS

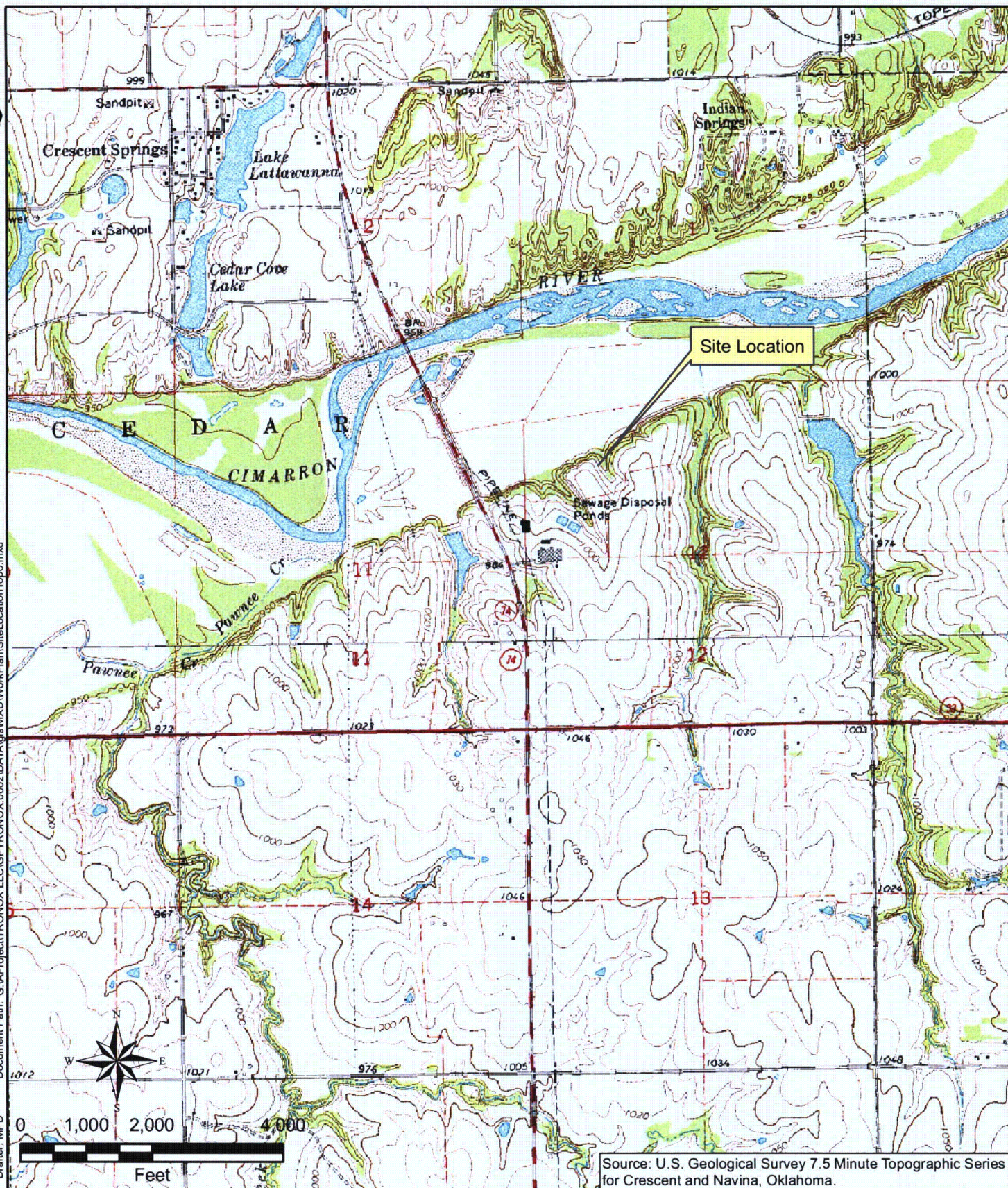
FIGURES



Document Path: G:\Project\TRONOX\0002\DATA\GIS\MXD\Work\Plan\Site\Location\Topo.mxd

Drafter: MPD

Date: 11/15/2006




Source: U.S. Geological Survey 7.5 Minute Topographic Series for Crescent and Navina, Oklahoma.

Program Manager  
Jim Harrington

Project Manager  
Todd Bechtel

Task Manager  
Janis Lutrick

Technical Review  
Paul Barnes

 **ARCADIS**

630 Plaza Drive, suite 200  
Highlands Ranch, Colorado 80129  
Tel: 720.344.3500  
Fax: 720.344.3535  
www.arcadis-us.com

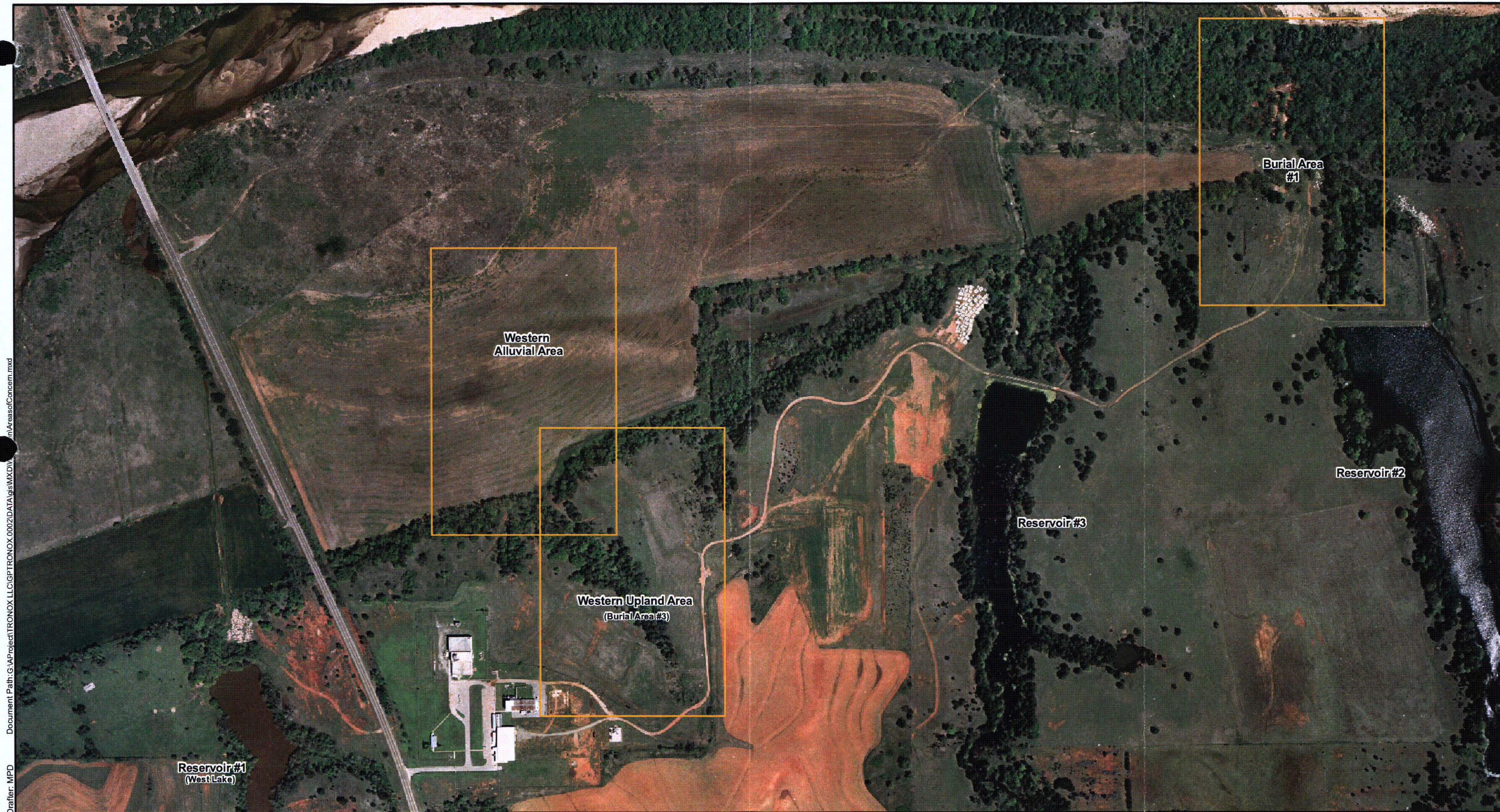
## Site Location Map

TRONOX, Inc.  
Crescent, Oklahoma

FIGURE

1





Document Path: G:\Project\TRONOX LLC\GPR\TRONOX.0002\DATA\gis\MXD\AreasOfConcern.mxd  
Drafter: MPD  
Date: 12/6/20

Program Manager  
Jim Harrington  
Project Manager  
Todd Bechtel  
Task Manager  
Janis Lutrick  
Technical Review  
Paul Barnes

**ARCADIS**

630 Plaza Drive, Suite 200  
Highlands Ranch, Colorado 80129  
Tel: 720-344-3500  
Fax: 720-344-3535  
www.arcadis-us.com

Areas of Concern

TRONOX, Inc.  
Crescent, Oklahoma

FIGURE

2



**Forward IRZ in Sandy Alluvial Zone:**

- Creates a barrier of reactive FeS matrix ahead of the leading edge of the plume to ensure treatment of any migrating groundwater.
- Up to 40 direct push injection points in a grid on 25 ft. centers around the leading edge of plume. Injected twice in the first and second full-scale quarterly injection events. 20,000 gallons of reagent (0.2% molasses solution) per injection point injected at 5 GPM. Injections complete after two quarterly events.

**Sandy Alluvial Zone:**

- Grid injection, beginning around the outside of the area.

**Optimistic**

- Up to 62 direct push injection points on 25 ft. centers. Injected quarterly over four consecutive quarters.
- Four quarters of 20,000 gallon injections per point, 0.2% molasses solution injected at 5 GPM. Dilute sulfate source added beginning in the second event, carbon source changed to methanol in the third event.

**Transition Alluvial Zone:**

- Grid injection, beginning around the outside of the area.
- Up to 30 direct push injection points on 25 ft. centers. Injected quarterly over four consecutive quarters.
- Four quarters of 20,000 gallon injections per point, 0.2% molasses solution injected at 5 GPM. Dilute sulfate source added beginning in the second event, carbon source changed to methanol in the third event. Injections complete after four quarterly events.

**Vadose Zone:**

- Surface infiltration to saturate and treat vadose zone to prevent infiltrating water from mobilizing vadose zone uranium (if present).
- Install up to 2,820 linear feet of shallow surface infiltration trenches, 2.5 ft. deep, filled with porous media. Injected quarterly for 2 quarters. Injection of 10,000 gallons of 0.2% molasses solution into each trench each event. TOC will slowly infiltrate into the vadose zone by surface recharge, facilitated by precipitation or irrigation during extended dry periods.


**Upland Bedrock Zone:**

- Combination of shallow trench and drilled well injection.
- Install four 2.5 ft deep infiltration trenches (960 lf) perpendicular to former burial trenches to facilitate infiltration of amendments into trench voids and induce reagent flow into natural pathways. Cover the remainder of the affected area by a grid of 15 drilled injection wells on 30 ft. centers, with at least two wells located in the footprint of each former burial trench. Four quarters of 20,000 gallon injections per point or trench, 0.2% molasses solution injected at 5 GPM. Dilute sulfate source added beginning in the second event, carbon source changed to methanol in the third event.

**Legend**

- Existing Monitoring Wells
- IRZ Injection Points (Approximate Locations)
- Extent of Uranium Impact (> 180 pCi/L)
- Escarpment Line
- Surface Trenches
- Vadose Zone
- Upland Bedrock Zone
- Transition Alluvial Zone
- Sandy Alluvial Zone
- Forward IRZ in Sandy Alluvial Zone
- Former Burial Trenches

Program Manager	Jim Harrington
Project Manager	Todd Bechtel
Task Manager	Janis Lutrick
Technical Review	Paul Barnes

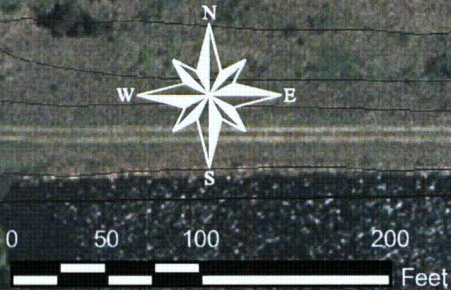


**ARCADIS**  
630 Plaza Drive, Suite 200  
Highlands Ranch, Colorado 80129  
Tel: 720-344-3500  
Fax: 720-344-3535  
www.arcadis-us.com

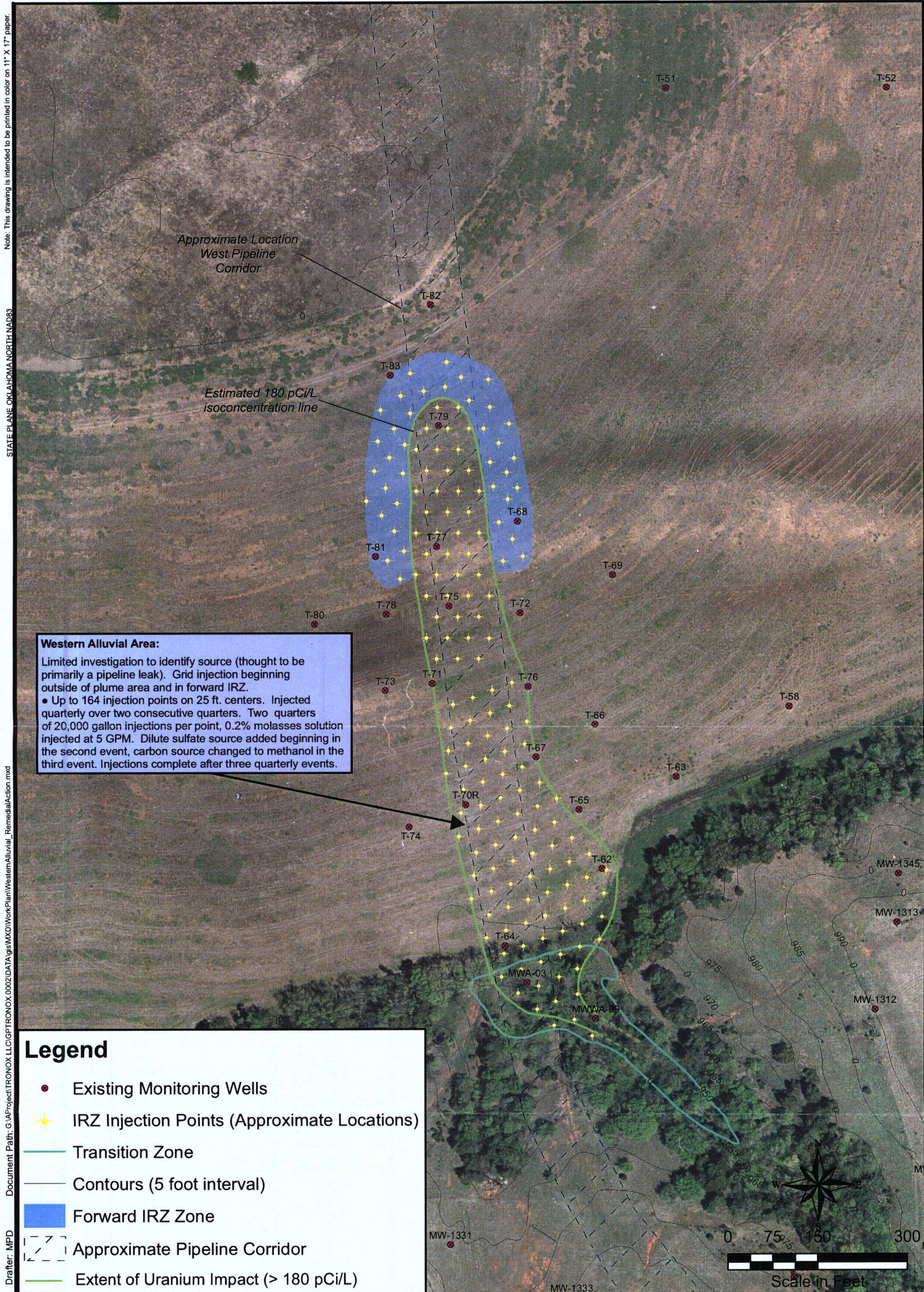
Burial Area 1 Remediation Plan

TRONOX, Inc.  
Crescent, Oklahoma


FIGURE  
3







Note: This drawing is intended to be printed in color on 11" X 17" paper.  
 STATE PLANE OKLAHOMA NORTH NAD83  
 Document Path: G:\Project\TRONOX LLC\GPT\TRONOX.0002\DATA\GIS\MXD\WorkPlan\WesternAlluvial\_RemedialAction.mxd  
 Drafter: MPD  
 Date: 12/6/2006

Program Manager Jim Harrington	 <b>ARCADIS</b>  630 Plaza Drive, Suite 200 Highlands Ranch, Colorado 80129 Tel: 720-344-3500 Fax: 720-344-3535 www.arcadis-us.com	Western Alluvial Area Remediation Plan   TRONOX, Inc. Crescent, Oklahoma	FIGURE  <b>4</b>
Project Manager Todd Bechtel			
Task Manager Janis Lutrick			
Technical Review Paul Barnes			



Note: This drawing is intended to be printed in color on 11" X 17" paper.

STATE PLANE OKLAHOMA NORTH NAD83


Document Path: G:\Project\TRONOX LLC\GPTRONOX.0002\DATA\GIS\MXD\WorkPlan\BurialArea3\_RemedialAction.mxd

Drafter: MPD

Date: 12/6/2006



Program Manager	Jim Harrington
Project Manager	Todd Bechtel
Task Manager	Janis Lutrick
Technical Review	Paul Barnes

**ARCADIS**

630 Plaza Drive, Suite 200  
Highlands Ranch, Colorado 80129  
Tel: 720-344-3500  
Fax: 720-344-3535  
www.arcadis-us.com

Western Upland Area  
Remediation Plan

TRONOX, Inc.  
Crescent, Oklahoma

FIGURE  
**5**





ARCADIS

## **APPENDIX A**

Geochemical Modeling Evaluation



## Geochemical Modeling of Reductive Precipitation of Uranium and Iron Sulfide with Subsequent Oxidative Dissolution and Sorption using One-Dimensional and Three-Dimensional Transport

---

### Objectives and Approach

The objective of this modeling analysis is to evaluate the fate and transport of soluble uranium in groundwater under various geochemical conditions representative of the Cimarron Site (Site) in which soluble uranium is reductively precipitated to the oxide mineral uraninite ( $\text{UO}_2$ ) via an engineered in-situ reactive (IRZ) zone treatment and to evaluate the stability of this low solubility mineral phase over time as geochemical conditions return to baseline.

Simulations involving geochemical reaction path modeling were performed with the software package Geochemists' Workbench (GWB; Rockworks, Golden, Colorado), a geochemical code capable of describing the precipitation, dissolution, and sorption of aqueous compounds including uranium under defined conditions in both batch and transport scenarios. Additionally, the numerical hydraulic flow software

MODFLOW with the transport module MT3DMS was used with a currently existing Site flow model and output from GWB to model sorption of uranium as a function of transport through the Burial Area #1.

GWB is capable of performing geochemical reaction path modeling with either an equilibrium approach or a kinetic approach. With an equilibrium approach the rate of reaction is not considered but a purely thermodynamic approach is used based on each reaction's equilibrium constant. This approach assumes that all chemical species in the system are at equilibrium with each other and would be considered conservative with respect to formation of reaction products. A kinetic approach assigns a rate to each reaction rather than assuming that each reaction goes to completion. In order to accurately use a kinetic model, a reliable reaction rate constant must be used.

This modeling study utilized the equilibrium approach for reaction path modeling because robust reaction rates for the species of interest are not widely available and proven. Rather than introduce additional uncertainty into the modeling approach, ARCADIS chose to use an equilibrium approach with extremely conservative assumptions. Equilibrium constant databases are constantly being updated. This approach is supported by multiple empirical studies which demonstrate the reductive precipitation of uranium with subsequent oxidative precipitation by iron sulfide (Abdelouas et al., 2000; Spear et al., 2000).



As discussed in the Work Plan (title), the proposed technology will involve the creation of electrochemically reducing conditions which will stimulate the biological reduction of soluble uranium to the insoluble uranium oxide, uraninite, along with reduced iron sulfide minerals. These reactions were simulated using actual Site conditions.

Upon the cessation of the treatment, oxidizing groundwater will flow into the treated area causing oxidative dissolution of the iron sulfides and the uraninite. These reactions were simulated as a batch reaction and considering transport with actual Site conditions and with various permutations of alkalinity and other possible geochemical conditions.

Once the system returns to oxidizing conditions the reduced iron sulfides will be oxidized to amorphous iron oxides and the uraninite will be gradually dissolved to form soluble uranyl carbonates. Simulations of the interaction between the highly sorptive amorphous iron oxides and the dissolved uranium were performed as both a batch reaction and considering transport. These reactions were simulated using actual Site conditions.

## **Scenario 1: Reductive Precipitation Simulations**

Reductive precipitation simulations were performed using actual Site data wherever possible to establish initial model conditions. Analytical data from groundwater and soil samples collected from the Burial Area #1 portion of the Site were used to define baseline geochemical conditions. These conditions were presented in the (ENSR 2006) and are listed in Table 1. Uranium concentrations for the Site groundwater are presented as activity, picoCuries per Liter (pCi/L), rather than mass, micrograms per Liter (ug/L). The majority of the uranium historically handled at the Site was slightly enriched with respect to the 235 isotope therefore a site specific activity to mass conversion factor of 1.6 pCi/ug, was available. However, in order to be overly conservative to the possible mass of uranium in groundwater, an activity to mass conversion factor for natural uranium of 0.67 pCi/ug was used to establish the initial mass of uranium in the Burial Area #1.

The physical conditions of the model were:

- Saturated sandstone with a porosity of 25 percent;
- Saturated volume equal to 1 kilogram (kg) of fluid;
- Unsaturated volume equal to 6 kg of sandstone;
- Sandstone mineralogy defined as 98 percent quartz, 1 percent calcite, 1 percent iron oxide as hematite (reactive portion varied by simulation); and
- Based on solid phase analysis, sandstone defined as having 4.5 milligrams per kilogram (mg/kg) uranium.

The initial uranium concentration used in the model is the sum of the highest recently reported groundwater concentration (Monitor Well TMW-9) of 1,793 pCi/L, equal to 2.67 mg/L (using natural uranium activity to mass conversion), and the mass of total uranium in soil from the same location, 4.5 milligrams per kilogram



(mg/kg). For the model domain this is 33.67 mg of uranyl carbonate. The current release criteria limit for uranium in solution at the Site is 180 pCi/L, equal to 110 ug/L.

In order to evaluate the potential mass of reduced iron sulfide minerals that would form during the creation of reducing conditions, the total mass of iron reported in soil from a sample collected in Burial Area #1 (TMW-9) of 6,900 mg/kg was varied from 10 percent to 100 percent in model simulations to account for bioavailability. Under Site geochemical conditions the mineral phases thermodynamically favored to form are amorphous iron sulfides such as mackinawite ( $\text{FeS}_{0.9}$ ) and Troilite ( $\text{FeS}$ ). Empirical studies of microbial processes stimulated in aquifer materials have demonstrated that  $\text{FeS}$  is the principal product of biogeochemical redox reactions with mackinawite being the dominant form (Suess, 1979; Matsunga et al., 1993; von Gunten and Zobrist, 1993). Mackinawite is commonly found with nickel and cobalt as impurities but is strictly defined as  $\text{FeS}_{0.9}$ . The molar ratio of iron to sulfur being less than one is due to imperfections in the atomic lattice structure and is directly related to the amorphous nature of this mineral.

In order to demonstrate no significant difference in the choice of the iron sulfide mineral, a simulation with troilite was also performed. The mass of mackinawite was varied based on varying percentages of the total iron mass being available for reaction.

## Approach and Assumptions

The model simulation design is that uraninite and mackinawite formation occurs on a saturated sandstone aquifer that contains oxidized uranium and iron oxide minerals in solution with dissolved uranium by the introduction of a reducing groundwater flow into the model domain. Rather than simulating induction of reducing conditions with the addition of an exogenous carbon source, a surrogate approach was used. A reductive groundwater flow (oxidation/reduction potential of -260 millivolts) equivalent to what will be produced by the IRZ was introduced through the model space to induce uraninite and mackinawite formation in the aquifer. The composition of this water is presented in Table 2. For some species in the introduced groundwater, such as dissolved iron and sodium, simulated concentrations were used to provide a charge balance for the model in order for it to converge on a solution. For instance, model convergence would not occur if the dissolved uranium concentration of the introduced groundwater was set to zero. However, a near zero value of  $1 \times 10^{-26}$  mg/L was used and model convergence was achieved.

For these simulations, the mass of iron available for reaction was varied by 10, 25, 50, 75, and 100 percent of the total iron present in the system. Iron was represented in the model as the crystalline oxide mineral hematite, a less reactive form of iron oxide, in order to be conservative in the prediction. Hematite was allowed to dissolve in order to yield the designated percentage of the total iron.

The reductive precipitation model simulations assume that mass is allowed to enter the system, but is not allowed to exit. The simulations were configured to add cumulative pore volumes of reducing fluid (water and solutes) to the initial system. Thus, the rock-water ratio decreases over the duration of the simulations. Because incoming pore volumes do not contain significant iron and uranium, both of these components remain essentially conserved within the local system. Additionally, it is assumed that all chemical reactions reach equilibrium without taking into account the rates of reaction and practical time scale of interest.



One impractical consequence of the above assumption is that thermodynamically stable, yet kinetically unlikely mineral phases can form during the simulation, even though such formation is clearly unrealistic due to kinetic limitations. An initial simulation resulted in the formation of both the realistic amorphous forms of uranium and iron minerals but also the formation of mature crystalline mineral forms. Therefore, a number of these crystalline mineral phases were excluded from consideration by the model. The minerals excluded were soddyite, dolomite, dolomite-dis, dolomite-ord, pyrite, pyrrhotite, haiweeite, rutherfordine,  $\text{UO}_2 \cdot (2.5\text{H}_2\text{O})$ ,  $\text{UO}_2\text{SO}_4 \cdot (3.5\text{H}_2\text{O})$ ,  $\text{UO}_2\text{SO}_4 \cdot 3\text{H}_2\text{O}$ ,  $\text{UO}_2\text{SO}_4 \cdot \text{H}_2\text{O}$ ,  $\text{U}_4\text{O}_9$ , magnesite, talc, gypsum, anhydrite, siderite, and elemental sulfur. The potential formation of siderite could be reasonable under certain circumstances. Simulations allowing siderite to form under various reactive iron percentages were performed.

## **Reductive Precipitation Simulation Results (Scenario 1)**

The resulting mineral phases and other species produced from the reductive precipitation of uraninite and mackinawite with various percentages of reactive iron are presented in Table 3. All of the uranium in the system (dissolved and sorbed phase) was converted to uraninite (32.34 milligrams [mg]). The mass of mackinawite varied from 7.15 grams (g) for the 10 percent reactive simulation to 71.56 g for the 100 percent reactive simulation. The various percentages of reactive iron yielded a uranium to iron sulfide ratio of 1:679 (10 percent reactive iron); 1:1699 (25 percent reactive iron); 1:3345 (50 percent reactive iron); and 1:6783 (100 percent reactive iron). The results in Table 3 are based on the exclusion of the above referenced minerals. Raw model output results are presented in Attachment Tables 1-5. When siderite was allowed to form, it did so as an intermediate product which then dissolved prior to the formation of mackinawite. Simulations were run allowing siderite to form under reactive iron percentages of 10, 50, and 100 percent. There were no differences in the final solution composition as compared to corresponding simulations in which siderite was suppressed. Raw model output results are presented in Attachment Tables 6-8. A model simulation in which no minerals were suppressed with the exception of uranophane (a model error occurred when uranophane was suppressed) was performed. This simulation produced pyrite as the final iron sulfide mineral and no difference in the uraninite concentration. Model results for unsuppressed simulations are presented in Attachment Tables 6-9. A simulation using troilite as the iron sulfide mineral with 10 percent reactive iron rather than mackinawite resulted in no significant difference in the ratio of uranium to iron sulfide suggesting that the choice of amorphous iron sulfide mineral is not important. Results of this simulation are presented in Attachment Table 10

## **Scenario 2: Oxidative Dissolution Simulations**

Scenario 2 simulates the effects of oxidative groundwater contacting a saturated sandstone aquifer in which mackinawite and uraninite had been reductively precipitated (Scenario 1). These simulations are designed to represent Site conditions after IRZ treatment has ceased and upgradient groundwater flows into the system. Oxidative dissolution simulations were performed using a batch approach as in the reductive precipitation scenario and considering one-dimensional transport, discussed in next section. To evaluate the effects of various chemical conditions that may exist at the Site and their affect on oxidative dissolution of mackinawite and uraninite, simulations under various dissolved oxygen, reactive iron concentrations, pH, total inorganic carbon concentrations, and calcite concentrations were conducted. The maximum observed dissolved oxygen concentration in Burial Area #1 is 1.2 mg/L however; the vast majority of all measured



values are substantially less. Oxidative dissolution simulations were performed using an introduced groundwater with a dissolved oxygen concentration of 1.2 mg/L and also with 8.0 mg/L to represent the extreme worst case scenario of full dissolved oxygen saturation.

The initial model conditions for the aqueous phase are the same as those listed in Table 2. The introduced oxidizing groundwater had the same composition as the solution in Table 2 with the exception of the parameters in Table 4, some of which were varied, as shown, for each permutation to evaluate the sensitivity of each parameter.

## **Oxidative Dissolution Simulation Results (Scenario 2 Batch)**

Under all scenarios, the mackinawite acted as a sacrificial reductant and was oxidized before any of the uraninite underwent oxidation. The resulting aqueous concentrations from the oxidative dissolution runs are presented in Tables 5 through 9. It is important to remember that these “batch runs” assume that oxygen is uniformly present throughout the entire treatment area immediately. As such they represent an extremely conservative depiction as oxygen entering the treatment area in groundwater will move as a front slowly reacting with and being consumed by the recently formed mackinawite in its path over a long time period.

The number of pore volumes required to pass through the system in order to oxidize the mackinawite varied as a function of the dissolved oxygen concentration and the initial mass of mackinawite (based on the percentage of reactive iron selected). No uraninite underwent dissolution until all mackinawite had been exhausted. Once the mackinawite had been oxidized, all of the uraninite underwent dissolution in a single pore volume. Depending on the dissolved oxygen concentration and the percentage of iron assumed to be available to form mackinawite (percentage of reactive iron), the pore volumes required to dissolve uraninite ranged from 500 (8.0 mg/L dissolved oxygen) to 1900 (1.2 mg/L dissolved oxygen) for 10 percent reactive iron and 5000 (8.0 mg/L dissolved oxygen) to 19,000 (1.2 mg/L dissolved oxygen) for 100 percent reactive iron simulation. The values presented in Tables 5 through 9 represent the composition of the pore volume immediately after all the mackinawite has been oxidized.

The concentration of uranium liberated once the mackinawite is exhausted was evaluated as a function of pH and dissolved oxygen concentrations as shown in Tables 5 through 9 and presented in micrograms per liter ( $\mu\text{g/L}$ ) and milligrams per liter ( $\text{mg/L}$ ). Soluble uranium is speciated in these Tables as the dominant carbonate forms with the total concentration being the sum of the two.

Under the 100 percent reactive iron permutations, the uranium concentration ranged from 1.47  $\mu\text{g/L}$  (1.2 mg/L dissolved oxygen, pH 5) to 8.96  $\mu\text{g/L}$  (8.0 mg/L dissolved oxygen, pH 6.8). Under the 75 percent reactive iron permutations, the uranium concentration ranged from 3.48  $\mu\text{g/L}$  (1.2 mg/L dissolved oxygen, pH 6.8) to 11.91  $\mu\text{g/L}$  (8.0 mg/L dissolved oxygen, pH 6.8). Under the 50 percent reactive iron permutations, the uranium concentrations ranged from 5.21  $\mu\text{g/L}$  (1.2 mg/L dissolved oxygen, pH 6.8) to 17.86  $\mu\text{g/L}$  (8.0 mg/L dissolved oxygen, pH 6.8). Under the 25 percent reactive iron permutations, the uranium concentrations ranged from 10.02  $\mu\text{g/L}$  (1.2 mg/L dissolved oxygen, pH 6.8) to 32.60  $\mu\text{g/L}$  (8.0 mg/L dissolved oxygen, pH 6.8). Under the 10 percent reactive iron permutations, the uranium concentrations ranged from 25.01  $\mu\text{g/L}$  (1.2 mg/L dissolved oxygen, pH 6.8) to 84.00  $\mu\text{g/L}$  (8.0 mg/L dissolved oxygen, pH 6.8). Varying other parameters such as pH, a lower bicarbonate concentration and the addition of 5 percent calcite to the solid phase did not result in significant differences in the final uranium



concentrations. Raw model output results for these simulations are presented in Attachment Tables 11 through 24. An oxidative dissolution simulation using troilite rather than mackinawite with 8 mg/l dissolved oxygen and 10 percent reactive iron was performed and yielded no significant difference in the soluble uranium concentration. Results of this simulation are presented in Attachment Table 25. In order to evaluate the effect of high concentrations of alkalinity on the stability of uraninite, an oxidative dissolution simulation was performed using a bicarbonate concentration of 1000 mg/L, approximately 5 times higher than average concentrations seen at the Site, and 372 mg/L higher than the highest reported value. The use of 1000 mg/L bicarbonate is considered extremely conservative and is intended to significantly overestimate the additional contribution of alkalinity from microbial respiration associated with the remediation technology. This simulation was performed under all other worst case conditions including 8.0 mg/L dissolved oxygen and 10 percent reactive iron. The concentration of uranium in solution for the simulation using 628 mg/L bicarbonate was 84 ug/L (Attachment Table 16) and the equivalent concentration when using 1000 mg/L bicarbonate was 85 ug/L (Attachment Table 28), thus there is no significant difference in the stability of uraninite under alkalinity concentrations considered realistic for the Site.

## **Oxidative Dissolution Simulations (Scenario 2 Transport)**

The previous simulations under Scenario 2 were done in a batch system and provide estimates of the number of pore volumes that must move through the system to dissolve the mackinawite and then the uraninite. An alternative to this scenario was run using the X1T module of GWB, which couples advective/dispersive transport to the geochemical reactions. This allows an estimate of the time required to exhaust the mackinawite based on a groundwater seepage velocity and therefore the stability of the uraninite mineral phase over time. For this purpose, simulations were run using the assumptions of 100 percent reactive iron and 8 mg/L dissolved oxygen in the system. Two simulations were conducted using different groundwater velocities (0.03 foot per day and 5 feet per day) based on observed velocities from the upland and alluvial portions of the Site. In order to observe the amount of time necessary for oxidation reactions to occur a model space was defined with the characteristics identified in Table 10.

## **Oxidative Dissolution Simulation Results (Scenario 2 Transport)**

- Using a worst case dissolved oxygen concentration of 8.0 mg/L and a 0.03 foot per day groundwater velocity, model simulations predict that mackinawite will be exhausted and uraninite dissolution will occur in approximately 25,925 years (14,065.7 pore volumes). Raw model output results are presented in Attachment Table 26.
- Using a worst case dissolved oxygen concentration of 8.0 mg/L and a 5 feet per day velocity, model simulations predict that mackinawite will be exhausted and uraninite dissolution will occur in approximately 155 years (14,065.6 pore volumes). Raw model output results are presented in Attachment Table 27.

## **Scenario 3: Sorption of Soluble Uranium Simulations**

Scenario 3 simulated uranium sorption onto iron oxide and iron hydroxide particles that exist in the system. Scenario 3 is intended to represent the behavior of uranium liberated into solution in Scenario 2 and how it interacts through sorption onto iron oxide coatings created from the oxidation of mackinawite in Scenario 2.



These simulations were coupled to oxidative dissolution reaction paths so that sorption occurred as mackinawite and subsequently uraninite were dissolving.

To estimate the sorption effect of iron-hydroxide and iron oxide mineral surfaces on dissolved uranium in solution, the double-layer theorem of Dzombak and Morel (1990) was used. Partition data for related sorbing minerals (goethite, ferrihydrite, and magnetite) were not deemed significantly different enough from hematite and, therefore, did not warrant modeling of complexation effects on other mineral surfaces. In order to investigate the effects of transport on uranium sorption onto iron oxide surfaces under various chemical conditions, one-dimensional transport simulations were also conducted.

The assumptions made for Scenario 1 and Scenario 2 were also applied to Scenario 3 simulations. In order to avoid the formation of thermodynamically stable mineral phases whose formation would be clearly unrealistic due to kinetic limitations, as discussed early, a number of mineral phases were excluded from consideration by the model in Scenario 3. These include uranophane, soddyite,  $U_4O_9$ , haiweeite, and  $U_3O_8$ .

The sorption behavior for iron oxides was modeled using the generalized double layer formulation. The partitioning behavior is dependent on surface area, reactive sites, and surface charge. The values for the surface properties used were the default values in the standard model for hematite (goethite and ferrihydrite sorption was not modeled because the variability in partitioning constants among the three phases is negligible). The uranium partitioning constants were estimated from the Dzombak and Morel compilation (1990). Actual surface properties may be somewhat different depending on the species of iron oxide formed. The standard model does not account for inclusions or solid solutions between uranium and iron oxide.

## **Sorption Simulations (Scenario 3 Batch)**

Scenario 3 (Batch) simulations were run to model the uranium sorption onto iron oxides when various concentrations of iron in the system was available to react and with a range of dissolved oxygen concentrations, at a lower pH environment, with a lower total inorganic carbon (TIC) concentration and when lower concentrations of calcite are available in the solid phase. Details of initial conditions are presented in Table 11.

The host sandstone was assumed to have a porosity of 25 percent, meaning that at saturation 1 kg of fluid is in contact with 6 kg of sandstone. Sandstone mineralogy was set at approximately 98 percent quartz (5.9 kg), 1 percent calcite (60 g) to buffer pH, 1 percent hematite (60 g – varied in each simulation), and minor uranium (based on solid phase composition) based on lithology description of soil at the Site.

The initial fluid compositions for Scenario 3 were taken from Scenario 2 (Batch) simulations along the reaction path where uraninite was completely dissolved. At this point, the dissolved oxygen concentration is not yet in equilibrium with the dissolved oxygen of the oxidizing fluid; therefore, the complexing model also takes into consideration the effect of additional oxygen entering the system as more pore volumes of fluid are flushed through. The system was flushed with 8 mg/L dissolved oxygen or 1.2 mg/L dissolved oxygen.

## **Sorption Simulation Results (Scenario 3 Batch)**



The simulations were repeated for each reactive iron concentration (10, 25, 50, 75, and 100 percent) under 8 and 1.2 mg/L of oxygen. Other simulations were performed using (a) 100 percent iron, 1.2 mg/L dissolved oxygen, average TIC; and (b) 100 percent iron, 1.2 mg/L dissolved oxygen, and decreased calcium concentration in the system, respectively. Last simulation conducted under Scenario 3 (Batch) was assuming 100 percent iron, 1.2 mg/L dissolved oxygen, and a pH of 5. Uranium concentrations in batch range from 1,460 ug/L to 362 ug/L. Results of the uranium concentration remaining in solution after instantaneous sorption but without transport are presented in Table 12. Note that these concentrations exist in a single point in space and do not account for transport into adjacent pores with additional sorptive capability.

## **Sorption Simulations (Scenario 3 Transport)**

Scenario 3 (Transport) simulations were conducted to model the uranium sorption onto iron oxide surfaces as it moves along a flow path to achieve a more realistic approach. For this purpose, simulations were made under the assumptions of 100 percent reactive iron and 8 mg/L dissolved oxygen or 1.2 mg/L dissolved oxygen concentrations in the system.

Additional simulations included lower TIC concentrations and higher calcium concentrations in the system. A groundwater velocity of 0.5 foot per day, rather than the reported velocity of 0.03 foot per day was used to enhance the numerical stability of the model software and is considered conservative since it is an order of magnitude faster, was used in the simulations since throughout most of the plume and downgradient of TMW 09, in the sandy alluvium the seepage velocity will be in this range. A length of 230 feet horizontal distance is assumed for the aquifer in the model space. This distance is based on the plume length from Monitor Well TMW-9 to the distal portion of the 180 pCi/L isoconcentration line.

The maximum observed uranium concentration under worst case conditions (10 percent reactive iron, 8.0 mg/L dissolved oxygen) in Scenario 3 (Batch) was that all uraninite dissolved and instantaneously released 1,460 ug/L of uranium into a solution. The more reasonable Site conditions, as shown in Table 12, indicate that a maximum worst case concentration of uranium is about 500 ug/L. This concentration was used in transport simulations for the incoming solution to evaluate the adsorption of uranium onto aquifer materials (iron oxides present in the system). Additionally, simulations were performed using a dissolved uranium concentration of 5,000 ug/L (equivalent to current Site concentrations) to represent an extreme worst case condition. A very small transport distance of 15 centimeters was chosen to evaluate the near immediate sorption onto iron oxides.

## **Sorption Simulation Results (Scenario 3 Transport)**

In all transport simulations, the vast majority of the soluble uranium is sorbed within a 15 centimeter distance including the simulation using 5000 ug/L of initial concentration. The maximum concentration of soluble uranium that occurs is 44.6 ug/L and is under extreme worst case conditions of 5000 ug/L uranium with 10 percent available iron and 1.2 mg/L dissolved oxygen. Results are presented in Table 13.



These simulations indicate that uranium sorption will happen almost instantaneously and that uranium concentrations will drop well below the regulatory limit of 110 µg/L within less than 1 foot of the source. Considering that this is a worst case scenario and that uranium concentrations this high (500 ug/L and 5000 ug/L) will not realistically enter the system instantaneously, it is unlikely that the regulatory limit of 110 µg/L uranium will be exceeded for any significant distance within the treatment area. It is important to note that sorptive capacity of the iron oxides in the system is based on the reduction of existing iron oxides during introduction of organic carbon and the re-oxidation of these iron oxides to the more sorptive amorphous mineral phase. This explains why the sorption of the 5000 ug/L uranium simulations (current Site concentration) is not occurring presently. However, it does indicate that the Site has enough sorptive ability after the iron oxides are reduced and re-precipitated, to reduce current Site uranium concentrations well below regulatory limits.

Simulations conducted to model uranium sorption under lower alkalinity concentration conditions did not result in significantly different results. In order to observe the amount of time necessary for oxidation reactions to occur a model space was defined with the characteristics identified in Table 14.

## **Transport Simulation Runs**

Two transport simulations were conducted with MT3DMS (Zheng and Wang 1999) in conjunction with the existing flow model constructed and calibrated by ENSR (2006). The flow model generates the velocity field necessary to simulate uranium transport when coupled with the contaminant transport code MT3DMS. The current transport simulations utilize solutions to the advection-dispersion equation (ADE), with porosity values selected by ENSR based on literature values (ENSR 2006; Table 3).

The runs simulated the possible dissolution of uranium previously co-precipitated with iron sulfide when oxygen enters the plume area (via rainwater and groundwater). The “area of appearance” of uranium into solution in the model corresponds to the extent of the existing uranium plume.

Transport simulations also assumed that the uranium plume is primarily attenuated by soil adsorption due to the presence of iron oxides, an oxidation product of ferrous sulfide. A linear distribution coefficient ( $K_d$ ) model was applied to the entire domain to address the adsorption of uranium to the iron oxides. Sensitivity analysis was conducted to evaluate the effect of the  $K_d$  value on uranium transport. The different  $K_d$  values were calculated by GWB based on different percentages of reactive iron oxides in the soil.

Scenario 4 assumes that all the uranium co-precipitated with iron sulfide enters the aqueous phase instantaneously, creating a plume at a constant concentration of 500 µg/L. This concentration is predicted by GWB in Scenario 2 above. Scenario 5 assumes that a fixed mass loading rate (0.1 pound per year of uranium) enters the aqueous phase each year.

## **Scenario 4: Instantaneous Solubilization of Uranium**

This scenario assumes all precipitated uranium is remobilized instantaneously when the ferrous sulfide in subsurface is exhausted by the dissolved oxygen from the fresh groundwater front, consequently causing a uranium plume with a constant and initial aqueous concentration of 500 µg/L. Vertically, the plume extends



approximately 25 feet below the water table, which coincides with the lowest elevation of concentrations over 180 picocuries per liter (pCi/L) (August 2004 Sampling Event).

All of the transport parameters are listed in Table 15.

Model results at four different simulation times (1, 10, 100, and 1000 years) are shown in Figure 1, respectively. The figures represent concentrations in Layer 5, which is the first layer that is entirely under the groundwater table due to the variable topography.

Results show that the concentrations of uranium never exceed the remediation target of 110 µg/L (180pCi/L). The highest simulated plume concentration for this scenario (1.1 µg/L) is two orders of magnitude smaller than this target concentration. Because the transport analysis assumes instantaneous sorption, the initial concentration of uranium released (500 µg/L) is immediately sorbed onto the reactive iron sites. The low simulated concentrations represent the release of aqueous uranium concentration from the sorbed phase due to the clean ground water front that contributes to the dissolution of the sorbed mass based on the specified  $K_d$ . In order to evaluate the effect of higher concentration loads of uranium during oxidizing conditions, a simulation run was conducted increasing the initial concentration of uranium from 500 µg/L to 5000 µg/L. The strong sorption capacity of the iron oxides attenuates linearly the uranium concentration to 11 µg/L. (highest simulated value for the 1000 years).

Because of the importance of the sorption parameters on the simulations results, a sensitivity analysis was conducted to evaluate the effect of the sorption distribution coefficient ( $K_d$ ) on the predicted concentration values. The different  $K_d$ 's were provided by batch studies using GWB to evaluate the difference in the sorption capacity based on the percentage of reactive iron available. Five scenarios were evaluated, ranging from 10% reactive iron ( $K_d = 19.38$  L/kg) to 100% reactive iron ( $K_d = 63.28$ ). The variations in aqueous concentrations are extremely small and cannot be appreciated in the plume snapshots as all the values of  $K_d$  result in a sorbed concentration of more than 99% of the total mass present. Figure 1 represents the simulation results for a  $K_d$  of 59 L/Kg (50% reactive iron available).

## **Scenario 5: Constant Mass Release of 0.1 Pound per Year**

This scenario assumes that 0.1 pound of uranium enters the aqueous phase in the plume area every year, simulating a gradual release of uranium from the oxidized iron sulfide. Assuming that 200 pounds of uranium are available, this constant uranium feed will persist until complete exhaustion of the available uranium mass (2000 years). The mass recharge was evenly distributed throughout the plume area. All of the transport parameters used are listed in Table 16.

Model results show that the mass released is almost entirely sorbed onto the reactive iron sites, leaving behind very low concentrations of uranium in solution (less than 0.1 µg/L). The concentrations do not exceed 0.1 µg/L until year 100, when enough mass is released due to oxidizing conditions to reach concentrations in the aqueous phase higher than 0.1 µg/L. The simulations show that even after 1000 years, the concentrations never exceed 1 µg/L of uranium.



The model assumes that the sorption reaction is fast enough, relative to groundwater velocity, to be treated as instantaneous; no kinetic limitations were considered between the solid and aqueous phase.

Groundwater transport modeling results indicate that, assuming an instantaneous remobilization of the uranium plume (Scenario 4), the concentrations never exceed the release criteria of 110 µg/L. Modeling of the scenario where 0.1 pound of uranium enters the aqueous phase annually (Scenario 5) resulted in an even lower uranium concentration estimation. When the effects of iron hydroxide adsorption and groundwater dilution are considered, the highest calculated uranium value in the plume area is 2.65 µg/L, which is an order of magnitude less than the release criteria.

## **Model Uncertainties and Assumptions**

Because of the numerical problems that were encountered during the calibration of some of the low permeability materials (clay and sandstones), the hydraulic conductivity of these layers was artificially high or calibrated to the high end to achieve convergence (ENSR Groundwater modeling report, 2006). This smoothing of the hydraulic conductivity field does not capture all field heterogeneities and, therefore, the model may not be able to reproduce or predict specific plume feature or irregularities. However, it is considered an acceptable simplification because it will provide a conservative plume velocity for risk assessment purposes.

The sorption model used in the MT3D transport simulations assumes an instantaneous, reversible and uniform sorption coefficient. The first two assumptions are considered reasonable based on the geochemistry of the site. The third assumption (uniformity) is also considered appropriate throughout the entire plume area as the well spacing will be design to create treatment zones that will overlap, ensuring appropriate distribution of iron hydroxide.

In general, the model is considered an appropriate representation of the Conceptual Site Model for the present purpose because it will most likely provide a conservative result.

## **Conclusions/Discussion**

A rigorous and conservative evaluation of Site conditions in which soluble uranium is precipitated through the introduction of organic carbon to the reduced oxide mineral uraninite, along with reduced iron sulfide minerals, was performed. These results supported by empirical studies indicate that under conditions present at the Site, uraninite and reduced iron sulfide minerals such as mackinawite will form. Once organic carbon addition is stopped and groundwater conditions return to oxidizing, the mackinawite has been demonstrated to be protective of the uraninite by acting as a sacrificial reductant. Using a range of groundwater velocities for the Site, the duration of mackinawite protection under worst case conditions ranged from 155 years to 25,925 years. Once the mackinawite is exhausted, the uranium begins to dissolve. Because this modeling approach used an equilibrium approach rather than a kinetic approach, the uranium dissolves all at once, which is again, a worst case condition. When this occurs there is instantaneous sorption of most of the uranium to the surrounding aquifer matrix. The highest uranium concentration remaining in solution without considering transport is approximately 1,400 µg/L under worst case conditions. When transport is considered on a very small scale (15 centimeters downgradient) the uranium concentrations immediately drop to very low levels, under a reasonably conservative case, the



uranium concentration drops two orders of magnitude below the regulatory limit of 110 ug/L. Beyond 15 centimeters the uranium concentrations become non-detectable.

In order to simulate extreme worst case conditions, the current Site uranium concentration of 5000 ug/L was used as a starting concentration to evaluate sorption. This simulation assumed that no reductive precipitation and subsequent re-oxidation and dissolution occurred. The simulation did assume that the existing crystalline iron oxides at the Site were converted to amorphous iron oxides by reduction and re-oxidation. In this simulation, soluble uranium did not exceed 45 ug/L at a distance of 15 centimeters downgradient indicating the enormous sorptive ability of amorphous iron oxides for uranium.

In addition to simulations using GWB, transport and sorption simulations were performed using MODFLOW with MT3DMS loaded with a Site-specific hydraulic flow model for the Site. The results for the attenuation of both 500 ug/L and 5000 ug/L uranium slugs released into the system are consistent with the GWB predictions.

This evaluation indicates that under multiple layers of conservative and worst case assumptions and conditions, that uranium treated by reductive precipitation will not re-dissolve to an aqueous concentration approaching the regulatory limit. Considering the degree of conservatism used in the evaluation, it is unlikely that the uranium concentration will ever exceed two to three orders of magnitude less than the regulatory limit.



## References

- Dzombak, D.A. and F.M.M. Morel. 1990. Surface Complexation Modeling and Hydrous Ferric Oxides. Wiley, New York, 393 pages.
- ENSR Corporation, Groundwater Modeling Report, September 2006.
- ENSR Corporation, Conceptual Site Model (Revision – 01), October 2006.
- Gerhar, L.W., C. Welty, and K.W. Rehfeldt. 1992. A critical review of data on field-scale dispersion in aquifers, *Water Resources and Research*, 28(7), 1955.
- Matsunga, T., G. Karametaxas, H.R. von Gunten, and P.C. Lichtner. 1993. Redox chemistry of iron and manganese minerals in river-recharged aquifers: A model interpretation of a column experiment. *Geochimica et Cosmochimica Acta* 57: 3895-3906.
- McDonald, M.G., and A.W. Harbaugh. 1988. MODFLOW. A numerical three-dimensional finite difference groundwater flow model. USGS Report 83-875.
- Suess, E. 1979. Mineral phases formed in anoxic sediments by microbial decomposition of organic matter. *Geochemica et Cosmochimica Acta* 43: 339-341.
- von Gunten, U. and J. Zobrist. 1993. Biogeochemical changes in groundwater-infiltration systems. Column studies. *Geochimica et Cosmochimica Acta* 57: 1691-1704.
- Xu, M., and Einstein. 1995. Use of weighted least-squares method in evaluation of the relationship between dispersivity and field scale. *Ground Water* 33, no 6, pp 905.
- Zheng, C. 1991. MT3D: A Modular Three-Dimensional Transport Model for Simulation of Advection, Dispersion, and Chemical Reactions of Contaminants in Groundwater Systems.
- Zheng, C., and P.P. Wang. 1999. MT3DMS: A Modular Three-Dimensional Multispecies Transport Model for Simulation of Advection, Dispersion, and Chemical Reactions of Contaminants in Groundwater Systems; Documentation and User's Guide



ARCADIS

TABLES



**Table 1. Initial Model Conditions – Chemical.**

Parameter	Value	Unit	Source Well/Boring
<b>Aqueous Phase</b>			
Dissolved Oxygen	8	mg/L	Equilibrium concentration with atmospheric oxygen
Nitrate	2.47	mg/L	MW 1315R
Bicarbonate	638	mg/L	MW 1315R
Sulfate	102	mg/L	MW 1315R
Uranium	2.67 <sup>1</sup>	mg/L	MW 1315R
Calcium	183	mg/L	MW 1315R
Chloride	22.5	mg/L	MW 1315R
Magnesium	70.9	mg/L	MW 1315R
Sodium	30.1	mg/L	MW 1315R
pH	6.8	s.u.	MW 1315R
<b>Solid Phase</b>			
Total Iron	6,900 <sup>2</sup>	mg/kg	TMW-9/10-10.5 ft bls
Total Uranium	4.5	mg/kg	TMW-9/10-10.5 ft bls

<sup>1</sup> Uranium reported as 1,793 picocuries per liter, equal to 1.1 mg/L. using Site specific activity conversion factor (1.63 pCi/ug). Model input used an activity conversion based on natural uranium (0.67 pCi/ug) to be conservative.

<sup>2</sup> The amount of iron available to react varied as a percentage of this value by model run.

mg/kg milligrams per kilogram.

mg/L milligrams per liter.

s.u. standard units.

ft bls feet below land surface.



# ARCADIS

**Table 2. Composition of Groundwater Introduced into System.**

Parameter	Value	Unit	Source Well/Boring
<b>Aqueous Phase</b>			
Dissolved Oxygen	-75	Log Activity	Simulated
Silicon Dioxide	6	mg/L	Simulated
Nitrate	2.47	mg/L	MW 1315R
Bicarbonate	628	mg/L	MW 1315R
Sulfate	102	mg/L	MW 1315R
Uranium	2.671	mg/L	MW 1315R
Calcium	90	mg/L	Simulated
Chloride	22.5	mg/L	MW 1315R
Magnesium	70.9	mg/L	MW 1315R
Sodium	7.28	mg/L	Simulated
Iron	1e-7	mg/L	Simulated
Uranium	1e-26	mg/L	Considered Zero
pH	6.8	s.u.	MW 1315R

mg/L milligrams per liter.

s.u. standard units.

-75 Log Activity for oxygen equal to -260 millivolts as Eh.

Uranium concentration of 1e-26 mg/L is essentially zero. This value used in solutions containing no uranium. Model convergence could not be achieved using a zero value.



**Table 3. Composition of Final Solution After Reductive Precipitation of Uraninite and Mackinawite As a Function of Available Iron.**

10% Reactive Iron		
Final Solution Composition		
Quartz	5.9	Kg
Mackinawite	7.15	G
Calcite	86.73	G
Uraninite	32.34	mg
O <sub>2</sub> (aq)	3.E-71	mg/L
HCO <sub>3</sub> <sup>-</sup>	438	mg/L
Ca <sup>2+</sup>	76.53	mg/L
pH	6.808	
SO <sub>4</sub> <sup>2-</sup>	2.E-03	mg/L
HS <sup>-</sup>	19.83	mg/L
H <sub>2</sub> S(aq)	15.16	mg/L
Na <sup>+</sup>	7.22	mg/L
Cl <sup>-</sup>	22.34	mg/L
NH <sub>4</sub> <sup>+</sup>	0.7145	mg/L
NH <sub>3</sub>	3.39E-03	mg/L
Mg <sup>2+</sup>	67.37	mg/L
CO <sub>2</sub> (g)	0.06835	fug
H <sub>2</sub> S(g)	0.004762	fug

25% Reactive Iron		
Final Solution Composition		
Quartz	5.9	kg
Mackinawite	17.89	g
Calcite	99.42	g
Uraninite	32.34	mg
O <sub>2</sub> (aq)	3.E-71	mg/L
HCO <sub>3</sub> <sup>-</sup>	438	mg/L
Ca <sup>2+</sup>	75.68	mg/L
pH	6.812	
SO <sub>4</sub> <sup>2-</sup>	1.88E-03	mg/L
HS <sup>-</sup>	19.41	mg/L
H <sub>2</sub> S(aq)	14.78	mg/L
Na <sup>+</sup>	7.22	mg/L
Cl <sup>-</sup>	22.34	mg/L
NH <sub>4</sub> <sup>+</sup>	0.7144	mg/L
NH <sub>3</sub>	3.40E-03	mg/L
Mg <sup>2+</sup>	67.37	mg/L
CO <sub>2</sub> (g)	0.06767	fug
N <sub>2</sub> (g)	9.28E-07	fug
S <sub>2</sub> (g)	4.90E-20	fug
H <sub>2</sub> S(g)	0.00464	fug

50% Reactive Iron		
Final Solution Composition		
Quartz	5.9	kg
Mackinawite	35.23	g
Calcite	112.1	g
Uraninite	32.34	mg
O <sub>2</sub> (aq)	3.E-71	mg/L
HCO <sub>3</sub> <sup>-</sup>	438.5	mg/L
Ca <sup>2+</sup>	74.6	mg/L
pH	6.819	
SO <sub>4</sub> <sup>2-</sup>	1.83E-03	mg/L
HS <sup>-</sup>	18.71	mg/L
H <sub>2</sub> S(aq)	14.15	mg/L
Na <sup>+</sup>	7.22	mg/L
Cl <sup>-</sup>	22.34	mg/L
NH <sub>4</sub> <sup>+</sup>	0.7144	mg/L
NH <sub>3</sub>	3.40E-03	mg/L
Mg <sup>2+</sup>	67.37	mg/L
CO <sub>2</sub> (g)	0.06666	fug
N <sub>2</sub> (g)	9.41E-07	fug
S <sub>2</sub> (g)	4.59E-20	fug
H <sub>2</sub> S(g)	0.00444	fug

75% Reactive Iron		
Final Solution Composition		
Quartz	5.9	kg
Mackinawite	53.67	g
Calcite	141.6	g
Uraninite	32.22	mg
O <sub>2</sub> (aq)	3.E-71	mg/L
HCO <sub>3</sub> <sup>-</sup>	458.7	mg/L
Ca <sup>2+</sup>	72.85	mg/L
pH	6.828	
SO <sub>4</sub> <sup>2-</sup>	1.77E-03	mg/L
HS <sup>-</sup>	17.96	mg/L
H <sub>2</sub> S(aq)	13.49	mg/L
Na <sup>+</sup>	7.22	mg/L
Cl <sup>-</sup>	22.34	mg/L
NH <sub>4</sub> <sup>+</sup>	0.7144	mg/L
NH <sub>3</sub>	3.40E-03	mg/L
Mg <sup>2+</sup>	67.37	mg/L
CO <sub>2</sub> (g)	0.06538	fug
N <sub>2</sub> (g)	9.55E-07	fug
S <sub>2</sub> (g)	4.17E-20	fug
H <sub>2</sub> S(g)	0.004236	fug

100% Reactive Iron		
Final Solution Composition		
Quartz	5.9	kg
Mackinawite	71.56	g
Calcite	162.7	g
Uraninite	32.34	mg
O <sub>2</sub> (aq)	3.E-71	mg/L
HCO <sub>3</sub> <sup>-</sup>	458.6	mg/L
Ca <sup>2+</sup>	71.43	mg/L
pH	6.835	
SO <sub>4</sub> <sup>2-</sup>	1.71E-03	mg/L
HS <sup>-</sup>	17.24	mg/L
H <sub>2</sub> S(aq)	12.85	mg/L
Na <sup>+</sup>	7.22	mg/L
Cl <sup>-</sup>	22.34	mg/L
NH <sub>4</sub> <sup>+</sup>	0.7144	mg/L
NH <sub>3</sub>	3.40E-03	mg/L
Mg <sup>2+</sup>	67.37	mg/L
CO <sub>2</sub> (g)	0.06424	fug
N <sub>2</sub> (g)	9.69E-07	fug
S <sub>2</sub> (g)	3.78E-20	fug
H <sub>2</sub> S(g)	0.004036	fug

kg kilogram.  
g gram.  
mg milligram.  
mg/L milligram per liter.  
(g) gaseous species.  
fug fugacity.



**Table 4. Scenario 2 (Batch) Permutations.**

Percentage of Total Iron that is Reactive	Dissolved Oxygen	pH (s.u.)	Total Inorganic Carbon
100% Reactive Iron	1.2 mg/L	5	628 mg/L
	1.2 mg/L	7.5	628 mg/L
	1.2 mg/L	6.8	628 mg/L
	1.2 mg/L	6.8	298 mg/L TIC
	1.2 mg/L	6.8	628 mg/L / 0.5% calcite
	8.0 mg/L	6.8	628 mg/L
75% Reactive Iron	1.2 mg/L	6.8	628 mg/L
	8.0 mg/L	6.8	628 mg/L
50% Reactive Iron	1.2 mg/L	6.8	628 mg/L
	8.0 mg/L	6.8	628 mg/L
25% Reactive Iron	1.2 mg/L	6.8	628 mg/L
	8.0 mg/L	6.8	628 mg/L
10% Reactive Iron	1.2 mg/L	6.8	628 mg/L
	8.0 mg/L	6.8	628 mg/L

s.u. standard units.  
mg/L milligrams per liter.



**Table 5. Oxidative Dissolution Simulations Using 100 Percent Reactive Iron.**

1.2 mg/L Dissolved Oxygen pH 5		
Quartz	5.9	kg
Hematite	59.04	g
Calcite	ND	
$\text{UO}_2(\text{CO}_3)_2^{2-}$	8.72E-04	mg/L
$\text{UO}_2(\text{CO}_3)$	6.01E-04	mg/L
$\text{O}_2(\text{aq})$	1.03E-05	mg/L
$\text{HCO}_3^-$	458.1	mg/L
$\text{Ca}^{2+}$	78.46	mg/L
pH	4.964	s.u.
$\text{SO}_4^{2-}$	77.57	mg/L
$\text{Na}^+$	7.124	mg/L
$\text{Cl}^-$	22.06	mg/L
$\text{NO}_3^{2-}$	2.74E-01	mg/L
$\text{Mg}^{2+}$	63.44	mg/L
$\text{CO}_2(\text{g})$	4.832	fug
$\text{N}_2(\text{g})$	0.02695	fug
Pore Volumes Required: 26,000		

1.2 mg/L Dissolved Oxygen pH 7.5		
Quartz	5.9	Kg
Hematite	59.04	G
Calcite	1833	G
$\text{UO}_2(\text{CO}_3)_2^{2-}$	1.62E-03	Mg/L
$\text{UO}_2(\text{CO}_3)$	1.04E-03	Mg/L
$\text{O}_2(\text{aq})$	3.33E-08	Mg/L
$\text{HCO}_3^-$	464.1	Mg/L
$\text{Ca}^{2+}$	45.74	Mg/L
pH	7.017	s.u.
$\text{SO}_4^{2-}$	82.67	Mg/L
$\text{Na}^+$	7.198	Mg/L
$\text{Cl}^-$	22.35	Mg/L
$\text{NO}_3^{2-}$	2.53E-02	Mg/L
$\text{Mg}^{2+}$	63.63	Mg/L
$\text{CO}_2(\text{g})$	0.04293	Fug
$\text{N}_2(\text{g})$	0.03017	Fug
Pore Volumes Required: 18,500		

1.2 mg/L Dissolved Oxygen pH 6.8		
Quartz	5.9	kg
Hematite	59.04	g
Calcite	26.91	g
$\text{UO}_2(\text{CO}_3)_2^{2-}$	1.86E-03	mg/L
$\text{UO}_2(\text{CO}_3)_3^{4-}$	7.52E-04	mg/L
$\text{O}_2(\text{aq})$	4.50E-08	mg/L
$\text{HCO}_3^-$	459.1	mg/L
$\text{Ca}^{2+}$	78.88	mg/L
pH	6.796	s.u.
$\text{SO}_4^{2-}$	79.09	mg/L
$\text{Na}^+$	7.201	mg/L
$\text{Cl}^-$	22.29	mg/L
$\text{NO}_3^{2-}$	1.93E-01	mg/L
$\text{Mg}^{2+}$	64.03	mg/L
$\text{CO}_2(\text{g})$	0.07026	fug
$\text{N}_2(\text{g})$	0.0302	fug
Pore Volumes Required: 19,000		

1.2 mg/L Dissolved Oxygen pH 6.8/298 mg/L TIC		
Quartz	5.9	kg
Hematite	59.04	g
Calcite	ND	
$\text{UO}_2(\text{CO}_3)_2^{2-}$	2.19E-03	mg/L
$\text{UO}_2(\text{CO}_3)_3^{4-}$	8.05E-05	mg/L
$\text{O}_2(\text{aq})$	1.22E-07	mg/L
$\text{HCO}_3^-$	144.1	mg/L
$\text{Ca}^{2+}$	83.21	mg/L
pH	6.3	s.u.
$\text{SO}_4^{2-}$	77.11	mg/L
$\text{Na}^+$	7.24	mg/L
$\text{Cl}^-$	22.29	mg/L
$\text{NO}_3^{2-}$	2.44E-02	mg/L
$\text{Mg}^{2+}$	66.01	mg/L
$\text{CO}_2(\text{g})$	0.06959	fug
$\text{N}_2(\text{g})$	0.03018	fug
Pore Volumes Required: 19,000		

1.2 mg/L Dissolved Oxygen pH 6.8 @ 0.5% Calcite		
Quartz	5.9	Kg
Hematite	59.04	G
Calcite	ND	
$\text{UO}_2(\text{CO}_3)_2^{2-}$	1.78E-03	Mg/L
$\text{UO}_2(\text{CO}_3)_3^{4-}$	7.21E-04	Mg/L
$\text{O}_2(\text{aq})$	2.60E-07	Mg/L
$\text{HCO}_3^-$	459.1	Mg/L
$\text{Ca}^{2+}$	78.88	Mg/L
pH	6.796	s.u.
$\text{SO}_4^{2-}$	79.09	Mg/L
$\text{Na}^+$	7.201	Mg/L
$\text{Cl}^-$	22.29	Mg/L
$\text{NO}_3^{2-}$	1.93E-01	Mg/L
$\text{Mg}^{2+}$	64.03	Mg/L
$\text{CO}_2(\text{g})$	0.0703	Fug
$\text{N}_2(\text{g})$	0.02808	Fug
Pore Volumes Required: 19,000		

8.0 mg/L Dissolved Oxygen pH 6.8		
Quartz	5.9	kg
Hematite	59.04	g
Calcite	ND	
$\text{UO}_2(\text{CO}_3)_2^{2-}$	6.44E-03	mg/L
$\text{UO}_2(\text{CO}_3)_3^{4-}$	2.52E-03	mg/L
$\text{O}_2(\text{aq})$	8.73E-08	mg/L
$\text{HCO}_3^-$	458.5	mg/L
$\text{Ca}^{2+}$	81.71	mg/L
pH	6.778	s.u.
$\text{SO}_4^{2-}$	85.78	mg/L
$\text{Na}^+$	7.201	mg/L
$\text{Cl}^-$	22.28	mg/L
$\text{NO}_3^{2-}$	0.05	mg/L
$\text{Mg}^{2+}$	63.8	mg/L
$\text{CO}_2(\text{g})$	0.07303	fug
$\text{N}_2(\text{g})$	0.02987	fug
Pore Volumes Required: 5,500		

kg kilogram.  
g gram.  
mg/L milligram per liter  
s.u. standard unit.

(g) gaseous species.  
fug fugacity.  
TIC total inorganic carbon.



**Table 6. Oxidative Dissolution Simulations Using 75 Percent Reactive Iron.**

1.2 mg/L Dissolved Oxygen pH 6.8		
Quartz	5.9	kg
Hematite	44.28	g
Calcite	35.88	g
$\text{UO}_2(\text{CO}_3)_2^{2-}$	2.48E-03	mg/L
$\text{UO}_2(\text{CO}_3)_3^{4-}$	1.00E-03	mg/L
$\text{O}_2(\text{aq})$	3.98E-08	mg/L
$\text{HCO}_3^-$	459.1	mg/L
$\text{Ca}^{2+}$	78.88	mg/L
pH	6.796	s.u.
$\text{SO}_4^{2-}$	79.20	mg/L
$\text{Na}^+$	7.201	mg/L
$\text{Cl}^-$	22.29	mg/L
$\text{NO}_3^{2-}$	1.91E-02	mg/L
$\text{Mg}^{2+}$	64.03	mg/L
$\text{CO}_2(\text{g})$	0.07026	fug
$\text{N}_2(\text{g})$	0.03024	fug
Pore Volumes Required: 9,000		

8.0 mg/L Dissolved Oxygen pH 6.8		
Quartz	5.9	kg
Hematite	44.28	g
Calcite	11.18	g
$\text{UO}_2(\text{CO}_3)_2^{2-}$	8.54E-03	mg/L
$\text{UO}_2(\text{CO}_3)_3^{4-}$	3.37E-03	mg/L
$\text{O}_2(\text{aq})$	1.43E-07	mg/L
$\text{HCO}_3^-$	459.4	mg/L
$\text{Ca}^{2+}$	82.01	mg/L
pH	6.781	s.u.
$\text{SO}_4^{2-}$	85.72	mg/L
$\text{Na}^+$	7.202	mg/L
$\text{Cl}^-$	22.28	mg/L
$\text{NO}_3^{2-}$	0.09	mg/L
$\text{Mg}^{2+}$	63.8	mg/L
$\text{CO}_2(\text{g})$	0.07278	fug
$\text{N}_2(\text{g})$	0.02936	fug
Pore Volumes Required: 2,750		

kg      kilogram.  
 g      gram.  
 mg/L      milligram per liter.  
 (g)      gaseous species.  
 fug      fugacity.  
 TIC      total inorganic carbon.  
 s.u.      standard unit.



**Table 7. Oxidative Dissolution Simulations Using 50 Percent Reactive Iron.**

1.2 mg/L Dissolved Oxygen pH 6.8		
Quartz	5.9	kg
Hematite	29.59	g
Calcite	43.92	g
$\text{UO}_2(\text{CO}_3)_2^{2-}$	3.71E-03	mg/L
$\text{UO}_2(\text{CO}_3)_3^{4-}$	1.50E-03	mg/L
$\text{O}_2(\text{aq})$	7.23E-09	mg/L
$\text{HCO}_3^-$	459.1	mg/L
$\text{Ca}^{2+}$	78.87	mg/L
pH	6.796	s.u.
$\text{SO}_4^{2-}$	79.21	mg/L
$\text{Na}^+$	7.201	mg/L
$\text{Cl}^-$	22.29	mg/L
$\text{NO}_3^{2-}$	2.29E-03	mg/L
$\text{Mg}^{2+}$	64.03	mg/L
$\text{CO}_2(\text{g})$	0.07026	fug
$\text{N}_2(\text{g})$	0.03045	fug
Pore Volumes Required: 9,000		

8.0 mg/L Dissolved Oxygen pH 6.8		
Quartz	5.9	kg
Hematite	29.59	g
Calcite	27.45	g
$\text{UO}_2(\text{CO}_3)_2^{2-}$	1.28E-02	mg/L
$\text{UO}_2(\text{CO}_3)_3^{4-}$	5.06E-03	mg/L
$\text{O}_2(\text{aq})$	6.27E-08	mg/L
$\text{HCO}_3^-$	459.4	mg/L
$\text{Ca}^{2+}$	82.01	mg/L
pH	6.781	s.u.
$\text{SO}_4^{2-}$	85.74	mg/L
$\text{Na}^+$	7.205	mg/L
$\text{Cl}^-$	22.28	mg/L
$\text{NO}_3^{2-}$	0.03	mg/L
$\text{Mg}^{2+}$	63.8	mg/L
$\text{CO}_2(\text{g})$	0.07278	fug
$\text{N}_2(\text{g})$	0.03008	fug
Pore Volumes Required: 2,750		

kg      kilogram.  
 g      gram.  
 mg/L      milligram per liter.  
 (g)      gaseous species.  
 fug      fugacity.  
 TIC      total inorganic carbon.  
 s.u.      standard unit.



**Table 8. Oxidative Dissolution Simulations Using 25 Percent Reactive Iron.**

1.2 mg/L dissolved Oxygen pH 6.8		
Quartz	5.9	kg
Hematite	14.76	g
Calcite	51.87	g
$\text{UO}_2(\text{CO}_3)_2^{2-}$	7.13E-03	mg/L
$\text{UO}_2(\text{CO}_3)_3^{4-}$	2.89E-03	mg/L
$\text{O}_2(\text{aq})$	4.67E-06	mg/L
$\text{HCO}_3^-$	459.1	mg/L
$\text{Ca}^{2+}$	78.87	mg/L
pH	6.796	s.u.
$\text{SO}_4^{2-}$	79.14	mg/L
$\text{Na}^+$	7.201	mg/L
$\text{Cl}^-$	22.29	mg/L
$\text{NO}_3^{2-}$	8.12E-02	mg/L
$\text{Mg}^{2+}$	64.03	mg/L
$\text{CO}_2(\text{g})$	0.07025	fug
$\text{N}_2(\text{g})$	0.02842	fug
Pore Volumes Required: 4,800		

8.0 mg/L Dissolved Oxygen pH 6.8		
Quartz	5.9	kg
Hematite	14.76	g
Calcite	43.75	g
$\text{UO}_2(\text{CO}_3)_2^{2-}$	2.26E-02	mg/L
$\text{UO}_2(\text{CO}_3)_3^{4-}$	1.00E-02	mg/L
$\text{O}_2(\text{aq})$	9.18E-09	mg/L
$\text{HCO}_3^-$	459.4	mg/L
$\text{Ca}^{2+}$	82	mg/L
pH	6.781	s.u.
$\text{SO}_4^{2-}$	85.71	mg/L
$\text{Na}^+$	7.213	mg/L
$\text{Cl}^-$	22.28	mg/L
$\text{NO}_3^{2-}$	2.97E-03	mg/L
$\text{Mg}^{2+}$	63.8	mg/L
$\text{CO}_2(\text{g})$	0.07277	fug
$\text{N}_2(\text{g})$	0.03044	fug
Pore Volumes Required: 1,370		

kg      kilogram.  
 g      gram.  
 mg/L    milligram per liter.  
 (g)      gaseous species.  
 fug      fugacity.  
 TIC      total inorganic carbon.  
 s.u.      standard unit.

**Table 9. Oxidative Dissolution Simulations Using 10 Percent Reactive Iron.**

1.2 mg/L Dissolved Oxygen pH 6.8		
Quartz	5.9	kg
Hematite	5.904	g
Calcite	56.72	g
$\text{UO}_2(\text{CO}_3)_2^{2-}$	1.78E-02	mg/L
$\text{UO}_2(\text{CO}_3)_3^{4-}$	7.21E-03	mg/L
$\text{O}_2(\text{aq})$	1.64E-07	mg/L
$\text{HCO}_3^-$	459.1	mg/L
$\text{Ca}^{2+}$	78.87	mg/L
pH	6.796	s.u.
$\text{SO}_4^{2-}$	79.09	mg/L
$\text{Na}^+$	7.209	mg/L
$\text{Cl}^-$	22.29	mg/L
$\text{Mg}^{2+}$	64.03	mg/L
$\text{CO}_2(\text{g})$	0.07025	fug
$\text{N}_2(\text{g})$	0.02911	fug
<b>Pore Volumes Required: 1,900</b>		

8.0 mg/L dissolved Oxygen pH 6.8		
Quartz	5.9	kg
Hematite	5.904	g
Calcite	53.12	g
$\text{UO}_2(\text{CO}_3)_2^{2-}$	6.00E-02	mg/L
$\text{UO}_2(\text{CO}_3)_3^{4-}$	2.40E-02	mg/L
$\text{O}_2(\text{aq})$	6.90	mg/L
$\text{HCO}_3^-$	459.4	mg/L
$\text{Ca}^{2+}$	81.98	mg/L
pH	6.781	s.u.
$\text{SO}_4^{2-}$	85.07	mg/L
$\text{Na}^+$	7.234	mg/L
$\text{Cl}^-$	22.28	mg/L
$\text{NO}_3^{2-}$	0.80	mg/L
$\text{Mg}^{2+}$	63.82	mg/L
$\text{CO}_2(\text{g})$	0.07274	fug
$\text{CO}_2(\text{g})$	0.07274	$\text{N}_2(\text{g})$
$\text{O}_2(\text{g})$	2.35E-08	fug
<b>Pore Volumes Required: 550</b>		

kg      kilogram.  
 g      gram.  
 mg/L      milligram per liter.  
 (g)      gaseous species.  
 fug      fugacity.  
 TIC      total inorganic carbon.  
 s.u.      standard unit.



**Table 10. Initial Conditions Scenario 2 (Transport).**

Parameter	Value
Aquifer Dimensions	12.192 m x 1 m x 1 m
Porosity	25%
Density (Sandstone)	2323 kg/m <sup>3</sup>
Density (Quartz)	2650 kg/m <sup>3</sup>
Density (Calcite)	2710 kg/m <sup>3</sup>
Density (Mackinawite)	4170 kg/m <sup>3</sup>
Density (Uraninite)	10970 kg/m <sup>3</sup>
Density (Hematite)	5300 kg/m <sup>3</sup>
Diffusion Coefficient	1e-6 cm <sup>2</sup> /sec
Longitudinal Dispersion	0.1 m
Sandstone mineralogy defined as 98% quartz, 0.998% mackinawite, 1% calcite, and 0.02% uraninite.	

m            meter.  
 kg/m<sup>3</sup>      kilogram per cubic meter.  
 cm<sup>2</sup>/sec    centimeter squared per second.  
 v/v         volume by volume.

**Table 11. Sorption Simulation Permutations (Scenario 3 Batch).**

Percentage of Total Iron that is Reactive	Dissolved Oxygen	pH (s.u.)	Total Inorganic Carbon
100% Reactive Iron	1.2 mg/L	5	638 mg/L
	1.2 mg/L	6.8	638 mg/L
	1.2 mg/L	6.8	298 mg/L TIC
	1.2 mg/L	6.8	638 mg/L / 10% Calcium
	8.0 mg/L	6.8	638 mg/L
75% Reactive Iron	1.2 mg/L	6.8	638 mg/L
	8.0 mg/L	6.8	638 mg/L
50% Reactive Iron	1.2 mg/L	6.8	638 mg/L
	8.0 mg/L	6.8	638 mg/L
25% Reactive Iron	1.2 mg/L	6.8	638 mg/L
	8.0 mg/L	6.8	638 mg/L
10% Reactive Iron	1.2 mg/L	6.8	638 mg/L
	8.0 mg/L	6.8	638 mg/L

s.u. standard units.

mg/L milligrams per liter.



**Table 12. Sorption Simulation Results (Scenario 3 Batch).**

Percentage of Total Iron that is Reactive	Dissolved Oxygen	pH (s.u.)	Total Inorganic Carbon	Uranium Remaining in Solution
100% Reactive Iron	1.2 mg/L	5	638 mg/L	8,860 µg/L
	1.2 mg/L	6.8	638 mg/L / 10% Calcium	363 µg/L
	1.2 mg/L	6.8	298 mg/L	463 µg/L
	1.2 mg/L	6.8	638 mg/L	463 µg/L
	8 mg/L	6.8	638 mg/L	483 µg/L
75% Reactive Iron	1.2 mg/L	6.8	638 mg/L	442 µg/L
	8 mg/L	6.8	638 mg/L	459 µg/L
50% Reactive Iron	1.2 mg/L	6.8	638 mg/L	479 µg/L
	8 mg/L	6.8	638 mg/L	494 µg/L
25% Reactive Iron	1.2 mg/L	6.8	638 mg/L	695 µg/L
	8 mg/L	6.8	638 mg/L	708 µg/L
10% Reactive Iron	1.2 mg/L	6.8	638 mg/L	1,450 µg/L
	8 mg/L	6.8	638 mg/L	1,460 µg/L

s.u. standard units.

mg/L milligrams per liter.

µg/L micrograms per liter.

**Table 13. Sorption Simulation Results (Scenario 3 Transport).**

Percentage of Total Iron that is Reactive	Dissolved Oxygen	pH (s.u.)	Initial Uranium Concentration	Total Inorganic Carbon	Distance from the Source	Uranium Remaining in Solution
50% Reactive Iron	1.2 mg/L	6.8	500 µg/L	638 mg/L	0.5 feet/ 15 cm	1.38 µg/L
	8 mg/L	6.8	500 µg/L	638 mg/L	0.5 feet/ 15 cm	1.38 µg/L
10% Reactive Iron	1.2 mg/L	6.8	500 µg/L	638 mg/L	0.5 feet/ 15 cm	2.92 µg/L
	1.2 mg/L	6.8	5000 µg/L	638 mg/L	0.5 feet/ 15 cm	44.6 µg/L
	8 mg/L	6.8	500 µg/L	638 mg/L	0.5 feet/ 15 cm	3.09 µg/L

s.u. standard units.

mg/L milligrams per liter.

µg/L micrograms per liter.



**Table 14. Initial Conditions Scenario 3 (Transport).**

Parameter	Value
Dimensions of the Aquifer	70.104 m x 1 m x 1 m
Porosity	0.25
Density	2323 kg/m <sup>3</sup> (sandstone)
Diffusion Coefficient	1e-5 cm <sup>2</sup> /sec
Longitudinal Dispersivity	0.1 m estimated
Density (Quartz)	2650 kg/m <sup>3</sup>
Density (Calcite)	2710 kg/m <sup>3</sup>
Density (Mackinawite)	4170 kg/m <sup>3</sup>
Density (Uraninite)	10970 kg/m <sup>3</sup>
Density (Hematite)	5300 kg/m <sup>3</sup>
Sandstone mineralogy is set at 86 percent v/v quartz, 0.4383 percent v/v hematite, and 0.857 percent v/v calcite. There is a negligible amount of uranium present in the aquifer.	

m meter.  
 kg/m<sup>3</sup> kilogram per cubic meter.  
 cm<sup>2</sup>/sec centimeter squared per second.  
 v/v volume by volume.

**Table 15. Transport Parameters in Scenario 4.**

Parameter	Value	Reference
Initial uranium concentration	500 µg/L	Output from Scenario 2
$K_d$	59 L/kg	Sorption equilibrium constant of uranium on iron oxides (Geochemists' Workbench)
Bulk density	2323 kg/m <sup>3</sup>	<a href="http://www.simetric.co.uk/si_materials.htm">http://www.simetric.co.uk/si_materials.htm</a>
Dispersivity	0.1 m	Conservative value based on Gelhar, 1992 and Xu and Einstein, 1995
Diffusion coefficient	10 <sup>-6</sup> cm <sup>2</sup> /sec	Default-GWB (Geochemists' Workbench Library)
Model duration	1000 yr	Time projection required by NRC
Step size	60 days	Determined by convergence requirement and computer hardware specifications

µg/L      microgram per liter.  
 L/kg      liter per kilogram.  
 kg/m<sup>3</sup>    kilogram per cubic meter.  
 $K_d$       distribution coefficient.  
 m          meter.  
 cm<sup>2</sup>/sec    centimeter squared per second.  
 yr          year.



**Table 16. Transport Parameters in Scenario 5.**

Parameter	Value	Reference
Uranium mass load	0.1 lb/yr	Assumed
$K_d$	59 L/kg	Sorption equilibrium constant of uranium on iron oxides (Geochemists' Workbench)
Bulk density	2323 kg/m <sup>3</sup>	<a href="http://www.simetric.co.uk/si_materials.htm">http://www.simetric.co.uk/si_materials.htm</a>
Dispersivity	0.1 m	Conservative value based on Gelhar, 1992 and Xu and Einstein, 1995
Diffusion coefficient	10 <sup>-6</sup> cm <sup>2</sup> /sec	Default-GWB (Geochemists' Workbench Library)
Model duration	2000 yr	Necessary time to release 200 pounds (estimated mass in Burial Area #1) of uranium at the prescribed mass release of 0.1 lb/year
Step size	60 days	Determined by convergence requirement and computer hardware specifications

lb/yr      pound per year.  
 L/kg      liter per kilogram.  
 $K_d$       distribution coefficient.  
 kg/m<sup>3</sup>    kilogram per cubic meter.  
 m          meter.  
 cm<sup>2</sup>/sec   squared centimeter per second.  
 yr          year.

ARCADIS

ATTACHMENT TABLES



Attachment Table 1. Hematite Dissolution, Iron and Uranium Reduction and the Precipitation of Uraninite and Mackinawite, 10 Percent Reactive Iron.

Database file used is Thermo\_mackinawite.dat

Initial Solution Composition - 1 kg of water

Quartz	5.9	kg
Hematite	6.5	g
Calcite	60	g
$\text{UO}_2(\text{CO}_3)_2^{2-}$	33.67	mg
$\text{O}_2(\text{aq})$	8	mg/l
$\text{HCO}_3^-$	638	mg/l
pH	6.8	s.u.
$\text{SO}_4^{2-}$	102	mg/l
$\text{Na}^+$	30.1	mg/l
$\text{Cl}^-$	22.5	mg/l
$\text{NO}_3^-$	2.47	mg/l
$\text{Mg}^{2+}$	70.9	mg/l

Reactants Composition 1 kg of water

$\text{SiO}_2(\text{aq})$	6	mg/l
$\text{Ca}^{2+}$	89.82	mg/l
pH	6.8	s.u.
$\text{SO}_4^{2-}$	102	mg/l
$\text{Na}^+$	7.28	mg/l
$\text{Cl}^-$	22.5	mg/l
$\text{NO}_3^-$	2.47	mg/l
$\text{Mg}^{2+}$	70.9	mg/l
$\text{Fe}^{2+}$	1.E-07	mg/l
$\text{U}^{4+}$	1.E-26	mg/l
$\text{O}_2(\text{aq})$	3.E-71	mg/l
$\text{HCO}_3^-$	628	mg/l

Final Solution Composition - 1 kg of water

Quartz	5.9	kg
Mackinawite	7.15	g
Calcite	561.5	g
Uraninite	32.34	mg
$\text{O}_2(\text{aq})$	3.E-71	mg/l
$\text{HCO}_3^-$	438	mg/l
$\text{Ca}^{2+}$	45.97	mg/l
pH	7.03	s.u.
$\text{SO}_4^{2-}$	2.E-03	mg/l
$\text{HS}^-$	19.83	mg/l
$\text{H}_2\text{S}(\text{aq})$	15.16	mg/l
$\text{Na}^+$	7.22	mg/l
$\text{Cl}^-$	22.34	mg/l
$\text{NH}_4^+$	0.7145	mg/l
$\text{NH}_3$	3.39E-03	mg/l
$\text{Mg}^{2+}$	67.37	mg/l

Main gases produced - fugacities

$\text{CO}_2(\text{g})$	0.03953
$\text{H}_2\text{S}(\text{g})$	0.004762

Attachment Table 2. Hematite Dissolution, Iron and Uranium Reduction and the Precipitation of Uraninite and Mackinawite, 25 Percent Reactive Iron.

Database file used is Thermo\_mackinawite.dat

Initial Solution Composition- 1 kg of water

Initial Solution Composition	5.9	kg
Hematite	16.25	g
Calcite	60	g
$\text{UO}_2(\text{CO}_3)_2^{2-}$	33.67	mg
$\text{O}_2(\text{aq})$	8	mg/l
$\text{HCO}_3^-$	638	mg/l
pH	6.8	s.u.
$\text{SO}_4^{2-}$	102	mg/l
$\text{Na}^+$	30.1	mg/l
$\text{Cl}^-$	22.5	mg/l
$\text{NO}_3^-$	2.47	mg/l
$\text{Mg}^{2+}$	70.9	mg/l

Reactants Composition- 1kg of water

$\text{SiO}_2(\text{aq})$	6	mg/l
$\text{Ca}^{2+}$	89.82	mg/l
pH	6.8	s.u.
$\text{SO}_4^{2-}$	102	mg/l
$\text{Na}^+$	7.28	mg/l
$\text{Cl}^-$	22.5	mg/l
$\text{NO}_3^-$	2.47	mg/l
$\text{Mg}^{2+}$	70.9	mg/l
$\text{Fe}^{2+}$	1.E-07	mg/l
$\text{U}^{4+}$	1.E-26	mg/l
$\text{O}_2(\text{aq})$	3.E-71	mg/l
$\text{HCO}_3^-$	628	mg/l

Final Solution Composition- 1 kg of water

Quartz	5.9	kg
Mackinawite	17.89	g
Calcite	564.4	g
Uraninite	32.34	mg
$\text{O}_2(\text{aq})$	3.E-71	mg/l
$\text{HCO}_3^-$	438	mg/l
$\text{Ca}^{2+}$	45.76	mg/l
pH	7.032	s.u.
$\text{SO}_4^{2-}$	1.88E-03	mg/l
$\text{HS}^-$	19.41	mg/l
$\text{H}_2\text{S}(\text{aq})$	14.78	mg/l
$\text{Na}^+$	7.22	mg/l
$\text{Cl}^-$	22.34	mg/l
$\text{NH}_4^+$	0.7144	mg/l
$\text{NH}_3$	3.40E-03	mg/l
$\text{Mg}^{2+}$	67.37	mg/l

Main gases produced - fugacities

$\text{CO}_2(\text{g})$	0.03937
$\text{N}_2(\text{g})$	9.28E-07
$\text{S}_2(\text{g})$	5.00E-20
$\text{H}_2\text{S}(\text{g})$	0.00464



Attachment Table 3. Hematite Dissolution, Iron and Uranium Reduction and the Precipitation of Uraninite and Mackinawite, 50 Percent Reactive Iron.

Database file used is Thermo\_mackinawite.dat

Initial Solution Composition - 1 kg of water

Quartz	5.9	kg
Hematite	32	g
Calcite	60	g
$\text{UO}_2(\text{CO}_3)_2^{2-}$	33.67	mg
$\text{O}_2(\text{aq})$	8	mg/l
$\text{HCO}_3^-$	638	mg/l
pH	6.8	s.u.
$\text{SO}_4^{2-}$	102	mg/l
$\text{Na}^+$	30.1	mg/l
$\text{Cl}^-$	22.5	mg/l
$\text{NO}_3^-$	2.47	mg/l
$\text{Mg}^{2+}$	70.9	mg/l

Reactants Composition 1 kg of water

$\text{SiO}_2(\text{aq})$	6	mg/l
$\text{Ca}^{2+}$	89.82	mg/l
pH	6.8	s.u.
$\text{SO}_4^{2-}$	102	mg/l
$\text{Na}^+$	7.28	mg/l
$\text{Cl}^-$	22.5	mg/l
$\text{NO}_3^-$	2.47	mg/l
$\text{Mg}^{2+}$	70.9	mg/l
$\text{Fe}^{2+}$	1.E-07	mg/l
$\text{U}^{4+}$	1.E-26	mg/l
$\text{O}_2(\text{aq})$	3.E-71	mg/l
$\text{HCO}_3^-$	628	mg/l

Final Solution Composition - 1 kg of water

Quartz	5.9	kg
Mackinawite	35.23	g
Calcite	569.1	g
Uraninite	32.34	mg
$\text{O}_2(\text{aq})$	3.E-71	mg/l
$\text{HCO}_3^-$	438.5	mg/l
$\text{Ca}^{2+}$	45.41	mg/l
pH	7.035	s.u.
$\text{SO}_4^{2-}$	1.83E-03	mg/l
$\text{HS}^-$	18.71	mg/l
$\text{H}_2\text{S}(\text{aq})$	14.15	mg/l
$\text{Na}^+$	7.22	mg/l
$\text{Cl}^-$	22.34	mg/l
$\text{NH}_4^+$	0.7144	mg/l
$\text{NH}_3$	3.40E-03	mg/l
$\text{Mg}^{2+}$	67.37	mg/l

Main gases produced - fugacities

$\text{CO}_2(\text{g})$	0.03913
$\text{N}_2(\text{g})$	9.41E-07
$\text{S}_2(\text{g})$	4.59E-20
$\text{H}_2\text{S}(\text{g})$	0.00444

Attachment Table 4. Hematite Dissolution, Iron and Uranium Reduction and the Precipitation of Uraninite and Mackinawite, 75 Percent Reactive Iron.

Database file used is Thermo\_mackinawite.dat

Initial Solution Composition - 1 kg of water

Quartz	5.9	kg
Hematite	48.75	g
Calcite	60	g
$\text{UO}_2(\text{CO}_3)_2^{2-}$	33.67	mg
$\text{O}_2(\text{aq})$	8	mg/l
$\text{HCO}_3^-$	638	mg/l
pH	6.8	s.u.
$\text{SO}_4^{2-}$	102	mg/l
$\text{Na}^+$	30.1	mg/l
$\text{Cl}^-$	22.5	mg/l
$\text{NO}_3^-$	2.47	mg/l
$\text{Mg}^{2+}$	70.9	mg/l

Reactants Composition 1 kg of water

$\text{SiO}_2(\text{aq})$	6	mg/l
$\text{Ca}^{2+}$	89.82	mg/l
pH	6.8	s.u.
$\text{SO}_4^{2-}$	102	mg/l
$\text{Na}^+$	7.28	mg/l
$\text{Cl}^-$	22.5	mg/l
$\text{NO}_3^-$	2.47	mg/l
$\text{Mg}^{2+}$	70.9	mg/l
$\text{Fe}^{2+}$	1.E-07	mg/l
$\text{U}^{4+}$	1.E-26	mg/l
$\text{O}_2(\text{aq})$	3.E-71	mg/l
$\text{HCO}_3^-$	628	mg/l

Final Solution Composition - 1 kg of water

Quartz	5.9	kg
Mackinawite	53.67	g
Calcite	574.1	g
Uraninite	32.22	mg
$\text{O}_2(\text{aq})$	3.E-71	mg/l
$\text{HCO}_3^-$	438.7	mg/l
$\text{Ca}^{2+}$	45.03	mg/l
pH	7.038	s.u.
$\text{SO}_4^{2-}$	1.77E-03	mg/l
$\text{HS}^-$	17.96	mg/l
$\text{H}_2\text{S}(\text{aq})$	13.49	mg/l
$\text{Na}^+$	7.22	mg/l
$\text{Cl}^-$	22.34	mg/l
$\text{NH}_4^+$	0.7144	mg/l
$\text{NH}_3$	3.40E-03	mg/l
$\text{Mg}^{2+}$	67.37	mg/l

Main gases produced - fugacities

$\text{CO}_2(\text{g})$	0.03886
$\text{N}_2(\text{g})$	9.55E-07
$\text{S}_2(\text{g})$	4.17E-20
$\text{H}_2\text{S}(\text{g})$	0.004236



Attachment Table 5. Hematite Dissolution, Iron and Uranium Reduction and the Precipitation of Uraninite and Mackinawite, 100 Percent Reactive Iron.

Database file used is Thermo\_mackinawite.dat

Initial Solution Composition - 1 kg of water

Quartz	5.9	kg
Hematite	65	g
Calcite	60	g
$\text{UO}_2(\text{CO}_3)_2^{2-}$	33.67	mg
$\text{O}_2(\text{aq})$	8	mg/l
$\text{HCO}_3^-$	638	mg/l
pH	6.8	s.u.
$\text{SO}_4^{2-}$	102	mg/l
$\text{Na}^+$	30.1	mg/l
$\text{Cl}^-$	22.5	mg/l
$\text{NO}_3^-$	2.47	mg/l
$\text{Mg}^{2+}$	70.9	mg/l

Reactants Composition 1 kg of water

$\text{SiO}_2(\text{aq})$	6	mg/l
$\text{Ca}^{2+}$	89.82	mg/l
pH	6.8	s.u.
$\text{SO}_4^{2-}$	102	mg/l
$\text{Na}^+$	7.28	mg/l
$\text{Cl}^-$	22.5	mg/l
$\text{NO}_3^-$	2.47	mg/l
$\text{Mg}^{2+}$	70.9	mg/l
$\text{Fe}^{2+}$	1.E-07	mg/l
$\text{U}^{4+}$	1.E-26	mg/l
$\text{O}_2(\text{aq})$	3.E-71	mg/l
$\text{HCO}_3^-$	628	mg/l

Final Solution Composition - 1 kg of water

Quartz	5.9	kg
Mackinawite	71.56	g
Calcite	579	g
Uraninite	32.34	mg
$\text{O}_2(\text{aq})$	3.E-71	mg/l
$\text{HCO}_3^-$	438.8	mg/l
$\text{Ca}^{2+}$	44.67	mg/l
pH	7.041	s.u.
$\text{SO}_4^{2-}$	1.71E-03	mg/l
$\text{HS}^-$	17.24	mg/l
$\text{H}_2\text{S}(\text{aq})$	12.85	mg/l
$\text{Na}^+$	7.22	mg/l
$\text{Cl}^-$	22.34	mg/l
$\text{NH}_4^+$	0.7144	mg/l
$\text{NH}_3$	3.40E-03	mg/l
$\text{Mg}^{2+}$	67.37	mg/l

Main gases produced - fugacities

$\text{CO}_2(\text{g})$	0.0386
$\text{N}_2(\text{g})$	9.69E-07
$\text{S}_2(\text{g})$	3.78E-20
$\text{H}_2\text{S}(\text{g})$	0.004036

Attachment Table 6. Hematite Dissolution, Iron and Uranium Reduction and the Precipitation of Uraninite and Mackinawite, 10 Percent Reactive Iron, Allowing Siderite Precipitation.

Database file used is Thermo\_mackinawite.dat

Initial Solution Composition - 1 kg of water

Quartz	5.9	kg
Hematite	6.5	g
Calcite	60	g
$\text{UO}_2(\text{CO}_3)_2^{2-}$	33.67	mg
$\text{O}_2(\text{aq})$	8	mg/l
$\text{HCO}_3^-$	638	mg/l
pH	6.8	s.u.
$\text{SO}_4^{2-}$	102	mg/l
$\text{Na}^+$	30.1	mg/l
$\text{Cl}^-$	22.5	mg/l
$\text{NO}_3^-$	2.47	mg/l
$\text{Mg}^{2+}$	70.9	mg/l

Reactants Composition - 1 kg of water

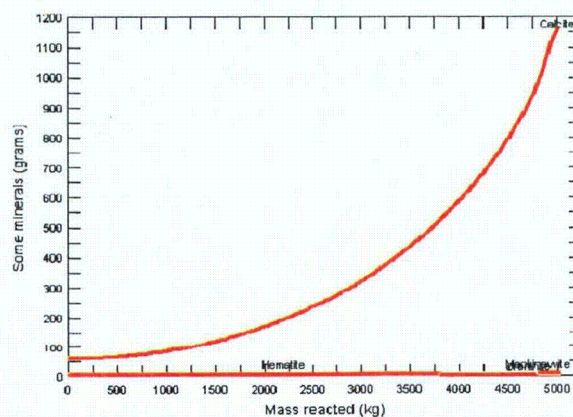
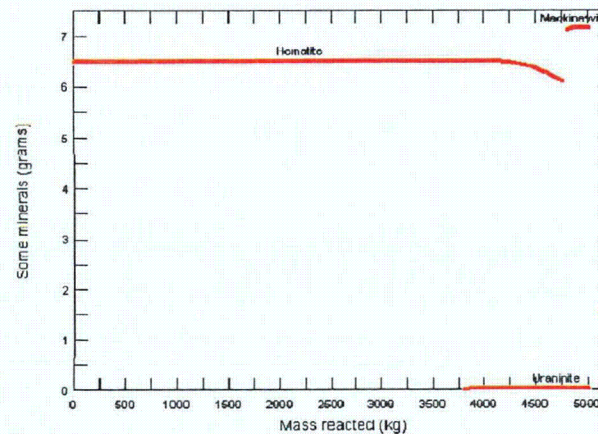
$\text{SiO}_2(\text{aq})$	6	mg/l
$\text{Ca}^{2+}$	89.82	mg/l
pH	6.8	s.u.
$\text{SO}_4^{2-}$	102	mg/l
$\text{Na}^+$	7.28	mg/l
$\text{Cl}^-$	22.5	mg/l
$\text{NO}_3^-$	2.47	mg/l
$\text{Mg}^{2+}$	70.9	mg/l
$\text{Fe}^{2+}$	1.E-07	mg/l
$\text{U}^{4+}$	1.E-26	mg/l
$\text{O}_2(\text{aq})$	3.E-71	mg/l
$\text{HCO}_3^-$	628	mg/l

Final Solution Composition - 1 kg of water

Quartz	5.9	kg
Mackinawite	7.157	g
Calcite	1166	g
Uraninite	32.34	mg
$\text{O}_2(\text{aq})$	3.E-71	mg/l
$\text{HCO}_3^-$	231.1	mg/l
$\text{Ca}^{2+}$	1.209	mg/l
pH	8.856	s.u.
$\text{SO}_4^{2-}$	2.10E-01	mg/l
$\text{HS}^-$	34.09	mg/l
$\text{H}_2\text{S}(\text{aq})$	0.40	mg/l
$\text{Na}^+$	7.247	mg/l
$\text{Cl}^-$	22.43	mg/l
$\text{NH}_4^+$	0.4984	mg/l
$\text{NH}_3$	0.1613	mg/l
$\text{Mg}^{2+}$	64.65	mg/l

Main gases produced - fugacities

$\text{CH}_4(\text{g})$	0.002474
$\text{CO}_2(\text{g})$	0.000316
$\text{N}_2(\text{g})$	2.08E-03
$\text{S}_2(\text{g})$	3.58E-23
$\text{H}_2\text{S}(\text{g})$	0.0001242





Attachment Table 7. Hematite Dissolution, Iron and Uranium Reduction and the Precipitation of Uraninite and Mackinawite, 50 Percent Reactive Iron, Allowing Siderite Precipitation.

Database file used is Thermo\_mackinawite.dat

Initial Solution Composition - 1 kg of water

Quartz	5.9	kg
Hematite	32	g
Calcite	60	g
$\text{UO}_2(\text{CO}_3)_2^{2-}$	33.67	mg
$\text{O}_2(\text{aq})$	8	mg/l
$\text{HCO}_3^-$	638	mg/l
pH	6.8	s.u.
$\text{SO}_4^{2-}$	102	mg/l
$\text{Na}^+$	30.1	mg/l
$\text{Cl}^-$	22.5	mg/l
$\text{NO}_3^-$	2.47	mg/l
$\text{Mg}^{2+}$	70.9	mg/l

Reactants Composition - 1 kg of water

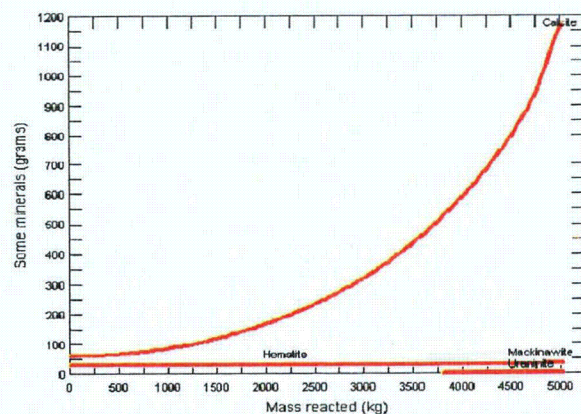
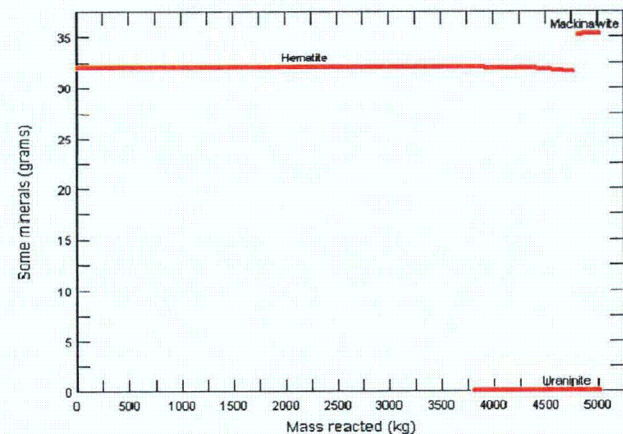
$\text{SiO}_2(\text{aq})$	6	mg/l
$\text{Ca}^{2+}$	89.82	mg/l
pH	6.8	s.u.
$\text{SO}_4^{2-}$	102	mg/l
$\text{Na}^+$	7.28	mg/l
$\text{Cl}^-$	22.5	mg/l
$\text{NO}_3^-$	2.47	mg/l
$\text{Mg}^{2+}$	70.9	mg/l
$\text{Fe}^{2+}$	1.E-07	mg/l
$\text{U}^{4+}$	1.E-26	mg/l
$\text{O}_2(\text{aq})$	3.E-71	mg/l
$\text{HCO}_3^-$	628	mg/l

Final Solution Composition - 1 kg of water

Quartz	5.9	kg
Mackinawite	35.23	g
Calcite	1167	g
Uraninite	32.34	mg
$\text{O}_2(\text{aq})$	3.E-71	mg/l
$\text{HCO}_3^-$	233.9	mg/l
$\text{Ca}^{2+}$	1.18	mg/l
pH	8.861	s.u.
$\text{SO}_4^{2-}$	2.00E-01	mg/l
$\text{HS}^-$	32.01	mg/l
$\text{H}_2\text{S}(\text{aq})$	14.15	mg/l
$\text{Na}^+$	7.247	mg/l
$\text{Cl}^-$	22.43	mg/l
$\text{NH}_4^+$	0.4963	mg/l
$\text{NH}_3$	1.63E-01	mg/l
$\text{Mg}^{2+}$	64.53	mg/l

Main gases produced - fugacities

$\text{CH}_4(\text{g})$	0.002474
$\text{CO}_2(\text{g})$	0.000316
$\text{N}_2(\text{g})$	2.11E-03
$\text{S}_2(\text{g})$	3.08E-23
$\text{H}_2\text{S}(\text{g})$	0.0001152





Attachment Table 8. Hematite Dissolution, Iron and Uranium Reduction and the Precipitation of Uraninite and Mackinawite, 100 Percent Reactive Iron, Allowing Siderite Precipitation.

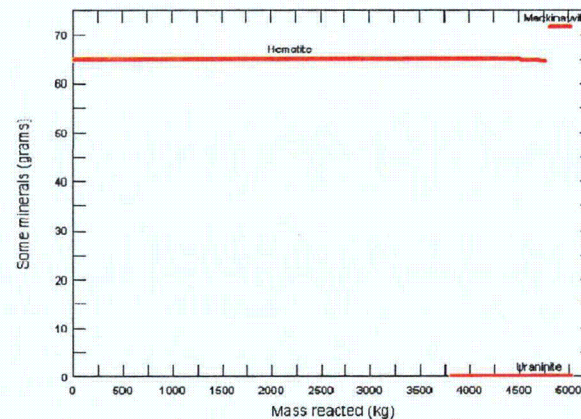
Database file used is Thermo\_mackinawite.dat

Initial Solution Composition - 1 kg of water

Quartz	5.9	kg
Hematite	65	g
Calcite	60	g
$\text{UO}_2(\text{CO}_3)_2^{2-}$	33.67	mg
$\text{O}_2(\text{aq})$	8	mg/l
$\text{HCO}_3^-$	638	mg/l
pH	6.8	s.u.
$\text{SO}_4^{2-}$	102	mg/l
$\text{Na}^+$	30.1	mg/l
$\text{Cl}^-$	22.5	mg/l
$\text{NO}_3^-$	2.47	mg/l
$\text{Mg}^{2+}$	70.9	mg/l

Reactants Composition - 1 kg of water

$\text{SiO}_2(\text{aq})$	6	mg/l
$\text{Ca}^{2+}$	89.82	mg/l
pH	6.8	s.u.
$\text{SO}_4^{2-}$	102	mg/l
$\text{Na}^+$	7.28	mg/l
$\text{Cl}^-$	22.5	mg/l
$\text{NO}_3^-$	2.47	mg/l
$\text{Mg}^{2+}$	70.9	mg/l
$\text{Fe}^{2+}$	1.E-07	mg/l
$\text{U}^{4+}$	1.E-26	mg/l
$\text{O}_2(\text{aq})$	3.E-71	mg/l
$\text{HCO}_3^-$	628	mg/l

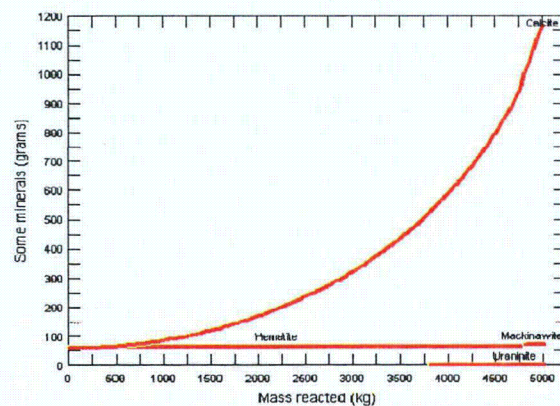


Final Solution Composition - 1 kg of water

Quartz	5.9	kg
Mackinawite	71.57	g
Calcite	1167	g
Uraninite	32.34	mg
$\text{O}_2(\text{aq})$	3.E-71	mg/l
$\text{HCO}_3^-$	237.4	mg/l
$\text{Ca}^{2+}$	1.145	mg/l
pH	8.868	s.u.
$\text{SO}_4^{2-}$	1.85E-01	mg/l
$\text{HS}^-$	29.32	mg/l
$\text{H}_2\text{S}(\text{aq})$	0.33	mg/l
$\text{Na}^+$	7.246	mg/l
$\text{Cl}^-$	22.43	mg/l
$\text{NH}_4^+$	0.4936	mg/l
$\text{NH}_3$	1.64E-01	mg/l
$\text{Mg}^{2+}$	64.38	mg/l

Main gases produced - fugacities

$\text{CH}_4(\text{g})$	0.002474
$\text{CO}_2(\text{g})$	0.000316
$\text{N}_2(\text{g})$	2.16E-03
$\text{S}_2(\text{g})$	2.51E-23
$\text{H}_2\text{S}(\text{g})$	0.000104





Attachment Table 9. Hematite Dissolution, Iron and Uranium Reduction and the Precipitation of Uraninite and Mackinawite, 10 Percent Reactive Iron, All Minerals Unsuppressed Except Uranophane

(When Uranophane unsuppressed- error message: Initial solution is too supersaturated)  
Database file used is Thermo\_mackinawite.dat

Initial Solution Composition- 1 kg of water

Quartz	5.9	kg
Hematite	6.5	g
Calcite	60	g
$\text{UO}_2(\text{CO}_3)_2^{2-}$	33.67	mg
$\text{O}_2(\text{aq})$	8	mg/l
$\text{HCO}_3^-$	638	mg/l
pH	6.8	
$\text{SO}_4^{2-}$	102	mg/l
$\text{Na}^+$	30.1	mg/l
$\text{Cl}^-$	22.5	mg/l
$\text{NO}_3^-$	2.47	mg/l
$\text{Mg}^{2+}$	70.9	mg/l

Reactants Composition- 1 kg of water

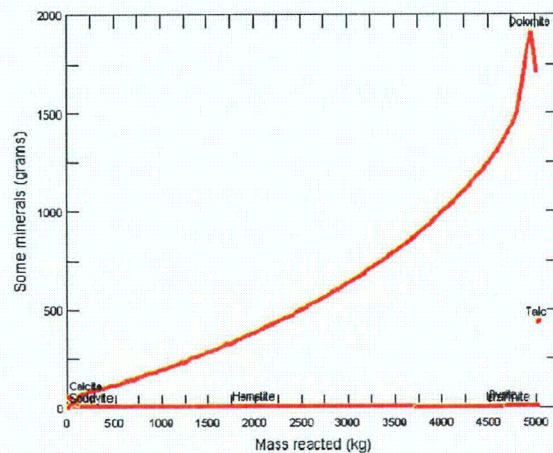
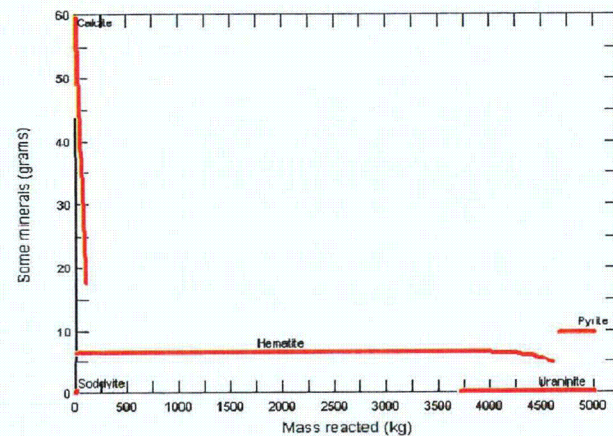
$\text{SiO}_2(\text{aq})$	6	mg/l
$\text{Ca}^{2+}$	89.82	mg/l
pH	6.8	
$\text{SO}_4^{2-}$	102	mg/l
$\text{Na}^+$	7.28	mg/l
$\text{Cl}^-$	22.5	mg/l
$\text{NO}_3^-$	2.47	mg/l
$\text{Mg}^{2+}$	70.9	mg/l
$\text{Fe}^{2+}$	1.E-07	mg/l
$\text{U}^{4+}$	1.E-26	mg/l
$\text{O}_2(\text{aq})$	3.E-71	mg/l
$\text{HCO}_3^-$	628	mg/l

Final Solution Composition- 1 kg of water

Quartz	5.628	kg
Pyrite	9.766	g
Uraninite	32.34	mg
Dolomite	1712	mg/l
Talc	428.7	mg/l
$\text{O}_2(\text{aq})$	3.E-71	mg/l
$\text{HCO}_3^-$	32.45	mg/l
$\text{Ca}^{2+}$	20.15	mg/l
pH	8.019	
$\text{SO}_4^{2-}$	2.53E-02	mg/l
$\text{HS}^-$	31.49	mg/l
$\text{H}_2\text{S}(\text{aq})$	2.61	mg/l
$\text{Na}^+$	7.278	mg/l
$\text{Cl}^-$	22.44	mg/l
$\text{NH}_4^+$	0.681	mg/l
$\text{NH}_3$	0.03334	mg/l
$\text{Mg}^{2+}$	9.24	mg/l

Main gases produced - fugacities

$\text{CH}_4(\text{g})$	0.002474
$\text{CO}_2(\text{g})$	0.000316
$\text{N}_2(\text{g})$	8.89E-05
$\text{S}_2(\text{g})$	1.56E-21
$\text{H}_2\text{S}(\text{g})$	0.0008184



Attachment Table 10. Hematite Dissolution, Iron and Uranium Reduction and the Precipitation of Uraninite and Troilite, 10 Percent Reactive Iron.

Database file used is Thermo\_mackinawite.dat

Initial Solution Composition - 1 kg of water

Quartz	5.9	kg
Hematite	6.5	g
Calcite	60	g
$\text{UO}_2(\text{CO}_3)_2^{2-}$	33.67	mg
$\text{O}_2(\text{aq})$	8	mg/l
$\text{HCO}_3^-$	638	mg/l
pH	6.8	s.u.
$\text{SO}_4^{2-}$	102	mg/l
$\text{Na}^+$	30.1	mg/l
$\text{Cl}^-$	22.5	mg/l
$\text{NO}_3^-$	2.47	mg/l
$\text{Mg}^{2+}$	70.9	mg/l

Reactants Composition - 1 kg of water

$\text{SiO}_2(\text{aq})$	6	mg/l
$\text{Ca}^{2+}$	89.82	mg/l
pH	6.8	s.u.
$\text{SO}_4^{2-}$	102	mg/l
$\text{Na}^+$	7.28	mg/l
$\text{Cl}^-$	22.5	mg/l
$\text{NO}_3^-$	2.47	mg/l
$\text{Mg}^{2+}$	70.9	mg/l
$\text{Fe}^{2+}$	1.E-07	mg/l
$\text{U}^{4+}$	1.E-26	mg/l
$\text{O}_2(\text{aq})$	3.E-71	mg/l
$\text{HCO}_3^-$	628	mg/l

Final Solution Composition - 1 kg of water

Quartz	5.9	kg
Troilite	7.134	g
Calcite	561.6	g
Uraninite	32.34	mg
$\text{O}_2(\text{aq})$	3.E-71	mg/l
$\text{HCO}_3^-$	438	mg/l
$\text{Ca}^{2+}$	45.97	mg/l
pH	6.808	s.u.
$\text{SO}_4^{2-}$	2.E-03	mg/l
$\text{HS}^-$	19.83	mg/l
$\text{H}_2\text{S}(\text{aq})$	15.16	mg/l
$\text{Na}^+$	7.22	mg/l
$\text{Cl}^-$	22.34	mg/l
$\text{NH}_4^+$	0.7145	mg/l
$\text{NH}_3$	3.39E-03	mg/l
$\text{Mg}^{2+}$	67.37	mg/l

Main gases produced - fugacities

$\text{CO}_2(\text{g})$	0.03953
$\text{H}_2\text{S}(\text{g})$	0.004762



Attachment Table 11. Oxidative Dissolution of Mackinawite and Uraninite, 10 Percent Reactive Iron with 1.2 mg/L Dissolved Oxygen.

Database file used is Thermo\_mackinawite.dat

Initial Solution Composition - 1 kg of water

Quartz	5.9	kg
Mackinawite	6.5	g
Calcite	60	g
Uraninite	33.67	mg
O <sub>2</sub> (aq)	3.00E-71	mg/l
HCO <sub>3</sub> <sup>-</sup>	638	mg/l
pH	6.8	s.u.
SO <sub>4</sub> <sup>2-</sup>	102	mg/l
Na <sup>+</sup>	30.1	mg/l
Cl <sup>-</sup>	22.5	mg/l
NO <sub>3</sub> <sup>-</sup>	2.47	mg/l
Mg <sup>2+</sup>	70.9	mg/l

Reactants Composition - 1 kg of water

SiO <sub>2</sub> (aq)	6	mg/l
Ca <sup>2+</sup>	89.82	mg/l
pH	6.8	s.u.
SO <sub>4</sub> <sup>2-</sup>	102	mg/l
Na <sup>+</sup>	7.28	mg/l
Cl <sup>-</sup>	22.5	mg/l
NO <sub>3</sub> <sup>-</sup>	2.47	mg/l
Mg <sup>2+</sup>	70.9	mg/l
Fe <sup>2+</sup>	1.E-07	mg/l
U <sup>4+</sup>	1.E-26	mg/l
O <sub>2</sub> (aq)	1.20	mg/l
HCO <sub>3</sub> <sup>-</sup>	628	mg/l

Final Solution Composition - 1 kg of water

Quartz	5.9	kg
Hematite	5.904	g
Calcite	56.72	g
UO <sub>2</sub> (CO <sub>3</sub> ) <sub>2</sub> <sup>2-</sup>	1.78E-02	mg/l
UO <sub>2</sub> (CO <sub>3</sub> ) <sub>3</sub> <sup>4-</sup>	7.21E-03	mg/l
O <sub>2</sub> (aq)	0.00	mg/l
HCO <sub>3</sub> <sup>-</sup>	459.1	mg/l
Ca <sup>2+</sup>	78.87	mg/l
pH	6.796	s.u.
SO <sub>4</sub> <sup>2-</sup>	79.09	mg/l
Na <sup>+</sup>	7.209	mg/l
Cl <sup>-</sup>	22.29	mg/l
Mg <sup>2+</sup>	64.03	mg/l

Main gases produced - fugacities

CO <sub>2</sub> (g)	0.07025
N <sub>2</sub> (g)	0.02911

All Uraninite dissolves at approx.

1,900 pore volumes

All Hematite is precipitated at approx.

1,900 pore volumes

Attachment Table 12. Oxidative Dissolution of Mackinawite and Uraninite, 25 Percent Reactive Iron with 1.2 mg/L Dissolved Oxygen.

Database file used is Thermo\_mackinawite.dat

Initial Solution Composition - 1 kg of water

Quartz	5.9	kg
Mackinawite	16.25	g
Calcite	60	g
Uraninite	33.67	mg
O <sub>2</sub> (aq)	3.00E-71	mg/l
HCO <sub>3</sub> <sup>-</sup>	638	mg/l
pH	6.8	s.u.
SO <sub>4</sub> <sup>2-</sup>	102	mg/l
Na <sup>+</sup>	30.1	mg/l
Cl <sup>-</sup>	22.5	mg/l
NO <sub>3</sub> <sup>-</sup>	2.47	mg/l
Mg <sup>2+</sup>	70.9	mg/l

Reactants Composition - 1 kg of water

SiO <sub>2</sub> (aq)	6	mg/l
Ca <sup>2+</sup>	89.82	mg/l
pH	6.8	s.u.
SO <sub>4</sub> <sup>2-</sup>	102	mg/l
Na <sup>+</sup>	7.28	mg/l
Cl <sup>-</sup>	22.5	mg/l
NO <sub>3</sub> <sup>-</sup>	2.47	mg/l
Mg <sup>2+</sup>	70.9	mg/l
Fe <sup>2+</sup>	1.E-07	mg/l
U <sup>4+</sup>	1.E-26	mg/l
O <sub>2</sub> (aq)	1.20	mg/l
HCO <sub>3</sub> <sup>-</sup>	628	mg/l

Final Solution Composition - 1 kg of water

Quartz	5.9	kg
Hematite	14.76	g
Calcite	51.87	g
UO <sub>2</sub> (CO <sub>3</sub> ) <sub>2</sub> <sup>2-</sup>	7.13E-03	mg/l
UO <sub>2</sub> (CO <sub>3</sub> ) <sub>3</sub> <sup>4-</sup>	2.89E-03	mg/l
O <sub>2</sub> (aq)	4.67E-06	mg/l
HCO <sub>3</sub> <sup>-</sup>	459.1	mg/l
Ca <sup>2+</sup>	78.87	mg/l
pH	6.796	s.u.
SO <sub>4</sub> <sup>2-</sup>	79.14	mg/l
Na <sup>+</sup>	7.201	mg/l
Cl <sup>-</sup>	22.29	mg/l
NO <sub>3</sub> <sup>2-</sup>	8.12E-02	mg/l
Mg <sup>2+</sup>	64.03	mg/l

Main gases produced - fugacities

CO <sub>2</sub> (g)	0.07025
N <sub>2</sub> (g)	0.02842

All Uraninite dissolves at approx.

4,800 pore volumes

All Hematite is precipitated at approx.

4,800 pore volumes



Attachment Table 13. Oxidative Dissolution of Mackinawite and Uraninite, 50 Percent Reactive Iron with 1.2 mg/L Dissolved Oxygen.

Database file used is Thermo\_mackinawite.dat

Initial Solution Composition - 1 kg of water

Quartz	5.9	kg
Mackinawite	32.58	g
Calcite	60	g
Uraninite	33.67	mg
O <sub>2</sub> (aq)	3.00E-71	mg/l
HCO <sub>3</sub> <sup>-</sup>	638	mg/l
pH	6.8	s.u.
SO <sub>4</sub> <sup>2-</sup>	102	mg/l
Na <sup>+</sup>	30.1	mg/l
Cl <sup>-</sup>	22.5	mg/l
NO <sub>3</sub> <sup>-</sup>	2.47	mg/l
Mg <sup>2+</sup>	70.9	mg/l

Reactants Composition - 1 kg of water

SiO <sub>2</sub> (aq)	6	mg/l
Ca <sup>2+</sup>	89.82	mg/l
pH	6.8	s.u.
SO <sub>4</sub> <sup>2-</sup>	102	mg/l
Na <sup>+</sup>	7.28	mg/l
Cl <sup>-</sup>	22.5	mg/l
NO <sub>3</sub> <sup>-</sup>	2.47	mg/l
Mg <sup>2+</sup>	70.9	mg/l
Fe <sup>2+</sup>	1.E-07	mg/l
U <sup>4+</sup>	1.E-26	mg/l
O <sub>2</sub> (aq)	1.20	mg/l
HCO <sub>3</sub> <sup>-</sup>	628	mg/l

Final Solution Composition - 1 kg of water

Quartz	5.9	kg
Hematite	29.59	g
Calcite	43.92	g
UO <sub>2</sub> (CO <sub>3</sub> ) <sub>2</sub> <sup>2-</sup>	3.71E-03	mg/l
UO <sub>2</sub> (CO <sub>3</sub> ) <sub>3</sub> <sup>4-</sup>	1.50E-03	mg/l
O <sub>2</sub> (aq)	7.23E-09	mg/l
HCO <sub>3</sub> <sup>-</sup>	459.1	mg/l
Ca <sup>2+</sup>	78.87	mg/l
pH	6.796	s.u.
SO <sub>4</sub> <sup>2-</sup>	79.21	mg/l
Na <sup>+</sup>	7.201	mg/l
Cl <sup>-</sup>	22.29	mg/l
NO <sub>3</sub> <sup>2-</sup>	2.29E-03	mg/l
Mg <sup>2+</sup>	64.03	mg/l

Main gases produced - fugacities

CO <sub>2</sub> (g)	0.07026
N <sub>2</sub> (g)	0.03045

All Uraninite dissolves at approx.  
All Hematite is precipitated at approx.

9,000 pore volumes  
9,000 pore volumes

Attachment Table 14. Oxidative Dissolution of Mackinawite and Uraninite, 75 Percent Reactive Iron with 1.2 mg/L Dissolved Oxygen.

Database file used is Thermo\_mackinawite.dat

Initial Solution Composition - 1 kg of water

Quartz	5.9	kg
Mackinawite	48.75	g
Calcite	60	g
Uraninite	33.67	mg
O <sub>2</sub> (aq)	3.00E-71	mg/l
HCO <sub>3</sub> <sup>-</sup>	638	mg/l
pH	6.8	s.u.
SO <sub>4</sub> <sup>2-</sup>	102	mg/l
Na <sup>+</sup>	30.1	mg/l
Cl <sup>-</sup>	22.5	mg/l
NO <sub>3</sub> <sup>-</sup>	2.47	mg/l
Mg <sup>2+</sup>	70.9	mg/l

Reactants Composition - 1 kg of water

SiO <sub>2</sub> (aq)	6	mg/l
Ca <sup>2+</sup>	89.82	mg/l
pH	6.8	s.u.
SO <sub>4</sub> <sup>2-</sup>	102	mg/l
Na <sup>+</sup>	7.28	mg/l
Cl <sup>-</sup>	22.5	mg/l
NO <sub>3</sub> <sup>-</sup>	2.47	mg/l
Mg <sup>2+</sup>	70.9	mg/l
Fe <sup>2+</sup>	1.E-07	mg/l
U <sup>4+</sup>	1.E-26	mg/l
O <sub>2</sub> (aq)	1.20	mg/l
HCO <sub>3</sub> <sup>-</sup>	628	mg/l

Final Solution Composition - 1 kg of water

Quartz	5.9	kg
Hematite	44.28	g
Calcite	35.88	g
UO <sub>2</sub> (CO <sub>3</sub> ) <sub>2</sub> <sup>2-</sup>	2.48E-03	mg/l
UO <sub>2</sub> (CO <sub>3</sub> ) <sub>3</sub> <sup>4-</sup>	1.00E-03	mg/l
O <sub>2</sub> (aq)	3.98E-08	mg/l
HCO <sub>3</sub> <sup>-</sup>	459.1	mg/l
Ca <sup>2+</sup>	78.88	mg/l
pH	6.796	s.u.
SO <sub>4</sub> <sup>2-</sup>	79.20	mg/l
Na <sup>+</sup>	7.201	mg/l
Cl <sup>-</sup>	22.29	mg/l
NO <sub>3</sub> <sup>2-</sup>	1.91E-02	mg/l
Mg <sup>2+</sup>	64.03	mg/l

Main gases produced - fugacities

CO <sub>2</sub> (g)	0.07026
N <sub>2</sub> (g)	0.03024

All Uraninite dissolves at approx.

14,000 pore volumes

All Hematite is precipitated at approx.

14,000 pore volumes



Attachment Table 15. Oxidative Dissolution of Mackinawite and Uraninite, 100 Percent Reactive Iron with 1.2 mg/L Dissolved Oxygen.

Database file used is Thermo\_mackinawite.dat

Initial Solution Composition - 1 kg of water

Quartz	5.9	kg
Mackinawite	65	g
Calcite	60	g
Uraninite	33.67	mg
O <sub>2</sub> (aq)	3.00E-71	mg/l
HCO <sub>3</sub> <sup>-</sup>	638	mg/l
pH	6.8	s.u.
SO <sub>4</sub> <sup>2-</sup>	102	mg/l
Na <sup>+</sup>	30.1	mg/l
Cl <sup>-</sup>	22.5	mg/l
NO <sub>3</sub> <sup>-</sup>	2.47	mg/l
Mg <sup>2+</sup>	70.9	mg/l

Reactants Composition - 1 kg of water

SiO <sub>2</sub> (aq)	6	mg/l
Ca <sup>2+</sup>	89.82	mg/l
pH	6.8	s.u.
SO <sub>4</sub> <sup>2-</sup>	102	mg/l
Na <sup>+</sup>	7.28	mg/l
Cl <sup>-</sup>	22.5	mg/l
NO <sub>3</sub> <sup>-</sup>	2.47	mg/l
Mg <sup>2+</sup>	70.9	mg/l
Fe <sup>2+</sup>	1.E-07	mg/l
U <sup>4+</sup>	1.E-26	mg/l
O <sub>2</sub> (aq)	1.20	mg/l
HCO <sub>3</sub> <sup>-</sup>	628	mg/l

Final Solution Composition - 1 kg of water

Quartz	5.9	kg
Hematite	59.04	g
Calcite	26.91	g
UO <sub>2</sub> (CO <sub>3</sub> ) <sub>2</sub> <sup>2-</sup>	1.86E-03	mg/l
UO <sub>2</sub> (CO <sub>3</sub> ) <sub>3</sub> <sup>4-</sup>	7.52E-04	mg/l
O <sub>2</sub> (aq)	4.50E-08	mg/l
HCO <sub>3</sub> <sup>-</sup>	459.1	mg/l
Ca <sup>2+</sup>	78.88	mg/l
pH	6.796	s.u.
SO <sub>4</sub> <sup>2-</sup>	79.09	mg/l
Na <sup>+</sup>	7.201	mg/l
Cl <sup>-</sup>	22.29	mg/l
NO <sub>3</sub> <sup>2-</sup>	1.93E-01	mg/l
Mg <sup>2+</sup>	64.03	mg/l

Main gases produced - fugacities

CO <sub>2</sub> (g)	0.07026
N <sub>2</sub> (g)	0.0302

All Uraninite dissolves at approx.

19,000 pore volumes

All Hematite is precipitated at approx.

19,000 pore volumes

Attachment Table 16. Oxidative Dissolution of Mackinawite and Uraninite, 10 Percent Reactive Iron with 8 mg/L Dissolved Oxygen.

Database file used is Thermo\_mackinawite.dat

Initial Solution Composition - 1 kg of water

Quartz	5.9	kg
Mackinawite	6.5	g
Calcite	60	g
Uraninite	33.67	mg
O <sub>2</sub> (aq)	3.00E-71	mg/l
HCO <sub>3</sub> <sup>-</sup>	638	mg/l
pH	6.8	s.u.
SO <sub>4</sub> <sup>2-</sup>	102	mg/l
Na <sup>+</sup>	30.1	mg/l
Cl <sup>-</sup>	22.5	mg/l
NO <sub>3</sub> <sup>-</sup>	2.47	mg/l
Mg <sup>2+</sup>	70.9	mg/l

Reactants Composition - 1 kg of water

SiO <sub>2</sub> (aq)	6	mg/l
Ca <sup>2+</sup>	89.82	mg/l
pH	6.8	s.u.
SO <sub>4</sub> <sup>2-</sup>	102	mg/l
Na <sup>+</sup>	7.28	mg/l
Cl <sup>-</sup>	22.5	mg/l
NO <sub>3</sub> <sup>-</sup>	2.47	mg/l
Mg <sup>2+</sup>	70.9	mg/l
Fe <sup>2+</sup>	1.E-07	mg/l
U <sup>4+</sup>	1.E-26	mg/l
O <sub>2</sub> (aq)	8	mg/l
HCO <sub>3</sub> <sup>-</sup>	628	mg/l

Final Solution Composition - 1 kg of water

Quartz	5.9	kg
Hematite	5.904	g
Calcite	53.12	g
UO <sub>2</sub> (CO <sub>3</sub> ) <sub>2</sub> <sup>2-</sup>	6.00E-02	mg/l
UO <sub>2</sub> (CO <sub>3</sub> ) <sub>3</sub> <sup>4-</sup>	2.40E-02	mg/l
O <sub>2</sub> (aq)	6.90	mg/l
HCO <sub>3</sub> <sup>-</sup>	459.4	mg/l
Ca <sup>2+</sup>	81.98	mg/l
pH	6.781	s.u.
SO <sub>4</sub> <sup>2-</sup>	85.07	mg/l
Na <sup>+</sup>	7.234	mg/l
Cl <sup>-</sup>	22.28	mg/l
NO <sub>3</sub> <sup>-</sup>	0.80	mg/l
Mg <sup>2+</sup>	63.82	mg/l

Main gases produced - fugacities

CO <sub>2</sub> (g)	0.07274
N <sub>2</sub> (g)	0.02052
O <sub>2</sub> (g)	2.35E-08

All Uraninite dissolves at approx.

550 pore volumes

All Hematite is precipitated at approx.

550 pore volumes

Attachment Table 17. Oxidative Dissolution of Mackinawite and Uraninite, 25 Percent Reactive Iron with 8 mg/L Dissolved Oxygen.

Database file used is Thermo\_mackinawite.dat

Initial Solution Composition - 1 kg of water

Quartz	5.9	kg
Mackinawite	16.25	g
Calcite	60	g
Uraninite	33.67	mg
O <sub>2</sub> (aq)	3.00E-71	mg/l
HCO <sub>3</sub> <sup>-</sup>	638	mg/l
pH	6.8	s.u.
SO <sub>4</sub> <sup>2-</sup>	102	mg/l
Na <sup>+</sup>	30.1	mg/l
Cl <sup>-</sup>	22.5	mg/l
NO <sub>3</sub> <sup>-</sup>	2.47	mg/l
Mg <sup>2+</sup>	70.9	mg/l

Reactants Composition - 1 kg of water

SiO <sub>2</sub> (aq)	6	mg/l
Ca <sup>2+</sup>	89.82	mg/l
pH	6.8	s.u.
SO <sub>4</sub> <sup>2-</sup>	102	mg/l
Na <sup>+</sup>	7.28	mg/l
Cl <sup>-</sup>	22.5	mg/l
NO <sub>3</sub> <sup>-</sup>	2.47	mg/l
Mg <sup>2+</sup>	70.9	mg/l
Fe <sup>2+</sup>	1.E-07	mg/l
U <sup>4+</sup>	1.E-26	mg/l
O <sub>2</sub> (aq)	8	mg/l
HCO <sub>3</sub> <sup>-</sup>	628	mg/l

Final Solution Composition - 1 kg of water

Quartz	5.9	kg
Hematite	14.76	g
Calcite	43.75	g
UO <sub>2</sub> (CO <sub>3</sub> ) <sub>2</sub> <sup>2-</sup>	2.26E-02	mg/l
UO <sub>2</sub> (CO <sub>3</sub> ) <sub>3</sub> <sup>4-</sup>	1.00E-02	mg/l
O <sub>2</sub> (aq)	9.18E-09	mg/l
HCO <sub>3</sub> <sup>-</sup>	459.4	mg/l
Ca <sup>2+</sup>	82	mg/l
pH	6.781	s.u.
SO <sub>4</sub> <sup>2-</sup>	85.71	mg/l
Na <sup>+</sup>	7.213	mg/l
Cl <sup>-</sup>	22.28	mg/l
NO <sub>3</sub> <sup>2-</sup>	2.97E-03	mg/l
Mg <sup>2+</sup>	63.8	mg/l

Main gases produced - fugacities

CO <sub>2</sub> (g)	0.07277
N <sub>2</sub> (g)	0.03044

All Uraninite dissolves at approx.

1,370 pore volumes

All Hematite is precipitated at approx.

1,370 pore volumes



Attachment Table 18. Oxidative Dissolution of Mackinawite and Uraninite, 50 Percent Reactive Iron with 8 mg/L Dissolved Oxygen.

Database file used is Thermo\_mackinawite.dat

Initial Solution Composition - 1 kg of water

Quartz	5.9	kg
Mackinawite	32.58	g
Calcite	60	g
Uraninite	33.67	mg
O <sub>2</sub> (aq)	3.00E-71	mg/l
HCO <sub>3</sub> <sup>-</sup>	638	mg/l
pH	6.8	s.u.
SO <sub>4</sub> <sup>2-</sup>	102	mg/l
Na <sup>+</sup>	30.1	mg/l
Cl <sup>-</sup>	22.5	mg/l
NO <sub>3</sub> <sup>-</sup>	2.47	mg/l
Mg <sup>2+</sup>	70.9	mg/l

Reactants Composition - 1 kg of water

SiO <sub>2</sub> (aq)	6	mg/l
Ca <sup>2+</sup>	89.82	mg/l
pH	6.8	s.u.
SO <sub>4</sub> <sup>2-</sup>	102	mg/l
Na <sup>+</sup>	7.28	mg/l
Cl <sup>-</sup>	22.5	mg/l
NO <sub>3</sub> <sup>-</sup>	2.47	mg/l
Mg <sup>2+</sup>	70.9	mg/l
Fe <sup>2+</sup>	1.E-07	mg/l
U <sup>4+</sup>	1.E-26	mg/l
O <sub>2</sub> (aq)	8	mg/l
HCO <sub>3</sub> <sup>-</sup>	628	mg/l

Final Solution Composition - 1 kg of water

Quartz	5.9	kg
Hematite	29.59	g
Calcite	27.45	g
UO <sub>2</sub> (CO <sub>3</sub> ) <sub>2</sub> <sup>2-</sup>	1.28E-02	mg/l
UO <sub>2</sub> (CO <sub>3</sub> ) <sub>3</sub> <sup>4-</sup>	5.06E-03	mg/l
O <sub>2</sub> (aq)	6.27E-08	mg/l
HCO <sub>3</sub> <sup>-</sup>	459.4	mg/l
Ca <sup>2+</sup>	82.01	mg/l
pH	6.781	s.u.
SO <sub>4</sub> <sup>2-</sup>	85.74	mg/l
Na <sup>+</sup>	7.205	mg/l
Cl <sup>-</sup>	22.28	mg/l
NO <sub>3</sub> <sup>2-</sup>	0.03	mg/l
Mg <sup>2+</sup>	63.8	mg/l

Main gases produced - fugacities

CO <sub>2</sub> (g)	0.07278
N <sub>2</sub> (g)	0.03008

All Uraninite dissolves at approx.

2,750 pore volumes

All Hematite is precipitated at approx.

2,750 pore volumes

Attachment Table 19. Oxidative Dissolution of Mackinawite and Uraninite, 75 Percent Reactive Iron with 8 mg/L Dissolved Oxygen.

Database file used is Thermo\_mackinawite.dat

Initial Solution Composition - 1 kg of water

Quartz	5.9	kg
Mackinawite	48.75	g
Calcite	60	g
Uraninite	33.67	mg
O <sub>2</sub> (aq)	3.00E-71	mg/l
HCO <sub>3</sub> <sup>-</sup>	638	mg/l
pH	6.8	s.u.
SO <sub>4</sub> <sup>2-</sup>	102	mg/l
Na <sup>+</sup>	30.1	mg/l
Cl <sup>-</sup>	22.5	mg/l
NO <sub>3</sub> <sup>-</sup>	2.47	mg/l
Mg <sup>2+</sup>	70.9	mg/l

Reactants Composition - 1 kg of water

SiO <sub>2</sub> (aq)	6	mg/l
Ca <sup>2+</sup>	89.82	mg/l
pH	6.8	s.u.
SO <sub>4</sub> <sup>2-</sup>	102	mg/l
Na <sup>+</sup>	7.28	mg/l
Cl <sup>-</sup>	22.5	mg/l
NO <sub>3</sub> <sup>-</sup>	2.47	mg/l
Mg <sup>2+</sup>	70.9	mg/l
Fe <sup>2+</sup>	1.E-07	mg/l
U <sup>4+</sup>	1.E-26	mg/l
O <sub>2</sub> (aq)	8	mg/l
HCO <sub>3</sub> <sup>-</sup>	628	mg/l

Final Solution Composition - 1 kg of water

Quartz	5.9	kg
Hematite	44.28	g
Calcite	11.18	g
UO <sub>2</sub> (CO <sub>3</sub> ) <sub>2</sub> <sup>2-</sup>	8.54E-03	mg/l
UO <sub>2</sub> (CO <sub>3</sub> ) <sub>3</sub> <sup>4-</sup>	3.37E-03	mg/l
O <sub>2</sub> (aq)	1.43E-07	mg/l
HCO <sub>3</sub> <sup>-</sup>	459.4	mg/l
Ca <sup>2+</sup>	82.01	mg/l
pH	6.781	s.u.
SO <sub>4</sub> <sup>2-</sup>	85.72	mg/l
Na <sup>+</sup>	7.202	mg/l
Cl <sup>-</sup>	22.28	mg/l
NO <sub>3</sub> <sup>2-</sup>	0.09	mg/l
Mg <sup>2+</sup>	63.8	mg/l

Main gases produced - fugacities

CO <sub>2</sub> (g)	0.07278
N <sub>2</sub> (g)	0.02936

All Uraninite dissolves at approx.

4,200 pore volumes

All Hematite is precipitated at approx.

4,200 pore volumes

Attachment Table 20. Oxidative Dissolution of Mackinawite and Uraninite, 100 Percent Reactive Iron with 8 mg/L Dissolved Oxygen.

Database file used is Thermo\_mackinawite.dat

Initial Solution Composition - 1 kg of water

Quartz	5.9	kg
Mackinawite	65	g
Calcite	60	g
Uraninite	33.67	mg
O <sub>2</sub> (aq)	3.00E-71	mg/l
HCO <sub>3</sub> <sup>-</sup>	638	mg/l
pH	6.8	s.u.
SO <sub>4</sub> <sup>2-</sup>	102	mg/l
Na <sup>+</sup>	30.1	mg/l
Cl <sup>-</sup>	22.5	mg/l
NO <sub>3</sub> <sup>-</sup>	2.47	mg/l
Mg <sup>2+</sup>	70.9	mg/l

Reactants Composition - 1 kg of water

SiO <sub>2</sub> (aq)	6	mg/l
Ca <sup>2+</sup>	89.82	mg/l
pH	6.8	s.u.
SO <sub>4</sub> <sup>2-</sup>	102	mg/l
Na <sup>+</sup>	7.28	mg/l
Cl <sup>-</sup>	22.5	mg/l
NO <sub>3</sub> <sup>-</sup>	2.47	mg/l
Mg <sup>2+</sup>	70.9	mg/l
Fe <sup>2+</sup>	1.E-07	mg/l
U <sup>4+</sup>	1.E-26	mg/l
O <sub>2</sub> (aq)	8	mg/l
HCO <sub>3</sub> <sup>-</sup>	628	mg/l

Final Solution Composition - 1 kg of water

Quartz	5.9	kg
Hematite	59.04	g
Calcite	ND	
UO <sub>2</sub> (CO <sub>3</sub> ) <sub>2</sub> <sup>2-</sup>	6.44E-03	mg/l
UO <sub>2</sub> (CO <sub>3</sub> ) <sub>3</sub> <sup>4-</sup>	2.52E-03	mg/l
O <sub>2</sub> (aq)	8.73E-08	mg/l
HCO <sub>3</sub> <sup>-</sup>	458.5	mg/l
Ca <sup>2+</sup>	81.71	mg/l
pH	6.778	s.u.
SO <sub>4</sub> <sup>2-</sup>	85.78	mg/l
Na <sup>+</sup>	7.201	mg/l
Cl <sup>-</sup>	22.28	mg/l
NO <sub>3</sub> <sup>2-</sup>	0.05	mg/l
Mg <sup>2+</sup>	63.8	mg/l

Main gases produced - fugacities

CO <sub>2</sub> (g)	0.07303
N <sub>2</sub> (g)	0.02987

All Uraninite dissolves at approx.

5,500 pore volumes

All Hematite is precipitated at approx.

5,500 pore volumes



Attachment Table 21. Oxidative Dissolution of Mackinawite and Uraninite, 100 Percent Reactive Iron with 1.2 mg/L Dissolved Oxygen and 0.5 Percent Calcite.

Database file used is Thermo\_mackinawite.dat

Initial Solution Composition - 1 kg of water

Quartz	5.9	kg
Mackinawite	65	g
Calcite	30	g
Uraninite	33.67	mg
O <sub>2</sub> (aq)	3.00E-71	mg/l
HCO <sub>3</sub> <sup>-</sup>	638	mg/l
pH	6.8	s.u.
SO <sub>4</sub> <sup>2-</sup>	102	mg/l
Na <sup>+</sup>	30.1	mg/l
Cl <sup>-</sup>	22.5	mg/l
NO <sub>3</sub> <sup>-</sup>	2.47	mg/l
Mg <sup>2+</sup>	70.9	mg/l

Reactants Composition - 1 kg of water

SiO <sub>2</sub> (aq)	6	mg/l
Ca <sup>2+</sup>	89.82	mg/l
pH	6.8	s.u.
SO <sub>4</sub> <sup>2-</sup>	102	mg/l
Na <sup>+</sup>	7.28	mg/l
Cl <sup>-</sup>	22.5	mg/l
NO <sub>3</sub> <sup>-</sup>	2.47	mg/l
Mg <sup>2+</sup>	70.9	mg/l
Fe <sup>2+</sup>	1.E-07	mg/l
U <sup>4+</sup>	1.E-26	mg/l
O <sub>2</sub> (aq)	1.20	mg/l
HCO <sub>3</sub> <sup>-</sup>	628	mg/l

Final Solution Composition - 1 kg of water

Quartz	5.9	kg
Hematite	59.04	g
Calcite	ND	
UO <sub>2</sub> (CO <sub>3</sub> ) <sub>2</sub> <sup>2-</sup>	1.78E-03	mg/l
UO <sub>2</sub> (CO <sub>3</sub> ) <sub>3</sub> <sup>4-</sup>	7.21E-04	mg/l
O <sub>2</sub> (aq)	2.60E-07	mg/l
HCO <sub>3</sub> <sup>-</sup>	459.1	mg/l
Ca <sup>2+</sup>	78.88	mg/l
pH	6.796	s.u.
SO <sub>4</sub> <sup>2-</sup>	79.09	mg/l
Na <sup>+</sup>	7.201	mg/l
Cl <sup>-</sup>	22.29	mg/l
NO <sub>3</sub> <sup>2-</sup>	1.93E-01	mg/l
Mg <sup>2+</sup>	64.03	mg/l

Main gases produced - fugacities

CO <sub>2</sub> (g)	0.0703
N <sub>2</sub> (g)	0.02808

All Uraninite dissolves at approx.

19,000 pore volumes

All Hematite is precipitated at approx.

19,000 pore volumes

Attachment Table 22. Oxidative Dissolution of Mackinawite and Uraninite, 100 Percent Reactive Iron with 1.2 mg/L Dissolved Oxygen and Average TIC.

Database file used is Thermo\_mackinawite.dat

Initial Solution Composition - 1 kg of water

Quartz	5.9	kg
Mackinawite	65	g
Calcite	60	g
Uraninite	33.67	mg
O <sub>2</sub> (aq)	3.00E-71	mg/l
HCO <sub>3</sub> <sup>-</sup>	298	mg/l
pH	6.8	s.u.
SO <sub>4</sub> <sup>2-</sup>	102	mg/l
Na <sup>+</sup>	30.1	mg/l
Cl <sup>-</sup>	22.5	mg/l
NO <sub>3</sub> <sup>-</sup>	2.47	mg/l
Mg <sup>2+</sup>	70.9	mg/l

Reactants Composition - 1 kg of water

SiO <sub>2</sub> (aq)	6	mg/l
Ca <sup>2+</sup>	89.82	mg/l
pH	6.8	s.u.
SO <sub>4</sub> <sup>2-</sup>	102	mg/l
Na <sup>+</sup>	7.28	mg/l
Cl <sup>-</sup>	22.5	mg/l
NO <sub>3</sub> <sup>-</sup>	2.47	mg/l
Mg <sup>2+</sup>	70.9	mg/l
Fe <sup>2+</sup>	1.E-07	mg/l
U <sup>4+</sup>	1.E-26	mg/l
O <sub>2</sub> (aq)	1.20	mg/l
HCO <sub>3</sub> <sup>-</sup>	298	mg/l

Final Solution Composition - 1 kg of water

Quartz	5.9	kg
Hematite	59.04	g
Calcite	ND	
UO <sub>2</sub> (CO <sub>3</sub> ) <sub>2</sub> <sup>2-</sup>	2.19E-03	mg/l
UO <sub>2</sub> (CO <sub>3</sub> ) <sub>3</sub> <sup>4-</sup>	8.05E-05	mg/l
O <sub>2</sub> (aq)	1.22E-07	mg/l
HCO <sub>3</sub> <sup>-</sup>	144.1	mg/l
Ca <sup>2+</sup>	83.21	mg/l
pH	6.3	s.u.
SO <sub>4</sub> <sup>2-</sup>	77.11	mg/l
Na <sup>+</sup>	7.24	mg/l
Cl <sup>-</sup>	22.29	mg/l
NO <sub>3</sub> <sup>2-</sup>	2.44E-02	mg/l
Mg <sup>2+</sup>	66.01	mg/l

Main gases produced - fugacities

CO <sub>2</sub> (g)	0.06959
N <sub>2</sub> (g)	0.03018

All Uraninite dissolves at approx.

19,000 pore volumes

All Hematite is precipitated at approx.

19,000 pore volumes

Attachment Table 23. Oxidative Dissolution of Mackinawite and Uraninite, 100 Percent Reactive Iron with 1.2 mg/L Dissolved Oxygen at pH 5.0 s.u.

Database file used is Thermo\_mackinawite.dat

Initial Solution Composition - 1 kg of water

Quartz	5.9	kg
Mackinawite	65	g
Calcite	60	g
Uraninite	33.67	mg
O <sub>2</sub> (aq)	3.00E-71	mg/l
HCO <sub>3</sub> <sup>-</sup>	638	mg/l
pH	5	s.u.
SO <sub>4</sub> <sup>2-</sup>	102	mg/l
Na <sup>+</sup>	30.1	mg/l
Cl <sup>-</sup>	22.5	mg/l
NO <sub>3</sub> <sup>-</sup>	2.47	mg/l
Mg <sup>2+</sup>	70.9	mg/l

Reactants Composition - 1 kg of water

SiO <sub>2</sub> (aq)	6	mg/l
Ca <sup>2+</sup>	89.82	mg/l
pH	5	s.u.
SO <sub>4</sub> <sup>2-</sup>	102	mg/l
Na <sup>+</sup>	7.28	mg/l
Cl <sup>-</sup>	22.5	mg/l
NO <sub>3</sub> <sup>-</sup>	2.47	mg/l
Mg <sup>2+</sup>	70.9	mg/l
Fe <sup>2+</sup>	1.E-07	mg/l
U <sup>4+</sup>	1.E-26	mg/l
O <sub>2</sub> (aq)	1.20	mg/l
HCO <sub>3</sub> <sup>-</sup>	628	mg/l

Final Solution Composition - 1 kg of water

Quartz	5.9	kg
Hematite	59.04	g
Calcite	ND	
UO <sub>2</sub> (CO <sub>3</sub> ) <sub>2</sub> <sup>2-</sup>	8.72E-04	mg/l
UO <sub>2</sub> (CO <sub>3</sub> )	6.01E-04	mg/l
O <sub>2</sub> (aq)	1.03E-05	mg/l
HCO <sub>3</sub> <sup>-</sup>	458.1	mg/l
Ca <sup>2+</sup>	78.46	mg/l
pH	4.964	s.u.
SO <sub>4</sub> <sup>2-</sup>	77.57	mg/l
Na <sup>+</sup>	7.124	mg/l
Cl <sup>-</sup>	22.06	mg/l
NO <sub>3</sub> <sup>2-</sup>	2.74E-01	mg/l
Mg <sup>2+</sup>	63.44	mg/l

Main gases produced - fugacities

CO <sub>2</sub> (g)	4.832
N <sub>2</sub> (g)	0.02695

All Uraninite dissolves at approx.  
All Hematite is precipitated at approx.

26,000 pore volumes  
27,500 pore volumes



Attachment Table 24. Oxidative Dissolution of Mackinawite and Uraninite, 100 Percent Reactive Iron with 1.2 mg/L Dissolved Oxygen at pH 7.5 s.u.

Database file used is Thermo\_mackinawite.dat

Initial Solution Composition - 1 kg of water

Quartz	5.9	kg
Mackinawite	65	g
Calcite	60	g
Uraninite	33.67	mg
O <sub>2</sub> (aq)	3.00E-71	mg/l
HCO <sub>3</sub> <sup>-</sup>	638	mg/l
pH	7.5	s.u.
SO <sub>4</sub> <sup>2-</sup>	102	mg/l
Na <sup>+</sup>	30.1	mg/l
Cl <sup>-</sup>	22.5	mg/l
NO <sub>3</sub> <sup>-</sup>	2.47	mg/l
Mg <sup>2+</sup>	70.9	mg/l

Reactants Composition - 1 kg of water

SiO <sub>2</sub> (aq)	6	mg/l
Ca <sup>2+</sup>	89.82	mg/l
pH	7.5	s.u.
SO <sub>4</sub> <sup>2-</sup>	102	mg/l
Na <sup>+</sup>	7.28	mg/l
Cl <sup>-</sup>	22.5	mg/l
NO <sub>3</sub> <sup>-</sup>	2.47	mg/l
Mg <sup>2+</sup>	70.9	mg/l
Fe <sup>2+</sup>	1.E-07	mg/l
U <sup>4+</sup>	1.E-26	mg/l
O <sub>2</sub> (aq)	1.20	mg/l
HCO <sub>3</sub> <sup>-</sup>	628	mg/l

Final Solution Composition - 1 kg of water

Quartz	5.9	kg
Hematite	59.04	g
Calcite	1833	g
UO <sub>2</sub> (CO <sub>3</sub> ) <sub>2</sub> <sup>2-</sup>	1.62E-03	mg/l
UO <sub>2</sub> (CO <sub>3</sub> )	1.04E-03	mg/l
O <sub>2</sub> (aq)	3.33E-08	mg/l
HCO <sub>3</sub> <sup>-</sup>	464.1	mg/l
Ca <sup>2+</sup>	45.74	mg/l
pH	7.017	s.u.
SO <sub>4</sub> <sup>2-</sup>	82.67	mg/l
Na <sup>+</sup>	7.198	mg/l
Cl <sup>-</sup>	22.35	mg/l
NO <sub>3</sub> <sup>2-</sup>	2.53E-02	mg/l
Mg <sup>2+</sup>	63.63	mg/l

Main gases produced - fugacities

CO <sub>2</sub> (g)	0.04293
N <sub>2</sub> (g)	0.03017

All Uraninite dissolves at approx.

18,500 pore volum

All Hematite is precipitated at approx.

18,500 pore volum

Attachment Table 25. Oxidative Dissolution of Troilite and Uraninite, 10 Percent Reactive Iron with 8 mg/L Dissolved Oxygen.

Database file used is Thermo\_mackinawite.dat

Initial Solution Composition - 1 kg of water

Quartz	5.9	kg
Troilite	6.5	g
Calcite	60	g
Uraninite	33.67	mg
O <sub>2</sub> (aq)	3.00E-71	mg/l
HCO <sub>3</sub> <sup>-</sup>	638	mg/l
pH	6.8	s.u.
SO <sub>4</sub> <sup>2-</sup>	102	mg/l
Na <sup>+</sup>	30.1	mg/l
Cl <sup>-</sup>	22.5	mg/l
NO <sub>3</sub> <sup>-</sup>	2.47	mg/l
Mg <sup>2+</sup>	70.9	mg/l

Reactants Composition - 1 kg of water

SiO <sub>2</sub> (aq)	6	mg/l
Ca <sup>2+</sup>	89.82	mg/l
pH	6.8	s.u.
SO <sub>4</sub> <sup>2-</sup>	102	mg/l
Na <sup>+</sup>	7.28	mg/l
Cl <sup>-</sup>	22.5	mg/l
NO <sub>3</sub> <sup>-</sup>	2.47	mg/l
Mg <sup>2+</sup>	70.9	mg/l
Fe <sup>2+</sup>	1.E-07	mg/l
U <sup>4+</sup>	1.E-26	mg/l
O <sub>2</sub> (aq)	8	mg/l
HCO <sub>3</sub> <sup>-</sup>	628	mg/l

Final Solution Composition - 1 kg of water

Quartz	5.9	kg
Hematite	5.904	g
Calcite	53.96	g
• U in fluid	2.40E-02	mg/l
O <sub>2</sub> (aq)	6.90	mg/l
HCO <sub>3</sub> <sup>-</sup>	459	mg/l
Ca <sup>2+</sup>	78.79	mg/l
pH	6.796	s.u.
SO <sub>4</sub> <sup>2-</sup>	77.48	mg/l
Na <sup>+</sup>	7.203	mg/l
Cl <sup>-</sup>	22.29	mg/l
NO <sub>3</sub> <sup>2-</sup>	2.44	mg/l
Mg <sup>2+</sup>	64.09	mg/l

Main gases produced - fugacities

CO <sub>2</sub> (g)	0.07017
N <sub>2</sub> (g)	1.24E-18
O <sub>2</sub> (g)	1.72E-01

All Uraninite dissolves at approx.

All Hematite is precipitated at approx.

550 pore volumes

600 pore volumes

Attachment Table 26. Oxidative Dissolution of Mackinawite and Uraninite at 40 Feet, 100 Percent Reactive Iron with 8 mg/L Dissolved Oxygen.

Database file used is Thermo\_mackinawite.dat

Initial Solution Composition- 1 kg of water

Quartz	6.83	kg
Mackinawite	69.67	g
Calcite	69.67	g
Uraninite	7.27	g
O <sub>2</sub> (aq)	3.00E-71	mg/l
HCO <sub>3</sub> <sup>-</sup>	638	mg/l
pH	6.8	s.u.
SO <sub>4</sub> <sup>2-</sup>	102	mg/l
Na <sup>+</sup>	30.1	mg/l
Cl <sup>-</sup>	22.5	mg/l
NO <sub>3</sub> <sup>-</sup>	2.47	mg/l
Mg <sup>2+</sup>	70.9	mg/l

Incoming Solution Composition- 1kg of water

SiO <sub>2</sub> (aq)	6	mg/l
Ca <sup>2+</sup>	90	mg/l
pH	6.8	s.u.
SO <sub>4</sub> <sup>2-</sup>	102	mg/l
Na <sup>+</sup>	7.28	mg/l
Cl <sup>-</sup>	22.5	mg/l
NO <sub>3</sub> <sup>-</sup>	2.47	mg/l
Mg <sup>2+</sup>	70.9	mg/l
Fe <sup>2+</sup>	1.E-07	mg/l
U <sup>4+</sup>	1.E-26	mg/l
O <sub>2</sub> (aq)	8	mg/l
HCO <sub>3</sub> <sup>-</sup>	628	mg/l

Hydrology and Transport information

Time ended	25925	years
Length	12.19	m
Width	1	m
Height	1	m
Specific Discharge	0.002275	m/day
Diffusion Coefficient	1.00E-06	cm <sup>2</sup> /sec
Porosity	0.25	Volume Fraction
Longitudinal Dispersivity	0.1	m
# of nodes	1	
groundwater velocity	0.03	ft/day

Final Solution Composition- 1 kg of water

Quartz	6.83	kg
Hematite	30.96	g
Calcite	39.94	g
• U in fluid	110	mg/l
O <sub>2</sub> (aq)	5.72E-01	mg/l
HCO <sub>3</sub> <sup>-</sup>	424.1	mg/l
Ca <sup>2+</sup>	88.53	mg/l
pH	6.794	s.u.
SO <sub>4</sub> <sup>2-</sup>	76.08	mg/l
Na <sup>+</sup>	7.187	mg/l
Cl <sup>-</sup>	22.27	mg/l
NO <sub>3</sub> <sup>2-</sup>	2.441	mg/l
Mg <sup>2+</sup>	64.54	mg/l

Main gases produced - fugacities

CO <sub>2</sub> (g)	0.06336
N <sub>2</sub> (g)	0.03048

distance	6.095	m
pore volumes displaced	14065.7	
time	25925	years



Attachment Table 27. Oxidative Dissolution of Mackinawite and Uraninite at 40 Feet under High Groundwater Velocity, 100 Percent Reactive Iron with 8 mg/L Dissolved Oxygen.

Database file used is Thermo\_mackinawite.dat

Initial Solution Composition - 1 kg of water

Quartz	6.83	kg
Mackinawite	69.67	g
Calcite	69.67	g
Uraninite	7.27	g
O <sub>2</sub> (aq)	3.00E-71	mg/l
HCO <sub>3</sub> <sup>-</sup>	638	mg/l
pH	6.8	s.u.
SO <sub>4</sub> <sup>2-</sup>	102	mg/l
Na <sup>+</sup>	30.1	mg/l
Cl <sup>-</sup>	22.5	mg/l
NO <sub>3</sub> <sup>-</sup>	2.47	mg/l
Mg <sup>2+</sup>	70.9	mg/l

Incoming Solution Composition - 1 kg of water

SiO <sub>2</sub> (aq)	6	mg/l
Ca <sup>2+</sup>	90	mg/l
pH	6.8	s.u.
SO <sub>4</sub> <sup>2-</sup>	102	mg/l
Na <sup>+</sup>	7.28	mg/l
Cl <sup>-</sup>	22.5	mg/l
NO <sub>3</sub> <sup>-</sup>	2.47	mg/l
Mg <sup>2+</sup>	70.9	mg/l
Fe <sup>2+</sup>	1.E-07	mg/l
U <sup>4+</sup>	1.E-26	mg/l
O <sub>2</sub> (aq)	8	mg/l
HCO <sub>3</sub> <sup>-</sup>	628	mg/l

Hydrology and Transport information

Time ended	154.8	years
Length	12.19	m
Width	1	m
Height	1	m
Specific Discharge	0.381	m/day
Diffusion Coefficient	1.E-06	cm <sup>2</sup> /sec
Porosity	0.25	Volume Fraction
Longitudinal Dispersivity	0.1	m
# of nodes	1	
groundwater velocity	5	ft/day

Final Solution Composition - 1 kg of water

Quartz	6.83	kg
Hematite	30.96	g
Calcite	39.97	g
• U in fluid	143	mg/l
O <sub>2</sub> (aq)	1.278E-45	mg/l
HCO <sub>3</sub> <sup>-</sup>	414.6	mg/l
Ca <sup>2+</sup>	90.69	mg/l
pH	6.794	s.u.
SO <sub>4</sub> <sup>2-</sup>	76.03	mg/l
Na <sup>+</sup>	7.188	mg/l
Cl <sup>-</sup>	22.27	mg/l
NO <sub>3</sub> <sup>-</sup>	2.62E-49	mg/l
Mg <sup>2+</sup>	64.64	mg/l

Main gases produced - fugacities

CO <sub>2</sub> (g)	0.06336
N <sub>2</sub> (g)	0.03048

distance	6.095 m
pore volumes displaced	14065.6
time	154.8 years

Attachment Table 28. Oxidative Dissolution of Mackinawite and Uraninite, 10 Percent Reactive Iron with 8 mg/L Dissolved Oxygen and 1000 mg/L Bicarbonate.

Database file used is Thermo\_mackinawite.dat

Initial Solution Composition - 1 kg of water

Quartz	5.9	kg
Mackinawite	6.5	g
Calcite	60	g
Uraninite	33.67	mg
O <sub>2</sub> (aq)	3.00E-71	mg/l
HCO <sub>3</sub> <sup>-</sup>	1000	mg/l
pH	6.8	s.u.
SO <sub>4</sub> <sup>2-</sup>	102	mg/l
Na <sup>+</sup>	30.1	mg/l
Cl <sup>-</sup>	22.5	mg/l
NO <sub>3</sub> <sup>-</sup>	2.47	mg/l
Mg <sup>2+</sup>	70.9	mg/l

Reactants Composition - 1 kg of water

SiO <sub>2</sub> (aq)	6	mg/l
Ca <sup>2+</sup>	89.82	mg/l
pH	6.8	s.u.
SO <sub>4</sub> <sup>2-</sup>	102	mg/l
Na <sup>+</sup>	7.28	mg/l
Cl <sup>-</sup>	22.5	mg/l
NO <sub>3</sub> <sup>-</sup>	2.47	mg/l
Mg <sup>2+</sup>	70.9	mg/l
Fe <sup>2+</sup>	1.E-07	mg/l
U <sup>4+</sup>	1.E-26	mg/l
O <sub>2</sub> (aq)	8	mg/l
HCO <sub>3</sub> <sup>-</sup>	1000	mg/l

Final Solution Composition - 1 kg of water

Quartz	5.9	kg
Hematite	5.904	g
Calcite	110.1	g
UO <sub>2</sub> (CO <sub>3</sub> ) <sub>2</sub> <sup>2-</sup>	5.01E-02	mg/l
UO <sub>2</sub> (CO <sub>3</sub> ) <sub>3</sub> <sup>4-</sup>	3.51E-02	mg/l
O <sub>2</sub> (aq)	6.90	mg/l
HCO <sub>3</sub> <sup>-</sup>	712	mg/l
Ca <sup>2+</sup>	47.05	mg/l
pH	6.834	s.u.
SO <sub>4</sub> <sup>2-</sup>	90.17	mg/l
Na <sup>+</sup>	7.2	mg/l
Cl <sup>-</sup>	22.34	mg/l
NO <sub>3</sub> <sup>2-</sup>	0.73	mg/l
Mg <sup>2+</sup>	62.07	mg/l

Main gases produced - fugacities

CO <sub>2</sub> (g)	0.09977
N <sub>2</sub> (g)	0.02145
O <sub>2</sub> (g)	1.94E-08

pore volumes needed to dissolve mackinawite

500

pore volumes needed to dissolve uraninite

550

Attachment Table 29. Sorption of Uranium onto Iron Hydroxides, 100 Percent Reactive Iron with 1.2 mg/L Dissolved Oxygen at pH 5 s.u.

Database file used is Thermo.dat  
Sorption Database used is FeOH+.dat  
System flushed with 1.2 mg/l O<sub>2</sub>

Initial Solution Composition - 1 kg of water

Quartz	5.9	kg
Hematite	60	g
Calcite	60	g
U <sup>4+</sup>	29.8	mg/l
O <sub>2</sub> (aq)	1.00E-08	mg/l
HCO <sub>3</sub> <sup>-</sup>	638	mg/l
pH	5	s.u.
SO <sub>4</sub> <sup>2-</sup>	102	mg/l
Na <sup>+</sup>	30.1	mg/l
Cl <sup>-</sup>	22.5	mg/l
NO <sub>3</sub> <sup>-</sup>	2.47	mg/l
Mg <sup>2+</sup>	70.8	mg/l

Final Solution Composition - 1 kg of water

Quartz	5.9	kg
Hematite	60	g
Calcite	59.92	g
Dolomite	0.11	g
• U in fluid	8.86	mg/l
O <sub>2</sub> (aq)	1.119	mg/l
HCO <sub>3</sub> <sup>-</sup>	6851	mg/l
Ca <sup>2+</sup>	471.3	mg/l
pH	4.998	s.u.
SO <sub>4</sub> <sup>2-</sup>	0.57	mg/l
Na <sup>+</sup>	24.6	mg/l
Cl <sup>-</sup>	19.74	mg/l
NO <sub>3</sub> <sup>2-</sup>	2.14	mg/l
Mg <sup>2+</sup>	32.08	mg/l

artifact due to charge balance

Surface Complexes

	moles
>(w)FeOHSO42-	0.0006403
>(w)FeSO4-	0.0004212
>(s)FeOHCa++	3.48E-05
>(s)FeOUO2+	7.21E-05
>(w)FeOUO2+	1.17E-05

Main gases produced - fugacities

CO <sub>2</sub> (g)	64.78
O <sub>2</sub> (g)	0.03155

Original Basis	mg/kg in fluid	mg/kg sorbed
U <sup>4+</sup>	8.86	18
Ca <sup>2+</sup>	866	1.27
Mg <sup>2+</sup>	50.7	0.0155
SO <sub>4</sub> <sup>2-</sup>	0.0263	95



Attachment Table 30. Sorption of Uranium onto Iron Hydroxides, 100 Percent Reactive Iron with 1.2 mg/L Dissolved Oxygen and 10 mg/L Calcite.

Database file used is Thermo.dat  
Sorption Database used is FeOH+.dat  
System flushed with 1.2 mg/l O<sub>2</sub>

Initial Solution Composition - 1 kg of water

Quartz	5.9	kg
Hematite	60	g
Calcite	10	mg
U <sup>4+</sup>	29.8	mg/l
O <sub>2</sub> (aq)	1.00E-08	mg/l
HCO <sub>3</sub> <sup>-</sup>	638	mg/l
pH	6.8	s.u.
SO <sub>4</sub> <sup>2-</sup>	102	mg/l
Na <sup>+</sup>	30.1	mg/l
Cl <sup>-</sup>	22.5	mg/l
NO <sub>3</sub> <sup>-</sup>	2.47	mg/l
Mg <sup>2+</sup>	70.8	mg/l

Final Solution Composition - 1 kg of water

Quartz	5.9	kg
Hematite	60	g
Calcite	N/A	
Dolomite	0.2513	g
• U in fluid	0.363	mg/l
O <sub>2</sub> (aq)	1.269	mg/l
HCO <sub>3</sub> <sup>-</sup>	769.9	mg/l
Ca <sup>2+</sup>	10.18	mg/l
pH	6.662	s.u.
SO <sub>4</sub> <sup>2-</sup>	0.50	mg/l
Na <sup>+</sup>	29.65	mg/l
Cl <sup>-</sup>	22.43	mg/l
NO <sub>3</sub> <sup>2-</sup>	2.46	mg/l
Mg <sup>2+</sup>	24.57	mg/l

Surface Complexes

	moles
>(w)FeOH <sub>2</sub> SO <sub>4</sub> -	0.0009895
>(w)FeSO <sub>4</sub> -	0.0001031
>(s)FeOH <sub>2</sub> Ca++	1.04E-04
>(s)FeOUO <sub>2</sub> +	1.06E-04
>(w)FeOUO <sub>2</sub> +	1.77E-05

Main gases produced - fugacities

CO <sub>2</sub> (g)	0.1636
O <sub>2</sub> (g)	0.03155

Original Basis	mg/kg in fluid	mg/kg sorbed
U <sup>4+</sup>	0.363	29.4
Ca <sup>2+</sup>	11.7	4.4
Mg <sup>2+</sup>	26.8	10.8
SO <sub>4</sub> <sup>2-</sup>	0.548	105

Attachment Table 31. Sorption of Uranium onto Iron Hydroxides, 100 Percent Reactive Iron with 1.2 mg/L Dissolved Oxygen and Average TIC.

Database file used is Thermo.dat  
Sorption Database used is FeOH+.dat  
System flushed with 1.2 mg/l O<sub>2</sub>

Initial Solution Composition - 1 kg of water

Quartz	5.9	kg
Hematite	60	g
Calcite	60	g
U <sup>4+</sup>	29.8	mg/l
O <sub>2</sub> (aq)	1.00E-08	mg/l
HCO <sub>3</sub> <sup>-</sup>	298	mg/l
pH	6.8	s.u.
SO <sub>4</sub> <sup>2-</sup>	102	mg/l
Na <sup>+</sup>	30.1	mg/l
Cl <sup>-</sup>	22.5	mg/l
NO <sub>3</sub> <sup>-</sup>	2.47	mg/l
Mg <sup>2+</sup>	70.8	mg/l

Final Solution Composition - 1 kg of water

Quartz	5.9	kg
Hematite	60	g
Calcite	59.69	g
Dolomite	0.4901	g
• U in fluid	0.463	mg/l
O <sub>2</sub> (aq)	1.269	mg/l
HCO <sub>3</sub> <sup>-</sup>	801	mg/l
Ca <sup>2+</sup>	52.67	mg/l
pH	6.694	s.u.
SO <sub>4</sub> <sup>2-</sup>	0.57	mg/l
Na <sup>+</sup>	29.64	mg/l
Cl <sup>-</sup>	22.37	mg/l
NO <sub>3</sub> <sup>2-</sup>	2.44	mg/l
Mg <sup>2+</sup>	3.888	mg/l

Surface Complexes

	moles
>(w)FeOHSO42-	0.0009898
>(w)FeSO4-	0.0001018
>(s)FeOHCa++	5.29E-04
>(s)FeOUO2+	1.04E-04
>(w)FeOUO2+	1.96E-05

Main gases produced - fugacities

CO <sub>2</sub> (g)	0.1576
O <sub>2</sub> (g)	0.03155

Original Basis	mg/kg in fluid	mg/kg sorbed
U <sup>4+</sup>	0.463	29.3
Ca <sup>2+</sup>	60.7	22.6
Mg <sup>2+</sup>	4.26	1.94
SO <sub>4</sub> <sup>2-</sup>	0.643	105

Attachment Table 32. Sorption of Uranium onto Iron Hydroxides, 100 Percent Reactive Iron with 1.2 mg/L Dissolved Oxygen.

Database file used is Thermo.dat  
Sorption Database used is FeOH+.dat  
System flushed with 1.2 mg/l O<sub>2</sub>

Initial Solution Composition - 1 kg of water

Quartz	5.9	kg
Hematite	60	g
Calcite	60	g
U <sup>4+</sup>	29.8	mg/l
O <sub>2</sub> (aq)	1.00E-08	mg/l
HCO <sub>3</sub> <sup>-</sup>	638	mg/l
pH	6.8	s.u.
SO <sub>4</sub> <sup>2-</sup>	102	mg/l
Na <sup>+</sup>	30.1	mg/l
Cl <sup>-</sup>	22.5	mg/l
NO <sub>3</sub> <sup>-</sup>	2.47	mg/l
Mg <sup>2+</sup>	70.8	mg/l

Final Solution Composition - 1 kg of water

Quartz	5.9	kg
Hematite	60	g
Calcite	59.69	g
Dolomite	0.4901	g
• U in fluid	0.46	mg/l
O <sub>2</sub> (aq)	1.269	mg/l
HCO <sub>3</sub> <sup>-</sup>	801	mg/l
Ca <sup>2+</sup>	52.67	mg/l
pH	6.694	s.u.
SO <sub>4</sub> <sup>2-</sup>	0.57	mg/l
Na <sup>+</sup>	29.64	mg/l
Cl <sup>-</sup>	22.37	mg/l
NO <sub>3</sub> <sup>2-</sup>	2.45	mg/l
Mg <sup>2+</sup>	3.888	mg/l

Surface Complexes

	moles
>(w)FeOHSO42-	0.0009898
>(w)FeSO4-	0.0001018
>(s)FeOHCa++	5.29E-04
>(s)FeOUO2+	1.04E-04
>(w)FeOUO2+	1.96E-05

Main gases produced - fugacities

CO <sub>2</sub> (g)	0.1576
O <sub>2</sub> (g)	0.03155

Original Basis	mg/kg in fluid	mg/kg sorbed
U <sup>4+</sup>	0.463	29.3
Ca <sup>2+</sup>	60.7	22.6
Mg <sup>2+</sup>	4.26	1.94
SO <sub>4</sub> <sup>2-</sup>	0.643	105



Attachment Table 33. Sorption of Uranium onto Iron Hydroxides, 100 Percent Reactive Iron with 8 mg/L Dissolved Oxygen.

Database file used is Thermo.dat  
Sorption Database used is FeOH+.dat  
System flushed with 8 mg/l O<sub>2</sub>

Initial Solution Composition - 1 kg of water

Quartz	5.9	kg
Hematite	60	g
Calcite	60	g
U <sup>4+</sup>	29.8	mg/l
O <sub>2</sub> (aq)	1.00E-08	mg/l
HCO <sub>3</sub> <sup>-</sup>	638	mg/l
pH	6.78	s.u.
SO <sub>4</sub> <sup>2-</sup>	102	mg/l
Na <sup>+</sup>	30.1	mg/l
Cl <sup>-</sup>	22.5	mg/l
NO <sub>3</sub> <sup>-</sup>	2.47	mg/l
Mg <sup>2+</sup>	70.8	mg/l

Final Solution Composition - 1 kg of water

Quartz	5.9	kg
Hematite	60	g
Calcite	59.69	g
Dolomite	0.4901	g
• U in fluid	0.483	mg/l
O <sub>2</sub> (aq)	8.00	mg/l
HCO <sub>3</sub> <sup>-</sup>	826.5	mg/l
Ca <sup>2+</sup>	54.1	mg/l
pH	6.672	s.u.
SO <sub>4</sub> <sup>2-</sup>	0.57	mg/l
Na <sup>+</sup>	29.62	mg/l
Cl <sup>-</sup>	22.37	mg/l
NO <sub>3</sub> <sup>2-</sup>	2.44	mg/l
Mg <sup>2+</sup>	3.991	mg/l

Surface Complexes

	moles
>(w)FeOHSO42-	0.00107
>(w)FeSO4-	0.000112
>(s)FeOHCa++	5.05E-04
>(s)FeOUO2+	1.04E-04
>(w)FeOUO2+	1.95E-05

Main gases produced - fugacities

CO <sub>2</sub> (g)	0.1711
O <sub>2</sub> (g)	0.1991

Original Basis	mg/kg in fluid	mg/kg sorbed
U <sup>4+</sup>	0.483	29.3
Ca <sup>2+</sup>	62.5	21.6
Mg <sup>2+</sup>	4.38	1.81
SO <sub>4</sub> <sup>2-</sup>	0.653	114

Attachment Table 34. Sorption of Uranium onto Iron Hydroxides, 75 Percent Reactive Iron with 1.2 mg/L Dissolved Oxygen.

Database file used is Thermo.dat  
Sorption Database used is FeOH+.dat  
System flushed with 1.2 mg/l O<sub>2</sub>

Initial Solution Composition - 1 kg of water

Quartz	5.9	kg
Hematite	44.38	g
Calcite	60	g
U <sup>4+</sup>	29.8	mg/l
O <sub>2</sub> (aq)	1.00E-08	mg/l
HCO <sub>3</sub> <sup>-</sup>	638	mg/l
pH	6.8	s.u.
SO <sub>4</sub> <sup>2-</sup>	102	mg/l
Na <sup>+</sup>	30.1	mg/l
Cl <sup>-</sup>	22.5	mg/l
NO <sub>3</sub> <sup>-</sup>	2.47	mg/l
Mg <sup>2+</sup>	70.8	mg/l

Final Solution Composition - 1 kg of water

Quartz	5.9	kg
Hematite	44.39	g
Calcite	59.68	g
Dolomite	0.4864	g
• U in fluid	0.442	mg/l
O <sub>2</sub> (aq)	1.269	mg/l
HCO <sub>3</sub> <sup>-</sup>	687.4	mg/l
Ca <sup>2+</sup>	63.26	mg/l
pH	6.679	s.u.
SO <sub>4</sub> <sup>2-</sup>	0.73	mg/l
Na <sup>+</sup>	29.7	mg/l
Cl <sup>-</sup>	22.35	mg/l
NO <sub>3</sub> <sup>2-</sup>	2.44	mg/l
Mg <sup>2+</sup>	4.672	mg/l

Surface Complexes

	moles
>(w)FeOHSO42-	0.0009865
>(w)FeSO4-	0.0001029
>(s)FeOHCa++	4.37E-04
>(s)FeOUO2+	1.03E-04
>(w)FeOUO2+	2.01E-05

Main gases produced - fugacities

CO <sub>2</sub> (g)	0.1404
O <sub>2</sub> (g)	0.03155

Original Basis	mg/kg in fluid	mg/kg sorbed
U <sup>4+</sup>	0.442	29.3
Ca <sup>2+</sup>	71.6	18.7
Mg <sup>2+</sup>	5.05	1.63
SO <sub>4</sub> <sup>2-</sup>	0.848	105

Attachment Table 35. Sorption of Uranium onto Iron Hydroxides, 75 Percent Reactive Iron with 8 mg/L Dissolved Oxygen.

Database file used is Thermo.dat  
Sorption Database used is FeOH+.dat  
System flushed with 8 mg/l O<sub>2</sub>

Initial Solution Composition - 1 kg of water

Quartz	5.9	kg
Hematite	44.39	g
Calcite	60	g
U <sup>4+</sup>	29.8	mg/l
O <sub>2</sub> (aq)	1.00E-08	mg/l
HCO <sub>3</sub> <sup>-</sup>	638	mg/l
pH	6.78	s.u.
SO <sub>4</sub> <sup>2-</sup>	102	mg/l
Na <sup>+</sup>	30.1	mg/l
Cl <sup>-</sup>	22.5	mg/l
NO <sub>3</sub> <sup>-</sup>	2.47	mg/l
Mg <sup>2+</sup>	70.8	mg/l

Final Solution Composition - 1 kg of water

Quartz	5.9	kg
Hematite	44.4	g
Calcite	59.68	g
Dolomite	0.486	g
• U in fluid	0.46	mg/l
O <sub>2</sub> (aq)	8.00	mg/l
HCO <sub>3</sub> <sup>-</sup>	707.7	mg/l
Ca <sup>2+</sup>	64.98	mg/l
pH	6.657	s.u.
SO <sub>4</sub> <sup>2-</sup>	0.74	mg/l
Na <sup>+</sup>	29.69	mg/l
Cl <sup>-</sup>	22.35	mg/l
NO <sub>3</sub> <sup>2-</sup>	2.44	mg/l
Mg <sup>2+</sup>	4.798	mg/l

Surface Complexes

	moles
>(w)FeOHSO42-	0.00107
>(w)FeSO4-	0.0001134
>(s)FeOHCa++	4.20E-04
>(s)FeOUO2+	1.03E-04
>(w)FeOUO2+	2.00E-05

Main gases produced - fugacities

CO <sub>2</sub> (g)	0.152
O <sub>2</sub> (g)	0.1991

Original Basis	mg/kg in fluid	mg/kg sorbed
U <sup>4+</sup>	0.459	29.3
Ca <sup>2+</sup>	73.8	18
Mg <sup>2+</sup>	5.2	1.53
SO <sub>4</sub> <sup>2-</sup>	0.866	114



Attachment Table 36. Sorption of Uranium onto Iron Hydroxides, 50 Percent Reactive Iron with 1.2 mg/L Dissolved Oxygen.

Database file used is Thermo.dat  
Sorption Database used is FeOH+.dat  
System flushed with 1.2 mg/l O<sub>2</sub>

Initial Solution Composition - 1 kg of water

Quartz	5.9	kg
Hematite	29.59	g
Calcite	60	g
U <sup>4+</sup>	29.8	mg/l
O <sub>2</sub> (aq)	1.00E-08	mg/l
HCO <sub>3</sub> <sup>-</sup>	638	mg/l
pH	6.8	s.u.
SO <sub>4</sub> <sup>2-</sup>	102	mg/l
Na <sup>+</sup>	30.1	mg/l
Cl <sup>-</sup>	22.5	mg/l
NO <sub>3</sub> <sup>-</sup>	2.47	mg/l
Mg <sup>2+</sup>	70.8	mg/l

Final Solution Composition - 1 kg of water

Quartz	5.9	kg
Hematite	29.6	g
Calcite	59.66	g
Dolomite	0.4818	g
• U in fluid	0.48	mg/l
O <sub>2</sub> (aq)	1.269	mg/l
HCO <sub>3</sub> <sup>-</sup>	594.2	mg/l
Ca <sup>2+</sup>	76.52	mg/l
pH	6.659	s.u.
SO <sub>4</sub> <sup>2-</sup>	1.07	mg/l
Na <sup>+</sup>	29.75	mg/l
Cl <sup>-</sup>	22.33	mg/l
NO <sub>3</sub> <sup>2-</sup>	2.44	mg/l
Mg <sup>2+</sup>	5.652	mg/l

Surface Complexes

	moles
>(w)FeOH <sub>2</sub> SO <sub>4</sub> 2-	0.0009792
>(w)FeSO <sub>4</sub> -	0.0001057
>(s)FeOH <sub>2</sub> Ca++	3.28E-04
>(s)FeOUO <sub>2</sub> +	1.02E-04
>(w)FeOUO <sub>2</sub> +	2.08E-05

Main gases produced - fugacities

CO <sub>2</sub> (g)	0.1269
O <sub>2</sub> (g)	0.03155

Original Basis	mg/kg in fluid	mg/kg sorbed
U <sup>4+</sup>	0.479	29.3
Ca <sup>2+</sup>	85.3	14.1
Mg <sup>2+</sup>	6.05	1.24
SO <sub>4</sub> <sup>2-</sup>	1.28	104

Attachment Table 37. Sorption of Uranium onto Iron Hydroxides, 50 Percent Reactive Iron with 8 mg/L Dissolved Oxygen.

Database file used is Thermo.dat  
Sorption Database used is FeOH+.dat  
System flushed with 8 mg/l O<sub>2</sub>

Initial Solution Composition - 1 kg of water

Quartz	5.9	kg
Hematite	29.59	g
Calcite	60	g
U <sup>4+</sup>	29.8	mg/l
O <sub>2</sub> (aq)	1.00E-08	mg/l
HCO <sub>3</sub> <sup>-</sup>	638	mg/l
pH	6.78	s.u.
SO <sub>4</sub> <sup>2-</sup>	102	mg/l
Na <sup>+</sup>	30.1	mg/l
Cl <sup>-</sup>	22.5	mg/l
NO <sub>3</sub> <sup>-</sup>	2.47	mg/l
Mg <sup>2+</sup>	70.8	mg/l

Final Solution Composition - 1 kg of water

Quartz	5.9	kg
Hematite	29.6	g
Calcite	59.66	g
Dolomite	0.481	g
• U in fluid	0.494	mg/l
O <sub>2</sub> (aq)	8.00	mg/l
HCO <sub>3</sub> <sup>-</sup>	609.9	mg/l
Ca <sup>2+</sup>	78.58	mg/l
pH	6.638	s.u.
SO <sub>4</sub> <sup>2-</sup>	1.10	mg/l
Na <sup>+</sup>	29.74	mg/l
Cl <sup>-</sup>	22.32	mg/l
NO <sub>3</sub> <sup>2-</sup>	2.44	mg/l
Mg <sup>2+</sup>	5.801	mg/l

Surface Complexes

	moles
>(w)FeOH <sub>2</sub> SO <sub>4</sub> 2-	0.001061
>(w)FeSO <sub>4</sub> -	0.0001167
>(s)FeOH <sub>2</sub> Ca++	3.19E-04
>(s)FeOUO <sub>2</sub> +	1.02E-04
>(w)FeOUO <sub>2</sub> +	2.07E-05

Main gases produced - fugacities

CO <sub>2</sub> (g)	0.1365
O <sub>2</sub> (g)	0.1991

Original Basis	mg/kg in fluid	mg/kg sorbed
U <sup>4+</sup>	0.494	29.3
Ca <sup>2+</sup>	87.8	13.6
Mg <sup>2+</sup>	6.22	1.17
SO <sub>4</sub> <sup>2-</sup>	1.32	113

Attachment Table 38. Sorption of Uranium onto Iron Hydroxides, 25 Percent Reactive Iron with 1.2 mg/L Dissolved Oxygen.

Database file used is Thermo.dat  
Sorption Database used is FeOH+.dat  
System flushed with 1.2 mg/l O<sub>2</sub>

Initial Solution Composition - 1 kg of water

Quartz	5.9	kg
Hematite	14.8	g
Calcite	60	g
U <sup>4+</sup>	29.8	mg/l
O <sub>2</sub> (aq)	1.00E-08	mg/l
HCO <sub>3</sub> <sup>-</sup>	638	mg/l
pH	6.8	s.u.
SO <sub>4</sub> <sup>2-</sup>	102	mg/l
Na <sup>+</sup>	30.1	mg/l
Cl <sup>-</sup>	22.5	mg/l
NO <sub>3</sub> <sup>-</sup>	2.47	mg/l
Mg <sup>2+</sup>	70.8	mg/l

Final Solution Composition - 1 kg of water

Quartz	5.9	kg
Hematite	14.81	g
Calcite	59.64	g
Dolomite	0.4752	g
• U in fluid	0.695	mg/l
O <sub>2</sub> (aq)	1.269	mg/l
HCO <sub>3</sub> <sup>-</sup>	513.9	mg/l
Ca <sup>2+</sup>	94.7	mg/l
pH	6.633	s.u.
SO <sub>4</sub> <sup>2-</sup>	2.33	mg/l
Na <sup>+</sup>	29.8	mg/l
Cl <sup>-</sup>	22.3	mg/l
NO <sub>3</sub> <sup>2-</sup>	2.44	mg/l
Mg <sup>2+</sup>	6.99	mg/l

Surface Complexes

	moles
>(w)FeOH <sub>2</sub> SO <sub>4</sub> 2-	0.0009542
>(w)FeSO <sub>4</sub> -	0.000114
>(s)FeOH <sub>2</sub> Ca++	1.93E-04
>(s)FeOUO <sub>2</sub> +	9.98E-05
>(w)FeOUO <sub>2</sub> +	2.25E-05

Main gases produced - fugacities

CO <sub>2</sub> (g)	0.1164
O <sub>2</sub> (g)	0.03155

Original Basis	mg/kg in fluid	mg/kg sorbed
U <sup>4+</sup>	0.695	29.1
Ca <sup>2+</sup>	104	8.29
Mg <sup>2+</sup>	7.43	0.728
SO <sub>4</sub> <sup>2-</sup>	2.89	103

Attachment Table 39. Sorption of Uranium onto Iron Hydroxides, 25 Percent Reactive Iron with 8 mg/L Dissolved Oxygen.

Database file used is Thermo.dat  
Sorption Database used is FeOH+.dat  
System flushed with 8 mg/l O<sub>2</sub>

Initial Solution Composition - 1 kg of water

Quartz	5.9	kg
Hematite	14.8	g
Calcite	60	g
U <sup>4+</sup>	29.8	mg/l
O <sub>2</sub> (aq)	1.00E-08	mg/l
HCO <sub>3</sub> <sup>-</sup>	638	mg/l
pH	6.78	s.u.
SO <sub>4</sub> <sup>2-</sup>	102	mg/l
Na <sup>+</sup>	30.1	mg/l
Cl <sup>-</sup>	22.5	mg/l
NO <sub>3</sub> <sup>-</sup>	2.47	mg/l
Mg <sup>2+</sup>	70.8	mg/l

Final Solution Composition - 1 kg of water

Quartz	5.9	kg
Hematite	14.81	g
Calcite	59.64	g
Dolomite	0.474	g
• U in fluid	0.708	mg/l
O <sub>2</sub> (aq)	8.00	mg/l
HCO <sub>3</sub> <sup>-</sup>	525.2	mg/l
Ca <sup>2+</sup>	97.06	mg/l
pH	6.615	s.u.
SO <sub>4</sub> <sup>2-</sup>	2.47	mg/l
Na <sup>+</sup>	29.79	mg/l
Cl <sup>-</sup>	22.29	mg/l
NO <sub>3</sub> <sup>2-</sup>	2.44	mg/l
Mg <sup>2+</sup>	7.161	mg/l

Surface Complexes

	moles
>(w)FeOH <sub>2</sub> SO <sub>4</sub> 2-	0.001033
>(w)FeSO <sub>4</sub> -	0.0001267
>(s)FeOH <sub>2</sub> Ca++	1.91E-04
>(s)FeOUO <sub>2</sub> +	9.98E-05
>(w)FeOUO <sub>2</sub> +	2.24E-05

Main gases produced - fugacities

CO <sub>2</sub> (g)	0.1239
O <sub>2</sub> (g)	0.1991

Original Basis	mg/kg in fluid	mg/kg sorbed
U <sup>4+</sup>	0.708	29.1
Ca <sup>2+</sup>	107	8.19
Mg <sup>2+</sup>	7.62	0.698
SO <sub>4</sub> <sup>2-</sup>	3.08	111



Attachment Table 40. Sorption of Uranium onto Iron Hydroxides, 10 Percent Reactive Iron with 1.2 mg/L Dissolved Oxygen.

Database file used is Thermo.dat  
Sorption Database used is FeOH+.dat  
System flushed with 1.2 mg/l O<sub>2</sub>

Initial Solution Composition - 1 kg of water

Quartz	5.9	kg
Hematite	5.9	g
Calcite	60	g
U <sup>4+</sup>	29.8	mg/l
O <sub>2</sub> (aq)	1.00E-08	mg/l
HCO <sub>3</sub> <sup>-</sup>	638	mg/l
pH	6.8	s.u.
SO <sub>4</sub> <sup>2-</sup>	102	mg/l
Na <sup>+</sup>	30.1	mg/l
Cl <sup>-</sup>	22.5	mg/l
NO <sub>3</sub> <sup>-</sup>	2.47	mg/l
Mg <sup>2+</sup>	70.8	mg/l

Final Solution Composition - 1 kg of water

Quartz	5.9	kg
Hematite	5.905	g
Calcite	59.62	g
Dolomite	0.4693	g
• U in fluid	1.45	mg/l
O <sub>2</sub> (aq)	1.269	mg/l
HCO <sub>3</sub> <sup>-</sup>	466.4	mg/l
Ca <sup>2+</sup>	109.5	mg/l
pH	6.617	s.u.
SO <sub>4</sub> <sup>2-</sup>	8.84	mg/l
Na <sup>+</sup>	29.82	mg/l
Cl <sup>-</sup>	22.27	mg/l
NO <sub>3</sub> <sup>2-</sup>	2.43	mg/l
Mg <sup>2+</sup>	8.073	mg/l

Surface Complexes

	moles
>(w)FeOH <sub>2</sub> SO <sub>4</sub> 2-	0.0008496
>(w)FeSO <sub>4</sub> -	0.0001314
>(s)FeOH <sub>2</sub> Ca++	9.58E-05
>(s)FeOUO <sub>2</sub> +	9.16E-05
>(w)FeOUO <sub>2</sub> +	2.75E-05

Main gases produced - fugacities

CO <sub>2</sub> (g)	0.1093
O <sub>2</sub> (g)	0.03155

Original Basis	mg/kg in fluid	mg/kg sorbed
U <sup>4+</sup>	1.45	28.3
Ca <sup>2+</sup>	120	4.11
Mg <sup>2+</sup>	8.57	0.371
SO <sub>4</sub> <sup>2-</sup>	11.3	94.2

Attachment Table 41. Sorption of Uranium onto Iron Hydroxides, 10 Percent Reactive Iron with 8 mg/L Dissolved Oxygen.

Database file used is Thermo.dat  
Sorption Database used is FeOH+.dat  
System flushed with 8 mg/l O<sub>2</sub>

Initial Solution Composition - 1 kg of water

Quartz	5.9	kg
Hematite	5.9	g
Calcite	60	g
U <sup>4+</sup>	29.8	mg/l
O <sub>2</sub> (aq)	1.00E-08	mg/l
HCO <sub>3</sub> <sup>-</sup>	638	mg/l
pH	6.78	s.u.
SO <sub>4</sub> <sup>2-</sup>	102	mg/l
Na <sup>+</sup>	30.1	mg/l
Cl <sup>-</sup>	22.5	mg/l
NO <sub>3</sub> <sup>-</sup>	2.47	mg/l
Mg <sup>2+</sup>	70.8	mg/l

Final Solution Composition - 1 kg of water

Quartz	5.9	kg
Hematite	5.905	g
Calcite	59.62	g
Dolomite	0.4678	g
• U in fluid	1.46	mg/l
O <sub>2</sub> (aq)	8.00	mg/l
HCO <sub>3</sub> <sup>-</sup>	474.4	mg/l
Ca <sup>2+</sup>	112	mg/l
pH	6.602	s.u.
SO <sub>4</sub> <sup>2-</sup>	9.85	mg/l
Na <sup>+</sup>	29.81	mg/l
Cl <sup>-</sup>	22.27	mg/l
NO <sub>3</sub> <sup>-</sup>	2.43	mg/l
Mg <sup>2+</sup>	8.253	mg/l

Surface Complexes

	moles
>(w)FeOH <sub>2</sub> SO <sub>4</sub> -	0.0009131
>(w)FeSO <sub>4</sub> -	0.0001477
>(s)FeOH <sub>2</sub> Ca++	9.78E-05
>(s)FeOUO <sub>2</sub> +	9.15E-05
>(w)FeOUO <sub>2</sub> +	2.76E-05

Main gases produced - fugacities

CO <sub>2</sub> (g)	0.115
O <sub>2</sub> (g)	0.1991

Original Basis	mg/kg in fluid	mg/kg sorbed
U <sup>4+</sup>	1.46	28.3
Ca <sup>2+</sup>	123	4.19
Mg <sup>2+</sup>	8.77	0.364
SO <sub>4</sub> <sup>2-</sup>	12.6	102

Attachment Table 42. Uranium Sorption onto Iron Oxides, 10 Percent Reactive Iron with 1.2 mg/L Dissolved Oxygen at 0.5 feet.

Database file used is Thermo.dat

Initial Solution Composition - 1 kg of water

Quartz	6.8	kg
Hematite	6.937	g
Calcite	69.67	g
U <sup>6+</sup>	1.00E-20	mg/l
O <sub>2</sub> (aq)	1.00E-08	mg/l
HCO <sub>3</sub> <sup>-</sup>	638	mg/l
pH	6.78	s.u.
SO <sub>4</sub> <sup>2-</sup>	102	mg/l
Na <sup>+</sup>	30.1	mg/l
Cl <sup>-</sup>	22.5	mg/l
NO <sub>3</sub> <sup>-</sup>	2.47	mg/l
Mg <sup>2+</sup>	70.8	mg/l

Incoming Solution Composition - 1 kg of water

SiO <sub>2</sub> (aq)	6	mg/l
Ca <sup>2+</sup>	90	mg/l
pH	6.8	s.u.
SO <sub>4</sub> <sup>2-</sup>	102	mg/l
Na <sup>+</sup>	30.1	mg/l
Cl <sup>-</sup>	22.5	mg/l
NO <sub>3</sub> <sup>-</sup>	2.47	mg/l
Mg <sup>2+</sup>	70.9	mg/l
Fe <sup>2+</sup>	1.E-20	mg/l
U <sup>6+</sup>	0.5	mg/l
O <sub>2</sub> (aq)	1.2	mg/l
HCO <sub>3</sub> <sup>-</sup>	628	mg/l

Hydrology and Transport information

Time ended	4	days
Length	15.24	cm
Width	1	cm
Height	1	cm
Specific Discharge	0.0381	m/day
Diffusion Coefficient	1.E-05	cm <sup>2</sup> /sec
Porosity	0.25	Volume Fraction
Longitudinal Dispersivity	0.1	m
# of nodes	10	

Highest Uranium concentration observed in water: 2.1 E-1 mg/kg at 0.762 cm distance at 15.36 hours  
Uranium concentrations beyond 12 cm of distance are below 10 ug/kg throughout the model run.

Note: Distance is divided into 10 nodes (15.24cm/10) and each node acts as a CSTR within itself, therefore the distance for each node is given as the mid point. The reason for reporting the concentration observed at 0.762 cm as the highest is because 0.762 cm is the shortest distance due to the amount of nodes (10).

Final Solution Composition at 4 days at 14.478 cm distance (beyond this concentration are extremely low)

Final Solution Composition - 1 kg of water

Quartz	6.83	kg
Hematite	6.937	g
Calcite	70.08	g
Dolomite	0.338	g
U in fluid	0.00292	mg/l
O <sub>2</sub> (aq)	1.20	mg/l
HCO <sub>3</sub> <sup>-</sup>	365.4	mg/l
Ca <sup>2+</sup>	136.1	mg/l
pH	6.629	s.u.
SO <sub>4</sub> <sup>2-</sup>	140.0	mg/l
Na <sup>+</sup>	7.19	mg/l
Cl <sup>-</sup>	22.23	mg/l
NO <sub>3</sub> <sup>-</sup>	2.43	mg/l
Mg <sup>2+</sup>	9.992	mg/l

Surface Complexes

	moles
>(w)FeOH <sub>2</sub> SO <sub>4</sub> 2-	1.15E-06
>(w)FeSO <sub>4</sub> -	3.81E-07
>(s)FeOH <sub>2</sub> Ca++	1.57E-07
>(s)FeOUO <sub>2</sub> +	1.62E-10
>(w)FeOUO <sub>2</sub> +	7.33E-11

Main gases produced - fugacities

CO <sub>2</sub> (g)	0.08701
O <sub>2</sub> (g)	0.0298

Original Basis	mg/kg in fluid	mg/kg sorbed
U <sup>6+</sup>	0.00292	0.277
Ca <sup>2+</sup>	162	32.7
Mg <sup>2+</sup>	11.4	2.13
SO <sub>4</sub> <sup>2-</sup>	183	730

distance	14.478	cm
pore volumes displaced	7.63553	
time	4	days

Attachment Table 43. Uranium Sorption onto Iron Oxides, 10 Percent Reactive Iron with 8 mg/L Dissolved Oxygen at 0.5 feet distance.

Database file used is Thermo.dat

Initial Solution Composition - 1 kg of water		
Quartz	6.8	kg
Hematite	6.937	g
Calcite	70.669	g
U <sup>6+</sup>	1.00E-20	mg/l
O <sub>2</sub> (aq)	1.00E-08	mg/l
HCO <sub>3</sub> <sup>-</sup>	638	mg/l
pH	6.78	s.u.
SO <sub>4</sub> <sup>2-</sup>	102	mg/l
Na <sup>+</sup>	30.1	mg/l
Cl <sup>-</sup>	22.5	mg/l
NO <sub>3</sub> <sup>-</sup>	2.47	mg/l
Mg <sup>2+</sup>	70.8	mg/l

Incoming Solution Composition - 1 kg of water		
SiO <sub>2</sub> (aq)	6	mg/l
Ca <sup>2+</sup>	90	mg/l
pH	6.8	s.u.
SO <sub>4</sub> <sup>2-</sup>	102	mg/l
Na <sup>+</sup>	30.1	mg/l
Cl <sup>-</sup>	22.5	mg/l
NO <sub>3</sub> <sup>-</sup>	2.47	mg/l
Mg <sup>2+</sup>	70.9	mg/l
Fe <sup>2+</sup>	1.E-20	mg/l
U <sup>6+</sup>	0.5	mg/l
O <sub>2</sub> (aq)	8	mg/l
HCO <sub>3</sub> <sup>-</sup>	628	mg/l

Hydrology and Transport information		
Time ended	4	days
Length	15.24	cm
Width	1	cm
Height	1	cm
Specific Discharge	0.0381	m/day
Diffusion Coefficient	1.E-05	cm <sup>2</sup> /sec
Porosity	0.25	Volume Fraction
Longitudinal Dispersivity	0.1	m
# of nodes	10	

Highest Uranium concentration observed in water: 0.240 mg/kg at 0.762 cm distance at 23.04 hours  
 Uranium concentrations beyond 12 cm of distance are below 10 µg/kg throughout the model run.

Note: Distance is divided into 10 nodes (15.24cm/10) and each node acts as a CSTR within itself, therefore the distance for each node is given as the mid point. The reason for reporting the concentration observed at 0.762 cm as the highest is because 0.762 cm is the shortest distance due to the amount of nodes (10).

Final Solution Composition at 4 days at 14.478 cm distance (beyond this concentration are extremely low)

Final Solution Composition - 1 kg of water		
Quartz	6.83	kg
Hematite	6.937	g
Calcite	70.669	g
Dolomite	0.34	g
U in fluid	0.00309	mg/l
O <sub>2</sub> (aq)	7.99	mg/l
HCO <sub>3</sub> <sup>-</sup>	385.6	mg/l
Ca <sup>2+</sup>	136.5	mg/l
pH	6.627	s.u.
SO <sub>4</sub> <sup>2-</sup>	140.9	mg/l
Na <sup>+</sup>	7.193	mg/l
Cl <sup>-</sup>	22.23	mg/l
NO <sub>3</sub> <sup>-</sup>	2.43	mg/l
Mg <sup>2+</sup>	10.02	mg/l

Surface Complexes	
	moles
>(w)FeOHSO42-	1.16E-06
>(w)FeSO4-	3.83E-07
>(s)FeOHCa++	1.57E-07
>(s)FeOUO2+	1.71E-10
>(w)FeOUO2+	7.75E-11

distance 14.478 cm  
 pore volumes displaced 7.63649  
 time 4 days

Main gases produced - fugacities	
CO <sub>2</sub> (g)	0.08727
O <sub>2</sub> (g)	0.1989

Original Basis	mg/kg in fluid	mg/kg sorbed
U <sup>4+</sup>	0.00309	0.292
Ca <sup>2+</sup>	162	32.7
Mg <sup>2+</sup>	11.5	2.13
SO <sub>4</sub> <sup>2-</sup>	184	731



Attachment Table 44 Uranium Sorption onto Iron Oxides, 50 Percent Reactive Iron with 1.2 mg/L Dissolved Oxygen at 0.5 feet.

Database file used is Thermo.dat

Initial Solution Composition - 1 kg of water

Quartz	6.8	kg
Hematite	34.69	g
Calcite	69.67	g
U <sup>6+</sup>	1.00E-20	mg/l
O <sub>2</sub> (aq)	1.00E-08	mg/l
HCO <sub>3</sub> <sup>-</sup>	638	mg/l
pH	6.78	s.u.
SO <sub>4</sub> <sup>2-</sup>	102	mg/l
Na <sup>+</sup>	30.1	mg/l
Cl <sup>-</sup>	22.5	mg/l
NO <sub>3</sub> <sup>-</sup>	2.47	mg/l
Mg <sup>2+</sup>	70.8	mg/l

Incoming Solution Composition - 1 kg of water

SiO <sub>2</sub> (aq)	6	mg/l
Ca <sup>2+</sup>	90	mg/l
pH	6.8	s.u.
SO <sub>4</sub> <sup>2-</sup>	102	mg/l
Na <sup>+</sup>	30.1	mg/l
Cl <sup>-</sup>	22.5	mg/l
NO <sub>3</sub> <sup>-</sup>	2.47	mg/l
Mg <sup>2+</sup>	70.9	mg/l
Fe <sup>2+</sup>	1.E-20	mg/l
U <sup>6+</sup>	0.5	mg/l
O <sub>2</sub> (aq)	1.2	mg/l
HCO <sub>3</sub> <sup>-</sup>	628	mg/l

Hydrology and Transport information

Time ended	4	days
Length	15.24	cm
Width	1	cm
Height	1	cm
Specific Discharge	0.0381	m/day
Diffusion Coefficient	1.E-05	cm <sup>2</sup> /sec
Porosity	0.25	Volume Fraction
Longitudinal Dispersivity	0.1	m
# of nodes	10	

Highest Uranium concentration observed in water: 2.5 E-1 mg/kg at 0.762 cm distance at 1 day  
Uranium concentrations beyond 8 cm of distance are zero throughout the model run.

Note: Distance is divided into 10 nodes (15.24cm/10) and each node acts as a CSTR within itself, therefore the distance for each node is given as the mid point. The reason for reporting the concentration observed at 0.762 cm as the highest is because 0.762 cm is the shortest distance due to the amount of nodes (10).

Final Solution Composition at 4 days at 14.478 cm distance (beyond this concentration are extremely low)

Final Solution Composition - 1 kg of water

Quartz	6.83	kg
Hematite	34.69	g
Calcite	70.08	g
Dolomite	0.488	g
U in fluid	0.00138	mg/l
O <sub>2</sub> (aq)	1.20	mg/l
HCO <sub>3</sub> <sup>-</sup>	586.9	mg/l
Ca <sup>2+</sup>	74.12	mg/l
pH	6.692	s.u.
SO <sub>4</sub> <sup>2-</sup>	80.4	mg/l
Na <sup>+</sup>	7.19	mg/l
Cl <sup>-</sup>	65.09	mg/l
NO <sub>3</sub> <sup>-</sup>	7.08	mg/l
Mg <sup>2+</sup>	5.46	mg/l

Surface Complexes

	moles
>(w)FeOH <sub>2</sub> SO <sub>4</sub> 2-	4.89E-08
>(w)FeSO <sub>4</sub> -	1.25E-06
>(s)FeOH <sub>2</sub> Ca++	6.03E-07
>(s)FeOUO <sub>2</sub> +	2.05E-10
>(w)FeOUO <sub>2</sub> +	6.17E-11

distance 6.858 cm  
pore volumes displaced 7.74853  
time 4 days

Main gases produced - fugacities

CO <sub>2</sub> (g)	0.1158
O <sub>2</sub> (g)	0.0298

Original Basis	mg/kg in fluid	mg/kg sorbed
U <sup>6+</sup>	0.00138	0.318
Ca <sup>2+</sup>	88	127
Mg <sup>2+</sup>	6.17	7.14
SO <sub>4</sub> <sup>2-</sup>	94.9	2.960

Attachment Table 45. Uranium Sorption onto Iron Oxides, 50 Percent Reactive Iron with 8 mg/L Dissolved Oxygen at 0.5 feet.

Database file used is Thermo.dat

Initial Solution Composition - 1 kg of water		
Quartz	6.8	kg
Hematite	34.685	g
Calcite	70.669	g
U <sup>6+</sup>	1.00E-20	mg/l
O <sub>2</sub> (aq)	1.00E-08	mg/l
HCO <sub>3</sub> <sup>-</sup>	638	mg/l
pH	6.78	s.u.
SO <sub>4</sub> <sup>2-</sup>	102	mg/l
Na <sup>+</sup>	30.1	mg/l
Cl <sup>-</sup>	22.5	mg/l
NO <sub>3</sub> <sup>-</sup>	2.47	mg/l
Mg <sup>2+</sup>	70.8	mg/l

Incoming Solution Composition - 1 kg of water		
SiO <sub>2</sub> (aq)	6	mg/l
Ca <sup>2+</sup>	90	mg/l
pH	6.8	s.u.
SO <sub>4</sub> <sup>2-</sup>	102	mg/l
Na <sup>+</sup>	30.1	mg/l
Cl <sup>-</sup>	22.5	mg/l
NO <sub>3</sub> <sup>-</sup>	2.47	mg/l
Mg <sup>2+</sup>	70.9	mg/l
Fe <sup>2+</sup>	1.E-20	mg/l
U <sup>6+</sup>	0.5	mg/l
O <sub>2</sub> (aq)	8	mg/l
HCO <sub>3</sub> <sup>-</sup>	628	mg/l

Hydrology and Transport information		
Time ended	4	days
Length	15.24	cm
Width	1	cm
Height	1	cm
Specific Discharge	0.0381	m/day
Diffusion Coefficient	1.E-05	cm <sup>2</sup> /sec
Porosity	0.25	Volume Fraction
Longitudinal Dispersivity	0.1	m
# of nodes	10	

Highest Uranium concentration observed in water: 0.240 mg/kg at 0.762 cm distance at 21.12 hours  
 Uranium concentrations beyond 8 cm of distance are zero throughout the model run.

Note: Distance is divided into 10 nodes (15.24cm/10) and each node acts as a CSTR within itself, therefore the distance for each node is given as the mid point. The reason for reporting the concentration observed at 0.762 cm as the highest is because 0.762 cm is the shortest distance due to the amount of nodes (10).

Final Solution Composition at 4 days at 14.478 cm distance (beyond this concentration are extremely low)  
 Final Solution Composition - 1 kg of water

Quartz	6.83	kg
Hematite	34.685	g
Calcite	70.78	g
Dolomite	0.461	g
U in fluid	0.00138	mg/l
O <sub>2</sub> (aq)	7.99	mg/l
HCO <sub>3</sub> <sup>-</sup>	586.9	mg/l
Ca <sup>2+</sup>	74.12	mg/l
pH	6.692	s.u.
SO <sub>4</sub> <sup>2-</sup>	80.4	mg/l
Na <sup>+</sup>	7.19	mg/l
Cl <sup>-</sup>	65.09	mg/l
NO <sub>3</sub> <sup>-</sup>	7.08	mg/l
Mg <sup>2+</sup>	5.46	mg/l

Surface Complexes	
	moles
>(w)FeOH <sub>2</sub> SO <sub>4</sub> 2-	4.89E-06
>(w)FeSO <sub>4</sub> -	1.25E-06
>(s)FeOH <sub>2</sub> Ca++	6.03E-07
>(s)FeOUO <sub>2</sub> +	2.05E-10
>(w)FeOUO <sub>2</sub> +	6.17E-11

Main gases produced - fugacities	
CO <sub>2</sub> (g)	0.1156
O <sub>2</sub> (g)	0.1988

Original Basis	mg/kg in fluid	mg/kg sorbed
U <sup>6+</sup>	0.00138	0.318
Ca <sup>2+</sup>	88	127
Mg <sup>2+</sup>	6.17	7.14
SO <sub>4</sub> <sup>2-</sup>	94.9	2,960

distance 8.858 cm  
 pore volumes displaced 7.74853  
 time 4 days

Attachment Table 46. Uranium Sorption onto Iron Oxides, 10 Percent Reactive Iron with 1.2 mg/L Dissolved Oxygen in a 5,000 µg/L System at 0.5 feet distance.

Database file used is Thermo.dat

Initial Solution Composition - 1 kg of water		
Quartz	6.8	kg
Hematite	6.937	g
Calcite	69.67	g
U <sup>6+</sup>	1.00E-20	mg/l
O <sub>2</sub> (aq)	1.00E-08	mg/l
HCO <sub>3</sub> <sup>-</sup>	638	mg/l
pH	6.78	s.u.
SO <sub>4</sub> <sup>2-</sup>	102	mg/l
Na <sup>+</sup>	30.1	mg/l
Cl <sup>-</sup>	22.5	mg/l
NO <sub>3</sub> <sup>-</sup>	2.47	mg/l
Mg <sup>2+</sup>	70.8	mg/l

Incoming Solution Composition - 1 kg of water		
SiO <sub>2</sub> (aq)	6	mg/l
Ca <sup>2+</sup>	90	mg/l
pH	6.8	s.u.
SO <sub>4</sub> <sup>2-</sup>	102	mg/l
Na <sup>+</sup>	30.1	mg/l
Cl <sup>-</sup>	22.5	mg/l
NO <sub>3</sub> <sup>-</sup>	2.47	mg/l
Mg <sup>2+</sup>	70.9	mg/l
Fe <sup>2+</sup>	1.E-20	mg/l
U <sup>6+</sup>	5	mg/l
O <sub>2</sub> (aq)	1.2	mg/l
HCO <sub>3</sub> <sup>-</sup>	628	mg/l

Hydrology and Transport information		
Time ended	30	days
Length	15.24	cm
Width	1	cm
Height	1	cm
Specific Discharge	0.0381	m/day
Diffusion Coefficient	1.E-05	cm <sup>2</sup> /sec
Porosity	0.25	Volume Fraction
Longitudinal Dispersivity	0.1	m
# of nodes	10	

Highest Uranium concentration observed in water: 2.5 mg/kg at 0.762 cm distance at 23.24 hours  
 Uranium concentrations beyond 14 cm of distance are below 50 µg/kg throughout the model run.

Note: Distance is divided into 10 nodes (15.24cm/10) and each node acts as a CSTR within itself there fore the distance for each node is given as the mid point. The reason for reporting the concentration observed at 0.762 cm as the highest is because 0.762 cm is the shortest distance due to the amount of nodes (10).

Final Solution composition at 30 days at 14.478 cm distance  
 Final Solution Composition - 1 kg of water

Quartz	6.83	kg
Hematite	6.937	g
Calcite	70.157	g
Dolomite	0.338	g
• U in fluid	0.0446	mg/l
O <sub>2</sub> (aq)	1.20	mg/l
HCO <sub>3</sub> <sup>-</sup>	385.7	mg/l
Ca <sup>2+</sup>	136.6	mg/l
pH	6.827	s.u.
SO <sub>4</sub> <sup>2-</sup>	141.2	mg/l
Na <sup>+</sup>	7.19	mg/l
Cl <sup>-</sup>	22.23	mg/l
NO <sub>3</sub> <sup>-</sup>	2.43	mg/l
Mg <sup>2+</sup>	7.192	mg/l

Surface Complexes		
	moles	
>(w)FeOH <sub>2</sub> SO <sub>4</sub> 2-		1.16E-06
>(w)FeSO <sub>4</sub> -		3.84E-07
>(s)FeOH <sub>2</sub> Ca++		1.55E-07
>(s)FeOUO <sub>2</sub> +		2.44E-09
>(w)FeOUO <sub>2</sub> +		1.12E-09

Main gases produced - fugacities		
CO <sub>2</sub> (g)		0.08736
O <sub>2</sub> (g)		0.0298

Original Basis	mg/kg in fluid	mg/kg sorbed
U <sup>6+</sup>	0.0446	4.19
Ca <sup>2+</sup>	163	32.4
Mg <sup>2+</sup>	11.5	2.12
SO <sub>4</sub> <sup>2-</sup>	185	732

distance 14.478 cm  
 pore volumes displaced 57.2699  
 time 30 days

ARCADIS

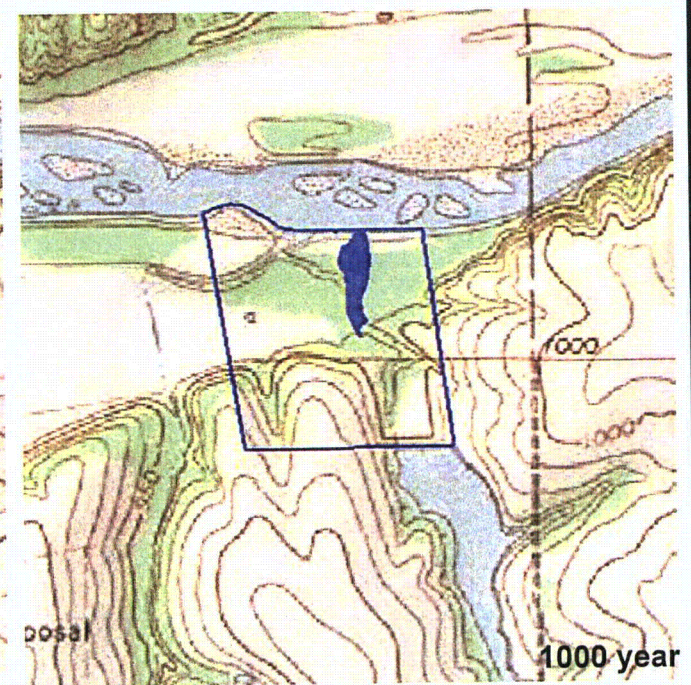
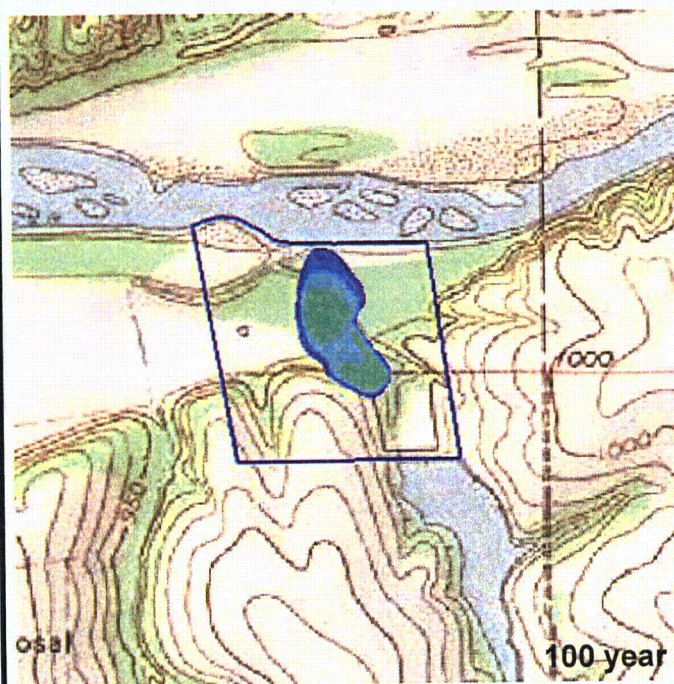
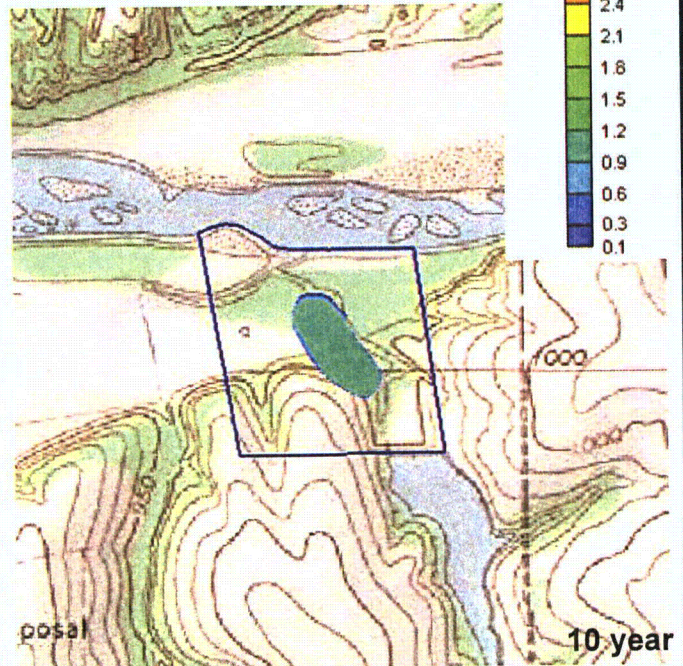
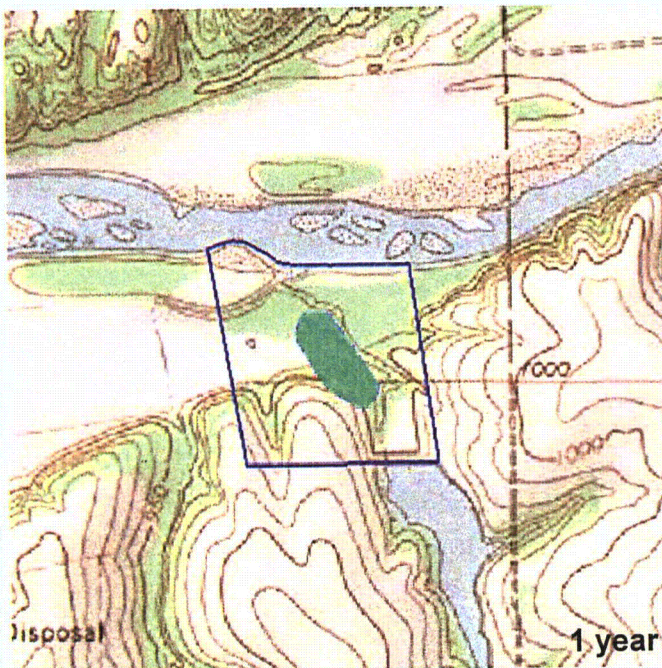
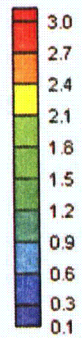
**ATTACHMENT FIGURES**

MT3DMS Transport





U Concentration  
( $\mu\text{g/L}$ )



**ARCADIS**

630 Plaza Drive  
Highlands Ranch, CO 80129  
Tel (720) 344-3500

Scenario 4: Uranium plume

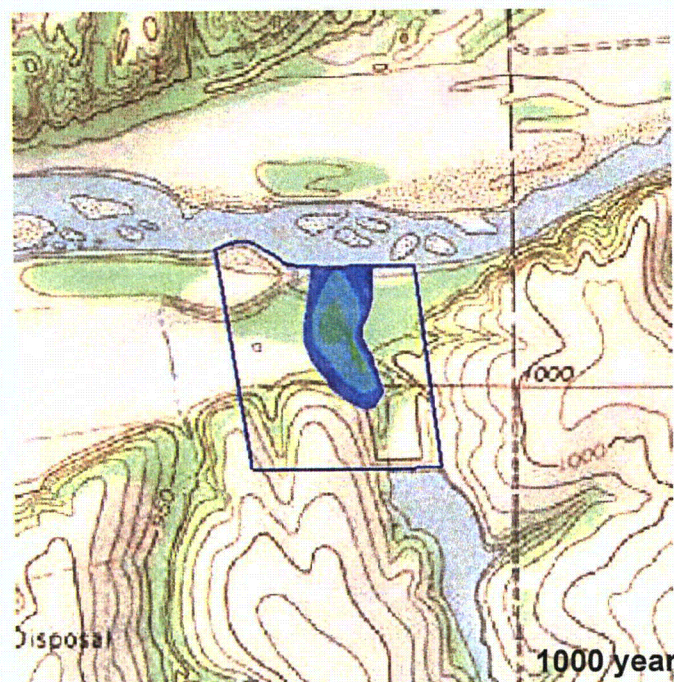
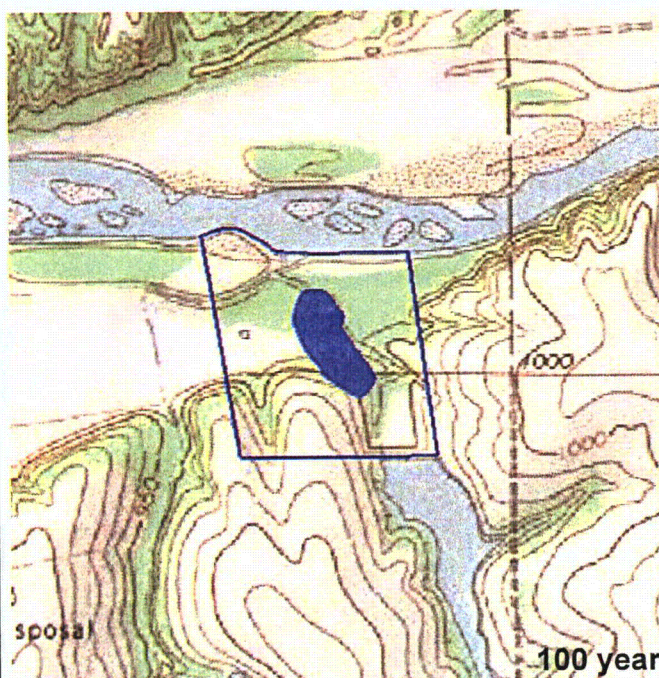
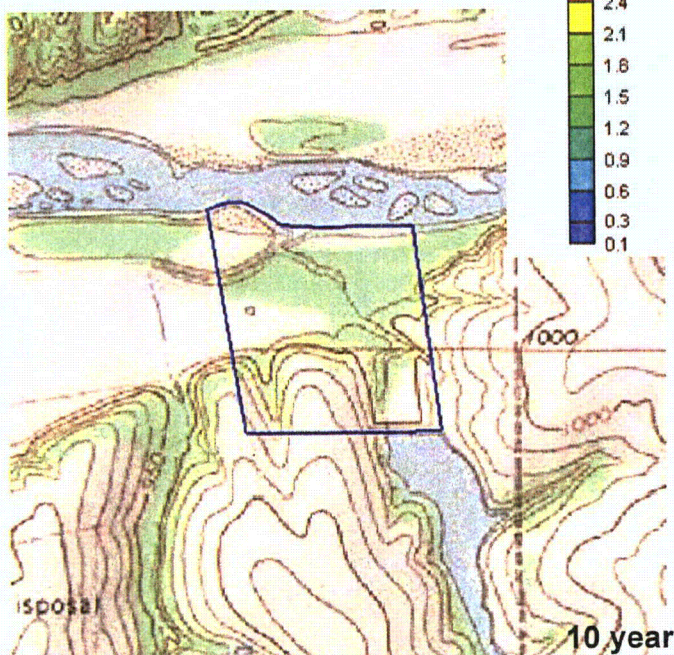
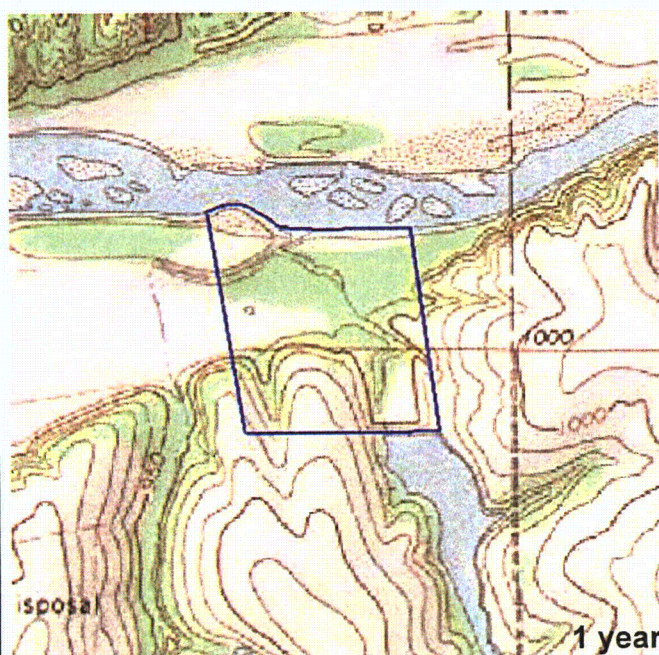
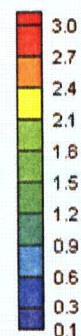
TRONOX  
Cimarron Site

PROJECT MANAGER YQ	DEPARTMENT MANAGER
DRAFTER YYQ	CHECKED EMB
PROJECT NUMBER GPTRONOX.0002	DRAWING NUMBER 1





U Concentration  
( $\mu\text{g/L}$ )



630 Plaza Drive  
Highlands Ranch, CO 80129  
Tel (720) 344-3500

### Scenario 5: Uranium plume

TRONOX  
Cimarron Site

PROJECT MANAGER YQ	DEPARTMENT MANAGER
DRAFTER YYQ	CHECKED EMB
PROJECT NUMBER GPTRONOX.0002	DRAWING NUMBER 2



**SDP ATTACHMENT 2**

**GROUNDWATER FLOW MODELING REPORT**

Prepared for:  
Cimarron Corporation (Tronox)  
Oklahoma City, Oklahoma

## Groundwater Flow Modeling Report

ENSR Corporation  
October 2006  
Document No.: 04020-044

**TRONOX**

ENSR | AECOM



Prepared for:  
Cimarron Corporation (Tronox)  
Oklahoma

# Groundwater Flow Modeling Report

Maya Desai and Ken Heim

Maya C. Desai Ken Heim  
Prepared By

Michael Meenan and James Cao

Michael Meenan James Cao  
Reviewed By

ENSR Corporation  
October 2006  
Document No.: 04020-044-327

**TRONOX**

ENSR | AECOM

# Contents

<b>1.0 INTRODUCTION.....</b>	<b>1-1</b>
1.1 Overview.....	1-1
1.2 Background and Objectives .....	1-1
<b>2.0 HYDROGEOLOGIC FRAMEWORK.....</b>	<b>2-1</b>
2.1 Site Setting .....	2-1
2.2 Precipitation .....	2-1
2.3 General Geology .....	2-1
2.4 Site-Specific Geology .....	2-2
2.4.1 BA #1 Area.....	2-2
2.4.2 Western Alluvial Area .....	2-2
2.5 Hydrogeology .....	2-3
2.6 Hydrologic Implications .....	2-3
2.7 Conceptual Model of Site Groundwater Flow.....	2-4
2.7.1 The Cimarron River .....	2-4
2.7.2 BA #1 Area.....	2-4
2.7.3 Western Alluvial Area .....	2-5
<b>3.0 MODELING APPROACH.....</b>	<b>3-1</b>
3.1 Groundwater Model Domain .....	3-1
3.1.1 BA #1 Area.....	3-2
3.1.2 WA Area.....	3-2
3.2 Hydrogeologic Physical Properties .....	3-3
3.3 Boundary Conditions .....	3-4
3.3.1 Recharge.....	3-4
3.3.2 Surface Water/Groundwater Interactions .....	3-4
3.3.3 Upgradient General Head Boundary .....	3-5
3.3.4 Underlying General Head Boundary .....	3-5
3.4 Summary of Modeling Approach .....	3-5
<b>4.0 MODEL CALIBRATION .....</b>	<b>4-1</b>
4.1 Calibration Approach.....	4-1
4.1.1 Measured and Predicted Water Levels.....	4-1
4.1.2 Volumetric Flow-Through Rate .....	4-1
4.1.3 Plume Migration.....	4-2
4.2 Calibration Parameters .....	4-2

## Contents, continued

4.3	Calibration Results .....	4-3
4.3.1	BA #1.....	4-3
4.3.2	WA area .....	4-4
4.3.3	Discussion.....	4-5
4.3.4	Summary of Calibration Results.....	4-5
4.4	Sensitivity Analysis .....	4-6
4.5	Uncertainties and Assumptions .....	4-7
<b>5.0</b>	<b>SUMMARY AND CONCLUSIONS .....</b>	<b>5-1</b>
<b>6.0</b>	<b>REFERENCES .....</b>	<b>6-1</b>

## List of Tables

- Table 1 - Summary of Slug and Aquifer Test Results
- Table 2 – Summary of Groundwater Elevation Data used for Calibration
- Table 3 - BA #1 Summary of Model Inputs
- Table 4 - WA Area Summary of Model Inputs

## List of Figures

- Figure 1 – Site Location Map
- Figure 2 – Geology Along the Cimarron River From Freedom to Guthrie, Oklahoma
- Figure 3 – BA #1 – Geological Cross-Section
- Figure 4 – Western Upland and Alluvial Areas – Geological Cross-Section
- Figure 5 – BA#1 Model Domain
- Figure 6 – WA Area Model Domain
- Figure 7 – BA #1 Boreholes and Cross-sections
- Figure 8 – BA #1 Solids Developed from Borehole data
- Figure 9 – BA #1 3D grid incorporating geologic information
- Figure 10 – WA Area Boreholes and Cross-sections
- Figure 11 – WA Area Solids Developed from Borehole data
- Figure 12 – WA Area 3D grid incorporating geologic information
- Figure 13 – BA #1 Calibration Results
- Figure 14 – WA Calibration Results



## 1.0 INTRODUCTION

### 1.1 Overview

In order to depict and predict groundwater flow and to evaluate groundwater remediation alternatives, two groundwater flow models were developed for the Cimarron Site. These two models address two of the three areas on site that require remediation of Uranium (U) in the groundwater. The two models included Burial Area #1 (BA #1) and the Western Alluvial (WA) area.

Calibration was evaluated by comparing measured groundwater elevations, flow path data, and water budgets, with simulated elevations, paths, and budgets. Both flow models achieved adequate calibration to the observed groundwater elevation data, to observed flow path trajectories, and to the estimated water budgets. Discrepancies between observations and predictions are considered reasonable. The overall water table configuration for each model was consistent with expectations based on observations of U concentrations. Overall hydrogeological concepts as presented in the Conceptual Site Model (CSM), Rev 01 (ENSR, 2006) were captured by the numerical models.

The resulting models are useful tools to evaluate groundwater flow characteristics (velocities, flux rates, etc.) and to evaluate different remediation scenarios including, but not limited to, understanding the permanence of the proposed remedial technique and to design the injection of reagents.

### 1.2 Background and Objectives

Cimarron Corporation's site near Crescent, Oklahoma is a former nuclear fuel manufacturing facility. Since stopping operations, the site has been undergoing decommissioning under the oversight of the Nuclear Regulatory Commission (NRC) and the Oklahoma Department of Environmental Quality (ODEQ). As a result of the facility processes there are several areas at the Cimarron Site that have residual concentrations of Uranium (U) in the groundwater. Cimarron Corporation is currently considering remedial actions in Burial Area #1, the Western Alluvial Area, and the Western Uplands area. To support the design of these remedial systems, numerical groundwater flow models were developed for two of these areas. These models, based largely on data and concepts presented in the Conceptual Site Model (Rev 01, ENSR, 2006), serve as tools to evaluate remediation strategies.

The overall objective of this modeling effort was to provide tools by which remediation alternatives could be evaluated. This objective was achieved by setting up the numerical models to include geologic and hydrologic conditions as observed and documented in the CSM-Rev 01 (ENSR, 2006). The models were then calibrated to specific targets. This calibration process yielded two models that compared well to observations and therefore could provide a frame of reference with which to evaluate impacts from remediation alternatives.

These models were initially developed to support ENSR's remediation via pump and treat. While Cimarron was considering remediation via pump and treat, they were also considering bioremediation. In this latter process, via additives, the geochemical conditions in the aquifer would be converted to a reducing environment which would immobilize the U. This process has been conceptualized and proposed by Arcadis. Data from these calibrated models and simulations using these numerical models can help to design either these or other remediation alternatives.

Note that even though there are detectable concentrations of U in the Western Upland area of the site, a numerical model was not constructed for that area. The conceptual site model for the WU area is presented in the CSM Rev 01 (ENSR, 2006). This conceptual site model forms the basis for ARCADIS' evaluation and selection of remedial design for this area. Given the extent of the U concentrations, complex numerical modeling for this area may not be necessary based on the remedial approach.

## 2.0 HYDROGEOLOGIC FRAMEWORK

Much of the following has been extracted and paraphrased from the CSM-Rev 01 Report (ENSR, 2006). This section largely focuses on the parts of the CSM that were directly used in the modeling effort.

### 2.1 Site Setting

The Cimarron Site lies within the Osage Plains of the Central Lowlands section of the Great Plains physiographic province, just south of the Cimarron River (**Figure 1**). The topography in the Cimarron area consists of low, rolling hills with incised drainages and floodplains along major rivers. Most of the drainages are ephemeral and receive water from storms or locally from groundwater base flow. The major drainage included in the models was the Cimarron River, which borders the site on the north. This river drains 4,186 square miles of Central Oklahoma from Freedom to Guthrie, Oklahoma (Adams and Bergman, 1995). The Cimarron River is a mature river with a well-defined channel and floodplain. The stream bed is generally flat and sandy and the river is bordered by terrace deposits and floodplain gravels and sands (Adams and Bergman, 1995). In the area of the Cimarron Site, the ancestral Cimarron River has carved an escarpment into the Garber-Wellington Formation. Floodplain alluvial sediments currently separate most of the river channel from the escarpment. Surface elevations in the Cimarron area range from 930 feet above mean sea level (amsl) along the Cimarron River to 1,010 feet amsl at the former plant site. Between the river and the escarpment, the ground surface is flat relative to the variable topography of the escarpment and leading up to the uplands. Vegetation in the area consists of native grasses and various stands of trees along and near drainages. Soil thickness in the project area ranges from about one to eight feet.

### 2.2 Precipitation

Adams and Bergman (1995) summarized the precipitation for the Cimarron River Basin from Freedom to Guthrie, Oklahoma. Their study showed that precipitation ranges from an average of 24 in/yr near Freedom, Oklahoma, in the northwest part of the Cimarron River floodplain in Oklahoma, to 32–42 in/yr at Guthrie, Oklahoma. Wet weather years occurred between 1950 and 1991, 1973–1975, 1985–1987, and 1990–1991. The wettest months of the year are May through September, while the winter months are generally the dry months. The period from 1973 through 1975 had a total measured rainfall that was 23 inches above normal (Carr and Marcher, 1977). Precipitation data collected by the National Oceanic and Atmospheric Administration (NOAA) for Guthrie County, Oklahoma, from 1971 to 2000 indicates that the annual average precipitation is 36.05 inches.

### 2.3 General Geology

The regional geology of the Cimarron area and the site-wide stratigraphic correlations for the project area can be combined into a general geological model for the Cimarron Site (**Figure 2**). The site consists of Permian-age sandstones and mudstones of the Garber-Wellington Formation of central Oklahoma overlain by soil in the upland areas and Quaternary alluvial sediments in the floodplains and valleys of incised streams. The Garber sandstones dip gently to the west and are overlain to the west of the Cimarron Site by the Hennessey Group. The Wellington Formation shales are found beneath the Garber sandstones at a depth of approximately 200 feet below ground surface in the project area. The Garber Formation at the project site is a fluvial deltaic sedimentary sequence consisting of channel sandstones and overbank mudstones. The channel sandstones are generally fine-grained, exhibit cross-stratification, and locally have conglomeratic zones of up to a few feet thick. The sandstones are weakly cemented with calcite, iron oxides, and hydroxides. The silt content of the sandstones is variable and clays within the fine fraction are generally kaolinite or montmorillonite. The mudstones are clay-rich and exhibit desiccation cracks and oxidation typical of overbank deposits. Some of the mudstones are continuous enough at the Cimarron Site to allow for separation of the sandstones into three main units, designated (from top to bottom) as Sandstones A, B, and C. Correlation of these three sandstone units is based primarily on elevation and the presence of a thick mudstone unit at the

base of Sandstones A and B that can be correlated between borings. Within each sandstone unit, there are frequent mudstone layers that are discontinuous and not correlative across the project area.

The Cimarron Site is located on part of an upland or topographic high between Cottonwood Creek and the Cimarron River. The project site is dissected by shallow, incised drainages that drain northward toward the Cimarron River. Groundwater base flow and surface water runoff during storms have been ponded in two reservoirs (Reservoirs #2 and #3) on the project site. The Cimarron River is a mature river that has incised the Garber Formation, forming escarpments that expose the upper part of the Garber sandstones. Within the Cimarron Site, the Cimarron River has developed a floodplain of unconsolidated sands, silts, and clays that separate the Garber sandstones exposed in an escarpment from the main river channel. Surface drainages within the project site flow toward the Cimarron River. Geological features of each modeled area of the Cimarron Site are as follows:

- **BA #1 Area** – The upland is underlain by a sequence of sandstone and mudstone units, namely, from top to bottom, Mudstone A, Sandstone B, Mudstone B, and Sandstone C. The alluvium can be divided into a transitional zone located within the erosional drainage area and an alluvial zone located north of the escarpment line. The transitional zone consists predominantly of clay and silt and overlies Sandstone B or Mudstone B. A paleochannel appears to exist in the transitional zone, which may control the flow of groundwater in the vicinity of the upland in this area. The alluvium consists of mainly sand and overlies Sandstone C and Mudstone B. Additional descriptions of the geology of this area are included in the CSM-Rev 01 Report (ENSR, 2006).
- **Western Alluvial Area** – Alluvial sediments in this area consist of predominantly sand with minor amounts of clay and silt. Sandstone B and Mudstone B exist beneath the alluvial sediments near the escarpment and Sandstone C underlies the alluvial sediments farther out in the floodplain. Additional descriptions of the geology of this area are included in the CSM-Rev 01 (ENSR, 2006).

## 2.4 Site-Specific Geology

### 2.4.1 BA #1 Area

Geologic logs from seventy-five boreholes were used to describe the subsurface geology in the immediate vicinity of the Uranium (U) plume at the BA #1 area. The lithologic logs collected from borehole cuttings described the subsurface geology as a sequence of interbedded layers of near surface unconsolidated alluvial material and deeper consolidated sandstones and mudstones. The logs identified twenty-seven unique material types, which included unconsolidated materials of varying degrees of sand, silt, and clay, anthropogenically disturbed surficial deposits, and sedimentary rock. In an effort to simplify the conceptualization of the subsurface geology these twenty-seven different material types were collapsed into nine distinct material types representing strata with significantly different hydrogeologic characteristics. The four unconsolidated materials include, fill, sand, silt, and clay, and the underlying consolidated units include Sandstone A, Sandstone B, and Sandstone C, interbedded with two distinct mudstone layers (**Figure 3**). The simplified lithologic units describe, from the surface downward, fill material in the uplands and widely scattered silt in the upland and alluvial areas. In the alluvial areas this is underlain by a thick sandstone unit with a relatively thick bed of clay within the unit. The upland areas and beneath the alluvium consist of interbedded sandstone and mudstone. Because of varied topography and elevation the exposure of materials at the site varies widely. In the upland areas most of the exposed material is either sandstone or mudstone while in the alluvium most of the exposed material is either sand or to a lesser extent silt and clay. All data in the lithologic logs was used in the development of the model

### 2.4.2 Western Alluvial Area

The subsurface geology at the WA area was depicted by geologic logs from twenty boreholes near the escarpment. In contrast to the geology of the BA#1 area, the subsurface of the WA area is a relatively flat, "pancake" geology where Sandstone C, the lowest sandstone indicated in the BA #1 area, is overlain by a continuous unit of unconsolidated alluvial sand, which is overlain by an intermittent unit of unconsolidated clay

(Figure 4). A simplification of the information from the lithologic logs was not necessary for the WA and the inconsistent distribution of clay around the site was largely due to topography and the erosion of the clay in the low lying areas. All data in the lithologic logs was used in the development of the model

## 2.5 Hydrogeology

Groundwater flow through above-described regional geologic units is governed by recharge areas and discharge areas.

Regionally, recharge is precipitation (rain, snow, etc) that infiltrates past the root zone to the water table. As discussed above, the average annual precipitation rate is approximately 30 in/yr. Recharge to the alluvium and terrace deposits along the Cimarron River was estimated to be 8 percent of precipitation based on baseflow calculations and the assumptions of steady-state equilibrium in the alluvium and terrace sands (Adams and Bergman, 1995). Rainfall recharge to groundwater is therefore estimated to be approximately 2.4 in/yr ( $5.5 \times 10^{-4}$  ft/day).

Discharge of groundwater occurs at low points in the watershed and generally coincides with streams and lakes. At this site the Cimarron River is a local and regional discharge boundary. Average annual baseflow in the Cimarron River should equal average annual recharge indicating that the recharge and discharge rates are balanced.

Recharge to the groundwater system typically occurs at topographic highs. The application of this water to the groundwater system results in downward gradients in the recharge areas; that is, there is a component of flow downward in addition to horizontal. Conversely, discharge from the groundwater system occurs at the topographic low points in any given watershed, for instance at a stream, river, or lake. Because of this, groundwater gradients tend to be upward in these areas; that is, there is component of flow upward in addition to horizontal. The flow path of any given unit of groundwater depends on where in the watershed it originates as recharge and how far it has to flow to discharge.

## 2.6 Hydrologic Implications

The site-specific geology suggests several hydrologic implications including:

- The alluvial material was largely deposited by the historical meandering of the Cimarron River and the deposition of overbank deposits that result from intermittent floods on the river. This inconsistent and repeating depositional cycle resulted in a series of inter-bedded unconsolidated material types that are collectively referred to as alluvium, which on a small scale can exhibit variable hydrogeologic characteristics but on a larger scale can be considered collectively.
- Groundwater discharged from the Garber-Wellington formation largely discharges through the alluvial deposits on its way to its final destination, the Cimarron River.
- Since both the WA and the BA #1 areas are within the Cimarron River alluvial valley, both areas receive groundwater from both upgradient discharge of groundwater to the alluvial deposits and from subsurface discharge of water from the deeper aquifer to the alluvium and river system. In general, flow from the southern upgradient sandstones to the alluvium is characterized as horizontal flow and flow from the sandstone underlying the alluvium is characterized as having a component of vertical (upward) flow.
- The sandstone and siltstone/mudstones of the Garber-Wellington formation are relatively impermeable when compared to the unconsolidated alluvial sands adjacent to the river. This suggests that the water table gradient in the sandstone would be relatively steep when compared to the alluvial sand. This would further suggest that water could be more easily withdrawn from the alluvial sand than from the consolidated sediments occurring both beneath, and upgradient of the alluvial material.



- In addition, within the bedrock, the sandstone units have higher permeability relative to the mudstones. Therefore, more groundwater flow is expected to take place horizontally within these water bearing units, with less flow between the units.

The hydrogeologic characteristics of the Cimarron River alluvial system are typical of a relatively permeable aquifer system receiving groundwater from an adjacent, less permeable bedrock aquifer and transferring the groundwater to the discharge zone, in this case the Cimarron River.

## 2.7 Conceptual Model of Site Groundwater Flow

The Conceptual Site Model (CSM) of the Cimarron River flow system was developed prior to the development of groundwater models for the WA area and the BA #1 area. The CSM was incorporated into the groundwater models to ensure that the models used existing information and an accepted interpretation of the site-wide geology. The conceptual models for the WA area and the BA #1 area were developed separately and as such are discussed separately. However, it is recognized that the conceptual models for the two areas must be consistent.

### 2.7.1 The Cimarron River

The Cimarron River is a significant hydrogeologic boundary for the entire Cimarron Site. The headwaters of this river are in New Mexico and from there it flows through Colorado, Kansas, and Oklahoma. In the vicinity of the Site (Freedom to Guthrie, OK) the Cimarron River is a gaining river. That is, it is a discharge zone for groundwater. Groundwater flow into the river is controlled by the difference in elevation of groundwater and in the river and by the conductivity of the river bottom sediments. The elevation of the river changes seasonally, but this can be represented as an average annual elevation for this steady-state modeling effort. Changes in the elevation of the river may result in short-term changes in the groundwater flow directions and gradients in the nearby alluvial materials. However, over the long-term, an average elevation is appropriate to reflect the average groundwater flow system. Cimarron River streamflows and associated water level elevations in the immediate vicinity of the Western Alluvial area and BA#1 model domains has not been historically measured. The variability in river water levels at the site were estimated using long term flow records (1973 through 2003) from the USGS stream gages at Dover (30.0 miles upstream to the west) and Guthrie (10.3 miles downstream to the east). Daily averaged water level elevations at each of the two sites were averaged and the average water level elevation for the area of the model domains was determined through linear interpolation to be 925.0 feet. A further statistical evaluation indicated that the 5<sup>th</sup> percentile of water level elevations at the site was 924.1 feet and the 95<sup>th</sup> percentile of water level elevations was 927.7 feet; therefore, 90% of the time the Cimarron River water level at the site varies within a range of 3.60 feet.

### 2.7.2 BA #1 Area

Groundwater in the vicinity of the BA #1 Area originates as precipitation that infiltrates into the shallow groundwater in recharge zones, both near the BA #1 area and in areas upgradient of the BA #1 area. The amount of water flowing from the sandstones into the modeled area and into the alluvial material is controlled by the changes in groundwater elevation and hydraulic conductivities between the two units.

Local to the BA #1 area, infiltrated rainwater recharges the shallow groundwater in the area of the former disposal trenches and then flows into Sandstone B. The reservoir also contributes water to the groundwater system. This groundwater then flows across an escarpment that is an interface for the Sandstone B water-bearing unit and the Cimarron River floodplain alluvium, and finally into and through the floodplain alluvium to the Cimarron River. Flow in Sandstone B is mostly northward west of the transitional zone and northeastward along the interface with the transitional zone. Flow is driven by a relatively steep hydraulic gradient (0.10 foot/foot) at the interface between Sandstone B and the floodplain alluvium. Once groundwater enters the transition zone of the floodplain alluvium, the hydraulic gradient decreases to around 0.023 foot/foot and flow is refracted to a more northwesterly direction. The decrease in hydraulic gradient is due in part to the much higher overall hydraulic conductivity in the floodplain alluvium compared to Sandstone B (10–3 to 10–2 cm/s in

alluvium versus 10–5 to 10–4 cm/s in Sandstone B). The refraction to the northwest is primarily due to a paleochannel in the floodplain alluvial sediments. The direction of this paleochannel is to the northwest near the buried escarpment and then is redirected to the north as it extends farther out into the floodplain. Once groundwater passes through the transitional zone, it enters an area where the hydraulic gradient is relatively flat. Data indicates that the gradient in the sandy alluvium is approximately 0.0007 ft/ft. **Figure 3-4** in the CSM-Rev 01 Report (ENSR, 2006) presents a potentiometric surface map of Sandstone B and the alluvium for the BA #1 area based on groundwater level measurements during August/September 2004. Seasonal data between 2003 and 2005 indicate that although groundwater levels may change seasonally, the hydraulic gradients and groundwater flow directions do not change significantly over time (ENSR, 2006).

### 2.7.3 Western Alluvial Area

Groundwater in the vicinity of the WA area originates as precipitation that infiltrates into the shallow groundwater in recharge zones both near the WA area and in areas upgradient of the WA area. Most of the groundwater in the WA area comes from the discharge of groundwater from Sandstones B and C to the alluvial materials. The amount of water flowing from the sandstones to the alluvial material is controlled by the difference in groundwater elevation and hydraulic conductivities between the two geologic units. Groundwater flow in the WA area is generally northward toward the Cimarron River; flow is driven by a relatively flat hydraulic gradient of 0.002 foot/foot. **Figure 3-6** in CSM-Rev 01 Report (ENSR, 2006) presents a potentiometric surface map of the alluvium for the WA area based on groundwater level measurements during August/September 2004. As with the BA#1 Area, although groundwater levels may change seasonally, there is little change over time in hydraulic gradient and groundwater flow directions.

### 3.0 MODELING APPROACH

Groundwater flow at the two Cimarron sites (BA #1 and WA areas) was simulated using the three-dimensional MODFLOW model (McDonald and Harbaugh, 1988). The MODFLOW model uses a block-centered finite-difference method to simulate groundwater flow in three dimensions. The MODFLOW model was selected because of its wide acceptance by the technical community, because of its robustness, and because several Windows® based applications support the model, including the GMS 6.0® modeling package, which was used for this project. The GMS 6.0® software package is a visualization package that facilitates easy manipulation of the MODFLOW input and output files. In addition to using the MODFLOW groundwater model, the MODPATH particle tracking program was used to simulate the transport of groundwater particles within the model domain as a direct result of a flow field predicted by MODFLOW.

#### 3.1 Groundwater Model Domain

The domains of the BA #1 area and WA groundwater models were set up to include the specific areas of interest and all important boundary conditions.

For the BA #1 area, the specific area of interest was located northwest of the Reservoir #2 from the source area in the uplands, downgradient through the transition zone, and into the alluvial sands (**Figure 5**). The downgradient boundary was the Cimarron River and the upgradient boundary was along an east-west line coincident with the Reservoir #2 dam. Groundwater flow is primarily northward, so boundaries parallel to groundwater flow were set up at locations upstream and downstream along the Cimarron River far enough away from the high U concentrations and parallel to flow lines to not influence the interior of the model domain during pumping simulations. The lower boundary (i.e., bottom) of the BA #1 model domain was fixed at elevation 900 feet, well below the lower extent of the alluvial aquifer.

In the case of the WA area, the specific area of interest was located just downgradient of the escarpment along a north-trending line of high U concentrations (**Figure 6**). The downgradient boundary was the Cimarron River and the upgradient boundary was set at the escarpment. Groundwater flow is primarily northward so boundaries parallel to groundwater flow were set up at locations upstream and downstream along the Cimarron River far enough away from the high U concentrations to not influence the interior of the model domain during pumping simulations. The lower boundary (i.e., bottom) of the WA area model domain was fixed at 870 feet, well below the lower extent of the alluvial aquifer.

The model domain for the BA #1 area was set up to include the area from the upgradient reservoir to the south, to the Cimarron River to the north, and to distances east and west adequate enough to have a negligible effect on the interior of the model domain. The model was developed with grid cells that are 10 feet square in the X-Y plane and with 12 layers extending from the land surface down to a depth of elevation 900 feet, resulting in approximately 270,000 grid cells within the model domain.

The model domain for the WA area was set up to include the area from the escarpment to the south to the Cimarron River to the north and east and west to distances adequate enough to have a negligible effect on the interior of the model domain. The model was developed with grid cells that are 10 feet square in the X-Y plane and with 2 layers extending from the land surface down to a depth of elevation 870 feet, resulting in 97,830 grid cells within the model domain. The high density of grid cells within each model domain was selected for two reasons including: 1) to provide for a finely discretized model within the area of the U plume for testing the effects of groundwater pumping, and 2) to provide for adequate representation of the subsurface geology into discrete geologic material types, particularly for the BA#1 area.

### 3.1.1 BA #1 Area

The model layers for the BA #1 area were developed directly from the lithologic information from the seventy-two boreholes that were available for the site. A simplification of the original borehole data, which had originally described 27 unique lithologic types, was imported directly into the GMS 6.0® modeling platform, as the basis for the groundwater model. The simplified geology included the following geologic units/materials: 1) fill, 2) silt, 3) an upper sand unit, 4) clay, 5) a lower sand unit, 6) an upper sandstone unit (Sandstone A), 7) an upper mudstone (A), 8) a middle sandstone unit (Sandstone B), 9) a lower mudstone (B), and 10) a lower sandstone unit (Sandstone C). Each of the boreholes was reviewed in light of the surrounding boreholes to ensure that the inter-relationships between boreholes were realistic and representative of the CSM-Rev 01 (ENSR, 2006) developed for the site. Following the importation and adjustment of the borehole information, each layer in each of the seventy-two boreholes was assigned a Horizon ID to indicate the layer's position in the depositional sequence at the Site. The GMS 6.0® modeling platform was then used to "connect" the boreholes to form cross-sections based on the Horizon IDs assigned to each of the boreholes. Since a cross-section was developed for every adjacent borehole, this resulted in a total of one hundred sixty-five cross-sections; each of which was reviewed to ensure the sensibility of the interpretations. In cases where the cross-section did not make geologic sense, the cross-section was manually modified (Figure 7).

Once the cross-sections were developed and checked for accuracy, the GMS 6.0® program was used to develop three-dimensional solids of each material type within the intended model X-Y model domain. Each of the 3-D solids was represented by upper and lower TIN (triangularly integrated network) surfaces and was created using the previously developed cross-sectional data. Each of the solids types corresponded to the nine geologic units indicated by the lithologic information for the boreholes (Figure 8).

The model boundaries were identified and incorporated into the GMS 6.0® platform, including the location of the river boundary, the general head boundary, and the recharge boundary (discussed in the next section). One of the last steps in the development of the BA #1 area groundwater model was to develop a generic, twelve layer 3D grid that encompassed the model domain on a 10 ft by 10ft horizontal spacing. The next step in the development of the model was to assign hydrogeologic properties to each of the material types and boundaries and then transition all of the 3-D solids information to the 3-D grid that is used by the MODFLOW and MODPATH models (Figure 9). The final step was to make modifications to the distribution of material types (i.e., hydraulic conductivities) to adjust for the discrepancies between the mathematically interpreted version of the distribution of soil types and the interpretation of soil types based on the CSM (ENSR, 2006).

### 3.1.2 WA Area

The model layers for the WA area were developed directly from the lithologic information from the twenty boreholes that were available for the site. The borehole data was imported directly into the GMS 6.0® modeling platform as the basis for the groundwater model. Each of the boreholes was reviewed in light of the surrounding boreholes to ensure that the inter-relationships between boreholes were realistic and representative of the CSM, Rev.1 (ENSR, 2006) developed for the site. Following the importation and adjustment of the borehole information, each layer in each of the twenty boreholes was assigned a Horizon ID to indicate the layer's position in the depositional sequence at the site. The GMS 6.0® modeling platform was then used to "connect" the boreholes to form cross-sections based on the Horizon IDs assigned to each of the boreholes. Since a cross-section was developed for every adjacent borehole, this resulted in a total of forty-one cross-sections; each of which was reviewed to ensure the sensibility of the interpretations. In cases where the cross-section did not make geologic sense, the cross-section was manually modified (Figure 10).

Once the cross-sections were developed and checked for accuracy, the GMS 6.0® program was used to develop three-dimensional solids of each material type within the intended model X-Y model domain. Each of the 3-D solids was represented by upper and lower TIN (triangularly integrated network) surfaces and was created using the previously developed cross-sectional data. Each of the solids types corresponded to the three geologic units indicated by the lithologic information for the boreholes (Figure 11). It should be noted that the geologic materials in the WA area consisted only of sandy alluvium and the underlying bedrock (Sandstone C), so this process was much simpler than for the BA#1 area.



The model boundaries were identified and incorporated into the GMS 6.0® platform including the location of the river boundary, the general head boundary, and the recharge boundary (discussed in the next section). One of the last steps in the development of the WA area groundwater model was to develop a generic, two layer 3D grid that encompassed the model domain on a 10 ft by 10 ft horizontal spacing. The final step in the development of the model was to assign hydrogeologic properties to each of the material types and boundaries and then transition all of the 3-D solids information to the 3-D grid that is used by the MODFLOW and MODPATH models (Figure 12).

### 3.2 Hydrogeologic Physical Properties

The physical property most commonly used to characterize subsurface permeability is the hydraulic conductivity. This parameter is applied to Darcy's Law as a proportionality constant relating groundwater flow rate to groundwater gradient and cross-sectional area, and is a measure of the ability of a soil matrix to transport groundwater through the subsurface. Hydraulic conductivity values are required to describe the permeability of each cell in the MODFLOW groundwater model because Darcy's equation is used by the model to solve for groundwater head in each model cell. If hydraulic conductivity values in the model area were spatially the same, the multiple model layers could act as a single layer. However, this degree of uniformity is not evident at the Cimarron site, so each model layer was assigned a unique horizontal and vertical hydraulic conductivity value consistent with the geology assigned to that layer.

In the case of the BA #1 area model, the MODFLOW model represents the complicated ten layer geologic system of largely continuous material types with twelve model layers. From the surface downward these include, 1) fill, 2) silt, 3) an upper sand unit, 4) clay, 5) a lower sand unit, 6) an upper sandstone unit (Sandstone A), 7) an upper mudstone (A), 8) a middle sandstone unit (Sandstone B), 9) a lower mudstone (B), and 10) a lower sandstone unit (Sandstone C). A single, constant hydraulic conductivity value was assigned to each of these 10 material types.

In the case of the WA area model, the MODFLOW groundwater model represents the (simple relative to the BA #1 model) subsurface by assigning the two dominant material types (sand and sandstone) to two different model layers. (Note: even though clay was present in the boring logs, it was not saturated, therefore was not modeled). These are 1) a sandy alluvium layer beneath the clay layer and exposed at several locations throughout the site and 2) an underlying sandstone layer beneath the sandy alluvial aquifer (Sandstone C). A single, constant hydraulic conductivity value was assigned to each of the two layers.

Hydraulic conductivity values for both the alluvium and the sandstone were derived from slug and pumping tests conducted during the field investigations, as described in the Burial Area #1 Groundwater Assessment Report (Cimarron Corporation, 2003). Table 1 summarizes the findings from these tests. Results for the alluvium ranged from 0.04 to 312 ft/day with a median value of 38 ft/day. Results for the sandstones ranged from 0.07 to 2.83 with a median value of 0.35 ft/day. The conductivity values are consistent with literature (Freeze & Cherry, 1979).

In general, the vertical hydraulic conductivity is assumed to be less than the horizontal because of the interbedding that occurs during sedimentary deposition. While relatively small layers and lenses of fine material do not significantly effect the lateral movement of groundwater they can effect the vertical movement by creating more tortuous pathway for groundwater flow, and resistance to vertical flow. In general, the vertical hydraulic conductivity in sedimentary or alluvial deposits can be 1 to 30% of the horizontal hydraulic conductivity.

The alluvial materials (sand, clay, silt) were assumed to have vertical components of flow consistent with a sedimentary environment. Therefore, the vertical hydraulic conductivity of the alluvial materials was set to 10% of horizontal hydraulic conductivity. For the sandstones and mudstones, the vertical hydraulic conductivity was set to 5% of horizontal hydraulic conductivity. The groundwater flow in sandstone and mudstone may be controlled not only by primary (matrix) pathways, but also secondary (remnant fracture) pathways. However, there is no data (i.e., groundwater elevation data) to suggest that fractures flow is significant at this site, especially on the scale of the entire model domain. Note that the conceptual

understanding of fractures at this site is that most of fractures occur on bedding planes (i.e., in the horizontal direction); thus, flow in the stone fractures would be controlled by horizontal hydraulic conductivity, not the vertical.

Anisotropy values are used if there is some reason to believe that the aquifer has a substantially different permeability along one horizontal axis than another. This is not believed to be the case in either the WA area or the BA #1 model domain and therefore the horizontal anisotropy was assumed to be unity.

### 3.3 Boundary Conditions

The boundary conditions at the perimeter of the model domain play an important role in the outcome of a groundwater simulation because of the dependence of hydraulic behavior within the interior of the model on the water levels and fluxes fixed at the model boundaries. Ideal model boundaries are natural hydrogeologic features (i.e., groundwater divides, rivers). Recharge to groundwater is also a boundary condition. Model predictions can be inaccurate when the areas of interest in the model domain are too close to a poorly selected boundary condition. In the absence of natural hydrogeologic boundaries, boundaries are chosen at distances great enough such that they do not affect the outcome of simulations in the area of interest. In the groundwater models of the Cimarron Site, the downgradient boundary was selected to coincide with the Cimarron River, a natural hydrogeologic boundary. Since there are no nearby natural features for the other boundaries, the domain was extended to distances sufficient such that simulations would not be significantly affected by the model boundaries.

#### 3.3.1 Recharge

Recharge to groundwater is simulated using the MODFLOW Recharge Package. This package can be used to apply a spatially and temporally distributed recharge rate to any layer within a model domain. In general, the recharge package is used to represent the fraction of precipitation that enters the subsurface as rainfall recharge directly to the groundwater water table. In model domains representing relatively small geographic regions, and without significant variability in site wide precipitation, the recharge package is applied uniformly throughout the model domain. The recharge package can be temporally varied in unsteady simulations to predict system response to unique or seasonal events but can be applied at a constant rate for steady state simulations. For the steady-state simulation of groundwater flow at the two Cimarron sites the recharge package was applied uniformly over the entire model domains at a constant rate. Since the model was steady-state and no losses of groundwater were assumed, the recharge rate, determined through model calibration, was expected to be similar to the rate indicated in the CSM-Rev 01 (ENSR, 2006) of 8% of precipitation or 2.4 in/yr.

#### 3.3.2 Surface Water/Groundwater Interactions

The Cimarron River is included in each of the models, as it is the regional groundwater discharge point. The Cimarron River is represented in the model domain using the MODFLOW River Package. The channel bed elevations at these sites were linearly interpolated from the gage datum of 999.2 feet at the USGS stream gage at Dover, OK (#07159100) located about 30 miles upstream, and the gage datum of 896.5 feet at the USGS stream gage at Guthrie, OK (#07160000) located about 10 miles downstream. The resulting value of 922.8 feet was assigned as the river bed elevation for both the BA #1 and WA areas. The surface water elevations were assumed to be 2 feet higher than the bed elevations at both locations resulting in a constant water surface elevation of 924.8 feet.

Depending on the difference between the measured river surface elevation and the predicted groundwater elevation in the cells adjacent to the river cells, the river will either be simulated to lose water to the aquifer or gain water from the aquifer. Based on the topography and hydrogeology of the site, the streams and rivers are generally expected to gain groundwater. The rate of water gain or loss from the Cimarron River is represented in MODFLOW using three parameters that include (1) the river bed area, (2) the channel bottom thickness, and (3) the hydraulic conductivity of the river bed sediments. While the product of the hydraulic conductivity

and the riverbed area divided by the bed thickness results in a conductance term (C), this value was established through model calibration rather than being calculated, due to a lack of site-specific information.

Model cells that were assigned river properties are shown with blue dots on **Figures 9 and 12** for the BA #1 and WA models, respectively.

The reservoir south of the BA#1 area was incorporated into the General Head Boundary condition as described below. None of the other intermittent surface waters, such as the drainageways, were included in the model, as their influence on the groundwater system is local and sporadic.

### **3.3.3 Upgradient General Head Boundary**

The upgradient boundaries for both the BA #1 and the WA area were represented as a General Head Boundary (GHB) in MODFLOW. Unlike a constant head boundary, which holds the water level constant and offers no control over the amount of water passing through the boundary, the GHB offers a way to limit the supply of upgradient water entering the model domain. This limitation provides a better representation of the system that is limited by the transfer of groundwater from the upgradient aquifer to the upgradient model boundary. The general head boundary requires the designation of a head, or groundwater elevation along the boundary, and conductivity. The head assigned to the GHB defines the groundwater level at the boundary and largely dictates the downgradient water levels and the gradients. The conductivity of the GHB defines the permeability of the boundary and controls the amount of water that can pass through the boundary. Water can pass into or out of the model domain through the general head boundary, depending on the relative hydraulic heads.

### **3.3.4 Underlying General Head Boundary**

In addition to representing the upgradient boundary using a GHB, the upward hydraulic gradient from the underlying bedrock described in the site CSM-Rev 01 (ENSR, 2006) can also be represented this way. Because the Cimarron River is a major discharge area, the discharge of deep groundwater through the alluvium and into the river is an expected phenomenon. To simulate this upward flow of groundwater a GHB was used in both model domains to varying degrees to represent a higher water level at depth than in the alluvial aquifer. The volumetric flow rate of water into the alluvial aquifer was limited by adjusting to a relatively low conductance during the calibration process.

Some of the model cells that were assigned general head boundary properties are shown with brown dots on **Figures 9 and 12** for the BA #1 and WA models, respectively. Other cells were also assigned this boundary type, but are not visible in this view of the model domain. Basically, all cells at the base of the models and at the southern limit were assigned GHB boundaries.

## **3.4 Summary of Modeling Approach**

Model parameters used to setup the groundwater models for the BA #1 and WA areas were developed from measured information and from interpretations made based on material characteristics. These parameters largely control the predictions made by the groundwater and pathline models.

## 4.0 MODEL CALIBRATION

### 4.1 Calibration Approach

Once the model domain was established, the model grid developed, and the model inputs entered, the calibration process began. The calibration process is a quality control step used to provide a frame of reference for evaluating simulation results. The calibration of groundwater models proceeds by making adjustments to the boundary conditions and the hydraulic conductivities until the simulated groundwater elevations adequately match the observed groundwater elevations. In addition to comparing model predicted elevations to observed elevations, a good calibration was also dependent on capturing gradients and flow directions such that simulated flow paths were congruent with inferred flow paths from U concentration data. The overall regional water balance was also considered. The following sections (4.1.1, 4.1.2, and 4.1.3) discuss the three ways the model calibration was evaluated.

#### 4.1.1 Measured and Predicted Water Levels

Comparing model predicted groundwater levels with measured levels is a rigorous, obvious, and straightforward way to evaluate the ability of a groundwater model to meet the project objectives. In steady-state models the groundwater predictions are generally compared with representative average groundwater water levels at several locations around the site. Since a single round of groundwater elevation measurements may not be representative of the average water table due to seasonal variations, it is preferable to use the results of several temporally distributed water level surveys to provide a better representation of the average water table.

The water level data used to evaluate the BA #1 and WA groundwater model calibrations was from each of the wells/boreholes used to develop the models. Water levels from each of four surveys including September 2003, December 2003, during August and September of 2004, and in May of 2005 were averaged to arrive at a set of average water levels for comparison to model predictions. **Table 2** summarizes the average groundwater elevations from four sampling rounds. This data set served as the calibration data set.

During the calibration, the model calibration parameters were adjusted in order to reach a quantitative target: the mean absolute difference between the predicted and measured water levels within 10% of the measured site-wide groundwater relief.

For the BA #1 area, the maximum groundwater elevation was 950.96 feet at Well 02W51 and the minimum elevation was 925.37 feet at Well 02W17; therefore, the calibration target is 10% of that difference or approximately 2.6 feet.

For the WA area, the maximum groundwater elevation in the model domain is 931.75 feet (at T-63) and the minimum elevation is 930.35 feet (at T-82), then the calibration target of 10% of the difference is approximately 0.14 feet.

In addition, it is recognized that the two models, although developed separately, must be consistent with each other. That is, values for inputs between the two models cannot be significantly different from each other.

#### 4.1.2 Volumetric Flow-Through Rate

Both of these models are dominated by the boundary conditions, that is, the boundary conditions have a strong influence on the model results. Therefore, in addition to simply matching steady-state water levels in the model domain by successive adjustment of aquifer properties and boundary conditions, comparing estimated steady-state flow-through rates was also considered as a means for evaluating calibration. There are a variety of ways to estimate a flow-through rate based on drainage area, baseflow, recharge, etc. This



section discusses one of the methods using one set of input values. Though not a rigorous calibration target, it is important to be mindful of the water budget, or flow-through volumes for the models. Therefore, the estimate of flow-through rate presented here is intended to provide a general, again not rigorous, frame of reference by which to evaluate the calibration.

One estimate of the steady-state flow rate through each model domain was made by multiplying an estimate of rainfall recharge by the total drainage area to arrive at an annual recharge rate. This recharge volume represents the water that enters the groundwater system over the entire watershed – not just the model domain and/or immediate site vicinity. However, this entire volume will pass through the model domain on its way to the regional discharge boundary – The Cimarron River. During the calibration process, the model boundary conditions were adjusted in consideration of this calculated annual flow-through rate. Note that in making this estimate, it is assumed that the surface water divides as represented from the topographic contours coincide with groundwater divides.

For the BA #1 area, the total drainage area upgradient and including the model domain is approximately 2.1 square miles. Based on an annual recharge rate of 2.4 in/yr over the BA #1 watershed, the total flow through rate for the BA #1 model domain was estimated to be approximately 32,000 ft<sup>3</sup>/day. For the WA area, the total upgradient drainage area and model domain is 0.32 mi<sup>2</sup> resulting in an estimated total flow through rate of the WA model domain of approximately 5,000 ft<sup>3</sup>/day.

During the calibration process, adjustments of hydrogeologic characteristics and boundary conditions were made in light of these estimates of flow. Comparing these estimates with the calibrated results provides one way to evaluate calibration.

#### 4.1.3 Plume Migration

In addition to accurately reproducing water levels and volumetric flow rate through the groundwater system, a pathline analysis was conducted to demonstrate an accurate representation of groundwater movement in the system. This was especially important for BA #1 area where there is ample water quality data by which to infer flow paths. In the case of the BA #1 site, the current distribution of the U plume was compared to predicted particle pathlines developed from particles initiated in the original U source area. By demonstrating that particles seeded in the source area would effectively follow the path of a measured plume, the pathline simulation can illustrate the accuracy of the model in representing flow directions and groundwater gradients.

For the BA #1 area, the MODPATH model was used to predict the fate of particles seeded at the approximate location of the initial U source. The results of the steady-state MODFLOW model were used as the groundwater flow driver for the MODPATH simulation and the predicted paths of the particles were compared with the plume map for U at the BA #1 area. For the simpler WA model, a pathline comparison was not required.

#### 4.2 Calibration Parameters

For both of these models there are strong boundary conditions. These are the general head boundary at the upgradient (south) edge of each of the models to simulate water entering the model domain from the sandstones, the general head boundary along the bottom of the models to simulate flow up from the sandstone into overlying soils, and the river where groundwater discharges. Flow and elevations in the model are dominated by the flow entering the model through the general head boundaries and flow leaving the model through the river. When models are so strongly influenced by these boundary conditions, calibrated solutions can result from a variety of non-unique combinations of boundaries and hydraulic conductivities.

Early in the calibration process, adjustments to hydraulic conductivity, recharge rate, and river conductance were made to simulate groundwater elevations similar to measured groundwater elevations. Once these initial adjustments were made, calibration focused on adjusting the head and conductance of the general head boundaries.

The general head boundary uses two variables to control the transfer of water across a model boundary including a water level (head) and a conductance term. The assigned groundwater elevation indicates the pressure head along the boundary. This is essentially the starting point for predicted heads along the boundary and adjacent water levels in the model are either higher or lower depending on boundary conditions and the additions or losses of water elsewhere within the model domain. The rate at which water enters the model through the general head boundary is controlled by the conductance term. A high conductance indicates a relatively limitless supply of water to the aquifer when the water table downgradient of the boundary is stressed and a low conductance indicates a limited supply of water to the aquifer. Limiting the conductance is of particular importance if only a portion of the total aquifer is included within the model domain and it is unrealistic to assume that the upgradient supply of water is limitless.

Each groundwater model was re-run several times with successive adjustment to the calibration parameters (general head boundaries) until the models were satisfactorily calibrated.

### 4.3 Calibration Results

In the following sections the results of each model's calibration is discussed with respect to the calibration targets discussed in Section 4.1.

#### 4.3.1 BA #1

In the calibration process, hydraulic conductivity, recharge, and river elevation and conductance were adjusted; the final calibration values are summarized in **Table 3**. The other adjusted parameters were the elevation and the conductance of the general head boundaries both at the back edge and on the bottom of the model. **Table 3** also includes the calibrated values for these inputs.

Through successive adjustment of the general head boundary parameters, the mean absolute error (MAE) between the measured and predicted water levels was calculated to be 1.2 feet. This value is much less than the 2.6 feet which is 10% of the total water table relief at the site; this indicates an acceptable model calibration. Additional adjustments to the shape and orientation of the underlying general head boundary were made to simulate flow paths (using MODPATH) consistent with that which is inferred from the concentrations downgradient of the burial area. Finally, adjustments to the general head boundary were also made to simulate an approximate flow-through volume consistent with what is expected based on the drainage area size and recharge rate. The following are calibration results that indicate transfer rates of groundwater through the BA #1 model domain.

- Calibrated transfer rate of water from the model domain to the Cimarron River is 19,100 ft<sup>3</sup>/day.
- Calibrated inflow rate from upgradient sandstone/mudstone units to the model domain is 16,900 ft<sup>3</sup>/day.
- Recharge rate to the aquifer is 1,200 ft<sup>3</sup>/day.

The difference between the total inflow (18,100 ft<sup>3</sup>/day) and the total outflow (19,100 ft<sup>3</sup>/day) equals ~1,000 ft<sup>3</sup>/day, which represents less than a 5% error in the water balance and is considered acceptable. **Figure 13** summarizes the calibration results showing the measured versus predicted groundwater elevations, the static simulated groundwater contours and a comparison of the particle pathlines originating from the burial area with the plume map as drawn from concentrations measured in August 2004. In the calibration process, targets with the best data (i.e., water level, flow path) are given preference over targets with less data (i.e., flow through rates). Thus, a good match of water levels, flow paths, and gradients is achieved, but justifiably at the expense, somewhat, of the flow-through match. The total calibrated flow through value above is less than the calculated flow-through rate based on drainage area and recharge presented in **Section 4.1.2**.

One of Arcadis' bioremediation design objectives is to estimate flux (dissolved oxygen) through the plume. Based on the calibrated flow-through rates, ZoneBudget (Harbaugh, 1990) was used in conjunction with the

MODFLOW output to calculate the flux through the plume areas only. The 2004 plume area for the BA #1 area is depicted on Figure 4-11 (CSM, Rev.1, ENSR, 2006); the plume was assumed to extend to the bottom of model Layer 7, which coincides with the lowest elevation where concentrations over 180 pCi/L were detected in August 2004. The flux was estimated at 19 gpm.

#### 4.3.2 WA area

In the calibration process, hydraulic conductivity, recharge, and river elevation and conductance were adjusted and the final calibration values are summarized in **Table 4**. The other adjusted parameter was the elevation and the conductance of the general head boundaries both at the back edge and on the bottom of the model. **Table 4** also includes the calibrated values for these inputs.

Conceptually the interaction of the sandstones with the alluvial materials should be very similar regardless of model area. That is, the conductance of Sandstone B and Sandstone C should be the same for the BA #1 model and for the WA model. Because the BA #1 model is so much more complicated, it was calibrated first and then the calibrated conductance values were applied to the WA model. In effect, calibration of the WA model relied almost exclusively on changing the elevations assigned to the general head boundaries.

Through successive adjustment of the general head boundary elevation the average absolute error between the measured and predicted water levels was determined to be 0.31 feet. This value is more than the target of 0.14 feet, which is 10% of the total water table relief at the site. When the gradient is very flat as it is in this case measured groundwater elevation differences over short distances can be very difficult to simulate, especially when spatial variations in hydraulic conductivity are not considered. Furthermore, because the calibration data set is averaged over several rounds of data, seasonal differences may be more apparent.

The flow paths generated based on the MODFLOW head field and the MODPATH model indicates that groundwater flow paths are generally from the south to the north, consistent with the conceptual model and with the inferred flow paths based on U concentrations from August 2004.

The following are calibration results that indicate transfer rates of groundwater through the WA area model domain.

- Calibrated transfer rate of water from the aquifer to the Cimarron River is 57,000 ft<sup>3</sup>/day.
- Calibrated inflow rate from upgradient sandstone/mudstone units to the model domain is 54,300 ft<sup>3</sup>/day.
- Recharge rate to the aquifer is 2,600 ft<sup>3</sup>/day.

The difference between the total inflow (56,900 ft<sup>3</sup>/day) and the total outflow (57,000 ft<sup>3</sup>/day) equals ~100 ft<sup>3</sup>/day, which represents less than a 1% error and is considered acceptable. **Figure 14** summarizes the calibration results showing the measured versus predicted groundwater elevations and the static simulated groundwater contours. In the calibration process, targets with the best data (i.e., water level, flow path) are given preference over targets with less data (i.e., flow through rates). Thus, a good match of water levels, flow paths, and gradients is achieved, but justifiably at the expense, somewhat, of the flow through match. The total flow through value presented above is more than the flow-through rate calculated based on drainage area and recharge presented in **Section 4.1.3**.

One of Arcadis's bioremediation design objectives is to estimate flux (dissolved oxygen) through the plume. Based on the calibrated flow-through rates, ZoneBudget (Harbaugh, 1990) was used in conjunction with the MODFLOW output to calculate the flux through the plume areas only. For the WA model the total U distribution was assumed to be an area that extends from near the base of the escarpment northward toward the Cimarron River, apparently originating where the western pipeline entered the alluvium north of the former Sanitary Lagoons. Uranium concentrations that exceeded 180 pCi/L in August 2004 are presented in Figure 4-15, CSM-Rev 01, ENSR, 2006). This impacted area extended only to the bottom of model Layer 1 since

there were no concentrations of U detected in the sandstone (i.e., Layer 2). The flux for this plume area was 31 gpm.

### 4.3.3 Discussion

In addition to evaluating the calibration of the model from the standpoint of quantitative targets, another way to evaluate the model is how well it aligns with the conceptual model. Because there is often aquifer test data (i.e., slug tests, pumping tests), comparison of calibrated and measured hydraulic conductivities is a good way to evaluate how well the model corresponds with the conceptual model. **Table 1** summarizes the measured hydraulic conductivities and **Tables 3 and 4** summarize the calibrated hydraulic conductivities. **Tables 3 and 4** also summarize the calibrated inputs for the river, recharge, and general head boundaries.

There are no measured hydraulic conductivity data for Fill, Silt, Clay, and Sandstone A. For Alluvium, the measured hydraulic conductivity values range from about 20 to more than 275 ft/day. Pumping tests generally provide a better estimate of aquifer hydraulic conductivity than slug tests. Focusing on just pumping test results, the hydraulic conductivity ranges from about 120 to about 275 ft/day. The calibrated value, 235 ft/day, is consistent with this range.

Slug test data was also available from four wells screened in Sandstone B. The hydraulic conductivity results ranged from approximately 0.1 to 2 ft/day. The calibrated value for Sandstone B was 5 ft/day. One slug test was completed in Sandstone C and the result was 0.2 ft/day, less than the calibrated value of 3 ft/day. In both instances, the calibrated values are higher than the measured. Values derived from pump tests and values from calibrated models are often higher than slug test data. The locations of slug tests represent only a tiny fraction of each Sandstone B and C. During model calibration, the values are adjusted upward and may ultimately be more representative of site conditions than just a few data points may indicate.

In some instances, the hydraulic conductivities were adjusted upward to provide numerical stability to the model. The model can become numerically unstable when there are large changes (in hydraulic conductivity, groundwater elevation, etc) over short distances. In the BA#1 model this happens, for instance where clay (hydraulic conductivity less than 1 ft/day) comes into contact with sand (over 200 ft/day). This instability can be mitigated by smoothing those contrasts. Sometimes this is done at the expense of making a perfect match with measured data. As long as the adjustments are consistent with the conceptual model, the conceptual understanding of how different soils transmit water, and are mindful of the project objectives, smoothing typically does not impact simulations. The model will simulate this general behavior whether the contrast is 100 or 1000 times different. This change was evaluated in the sensitivity analyses, discussed below.

In the absence of data for fill, silt, clay and Sandstone A, estimates were made based on literature values and on qualitative site observations. Adjustments to these values were made during the calibration to encourage a good match of simulated and measured groundwater elevation and to encourage numerical stability.

**Figures 13 and 14** summarize the calibration results. The graph shows the measured versus predicted groundwater elevations. Each point represents the groundwater elevation at a particular well. The closer the point is to the line, the less difference there is between the simulated and observed groundwater elevation. These figures also show the simulated groundwater contour map. Overall these match well for both models. For the BA#1 model, **Figure 13** also shows a comparison of a particle pathline originating from the Burial Area with the plume map as drawn from U concentrations measured on August 2004. As discussed above, these pathlines are a good match for the groundwater flow paths suggested by the distribution of U in groundwater.

### 4.3.4 Summary of Calibration Results

Three calibration targets were set as objectives prior to model calibration: achieve a good match between simulated and measured groundwater elevations and gradients, achieve a good match with the site conceptual model, and yield relatively consistent correlation of water budget estimates. For the most part, the first two objectives were achieved without difficulty. The measured and simulated groundwater elevations are in



concert and especially for the BA#1 model, the simulated flow directions agree with flow directions indicated by U concentrations. Discrepancies between measured and simulated groundwater elevations, flow paths, and water budgets are explainable and can be accounted for when interpreting simulation results. Ultimately, the discrepancies in estimated flow-through volumes and simulated flow-through volumes are explained by ranges in recharge to and discharge from the site as well as uncertainties inherent in the modeling.

#### 4.4 Sensitivity Analysis

In order to characterize the effects of uncertainty in the modeling parameters (recharge, hydraulic conductivity, and general head boundaries) on model predictions, sensitivity runs were conducted. In these runs, each parameter was varied from the base run (calibrated model). Differences were noted and these differences help in understanding the range of possible predictions, and how uncertainties in these parameters may affect model predictions.

Rainfall recharge, hydraulic conductivity and the general head boundary were the three primary variables tested in the sensitivity evaluation. Rainfall recharge has a direct impact on the amount of water moving through the aquifer and an impact on the amount of water that can be withdrawn from an aquifer. The conductivity is the fundamental parameter describing how effectively groundwater is transmitted in an aquifer. The sensitivity evaluation was focused on the hydraulic conductivity of the sand. The upgradient head boundary and the aquifer bottom boundary in the model of the BA #1 area were both represented using the general head boundary (GHB) in MODFLOW. This boundary fixes a water level at a specific group of cells in a model domain and uses a conductance term to facilitate the calculation of the volume of water that can be moved across the general head boundary. Like recharge, the general head boundary has a significant effect on the hydrologic budget and can largely control the amount of water entering or leaving the model domain. Therefore the models' sensitivity to this parameter was evaluated also.

One parameter was adjusted to complete the sensitivity analysis of the BA #1 area to enable this already complex and numerically sensitive model to iterate to a solution under the range of conditions imposed by the sensitivity analysis. During the sensitivity analysis, the horizontal hydraulic conductivity of the clay was increased from the 0.5 ft/day that was used during the model calibration, to 10 ft/day. By increasing the hydraulic conductivity of the clay, the gradients were decreased resulting in a smoother transition across adjacent model cells and therefore, a more stable model.

With the parameters selected for the sensitivity analysis a sequence of model scenarios were developed and run to evaluate the effect of varying the magnitudes of the selected parameters on the calibration. The results are as follows.

For the BA #1 area, with the increased hydraulic conductivity of the clay, calibration results were marginally different results then when the original calibrated clay conductivity value was used.

Modification of the recharge rate by a factor of 50% and 200% resulted in only minor changes to the steady-state head calibration. This is largely because of the relatively small component of the hydrologic budget that surface recharge represents in the calibrated model, which is less than 10% of the overall budget.

Changing the hydrologic conductivity in the sand aquifer by a factor of 50% and 200% resulted in a relatively minor change to the steady state calibration. Small differences in the Mean Absolute Error (MAE) between the calibration run and the sensitivity runs are primarily because the Mean Absolute Error value is calculated using several wells outside of the sand aquifer that were relatively unaffected by the change and because the flow regime is so strongly controlled by the recharge and discharge boundary conditions.

Changes made independently to the head and the conductance of the subsurface general head boundary by factors of 50% and 200% resulted in fairly substantial changes to the steady state calibration. This is because water flowing into the model through the subsurface general head boundary represents a significant portion of

the total water budget in the model. Both the elevation and the conductance are strong controllers of how much water is permitted to enter the model, thus have obvious impacts to model predictions.

## 4.5 Uncertainties and Assumptions

In order to fully understand the predictions and simulations, it is important to understand the factors that contribute to model uncertainty. Addressing these uncertainties allows users to understand and interpret the results of the simulations.

### Flow-Through Volumes

As discussed above, estimates of flow-through volume were made based on drainage area and recharge rates. Comparing these estimates to simulated flow-through volumes was one way calibration was evaluated. Other methods can also be used to estimate flow-through volumes. For instance, one method varies recharge rates based on the ranges of annual precipitation rates of 24 inches, 30 inches, 32 inches, and 42 inches (CSM-Rev 01, ENSR, 2006). Another method uses streamflow measurements collected by the USGS on the Cimarron River at Dover (upstream) and Guthrie (downstream) and basin scaling to estimate the rate of groundwater discharge from the Western Alluvial area and the Burial Area #1. These approaches indicated that flow-through volume estimates may range over more than an order of magnitude depending on the methodology for making the estimate. In turn, depending on the technique to calculate flow-through volumes, different groundwater fluxes through the plume areas may be calculated.

### Equivalent Porous Media Assumption

The MODFLOW model assumes that flow is through a porous media. That is, MODFLOW is designed to model groundwater flow through unconsolidated materials. MODFLOW is often used to model consolidated soils and bedrock, but flow through these materials may be governed by fractured flow, not porous media flow. The presence of fractures may greatly affect the direction and rate of groundwater flow especially on a local scale. For example, if the local groundwater flow system is dominated by a single fracture, the orientation of the fracture will control the direction of travel. Depending on the fracture's size, groundwater velocity through the fracture may be higher than would occur in more diffuse flow through a porous media even if the flux is the same. There is no evidence that groundwater flow and contaminant transport at the Cimarron Site are necessarily controlled by fracture flow. However, there may be local effects associated with fracturing the bedrock units. It is beyond the capabilities of the current model to accurately predict the time of travel through fractures in the consolidated soils or bedrock. Travel times through the consolidated units (sandstones and mudstones) can be calculated by MODPATH based on the assumption that the consolidated units are an equivalent porous media. The use of equivalent porous media assumptions are best suited for predictions over the scale of the model and may not provide accurate predictions local to a fracture or fracture system. Despite this uncertainty, groundwater flow is still likely to coincide generally with the surface water catchments and groundwater will discharge to the surface waters located within and adjacent to the site.

### Steady-State Assumption

If the model should be used to simulate either groundwater extraction or injection, it should be noted that the groundwater model assumes that steady-state is reached instantaneously. In fact, there will be some time that will elapse before steady-state will be reached. Simulated pumping or injection also assumes that groundwater will be extracted from or injected into the entire cell saturated thickness. In fact, depending on where the well screen is placed and where the pump is set, this may not hold true. Simulated pumping or injection also occurs throughout the entire 10 foot by 10 foot cell. For these reasons, pumping and injection scenarios implemented in the field may result in drawdown and flow rates different from what has been predicted. Because the model accurately represents the conceptual model and overall observed flow rates, directions, and gradients, overall capture zones should be relatively accurate. As field data become available, they may be used to update and refine the model.

### Fate and Transport Issues

It should be noted that this application is a flow model and, as such, only considers the movement of water in the subsurface. Constituents dissolved in groundwater may be subject to processes that result in migration that cannot be explained exclusively by groundwater velocity (i.e., advection).

Groundwater velocities generated by the model and presented in the CSM, Rev.1 (ENSR, 2006) require input of a value for porosity for each of the geologic materials. There are no site-specific data on porosities, and they are likely to be very variable. Literature values were used. It should be recognized that the calculated velocities are directly dependent on these input values of porosity. Changes to the porosity values could potentially change estimate velocities by more than an order of magnitude.

## 5.0 SUMMARY AND CONCLUSIONS

Numerical groundwater models for the BA #1 and the WA areas have been conceptualized, developed, and calibrated to provide tools by which groundwater flow can be evaluated and changes to groundwater flow can be assessed as different remedial alternatives are simulated. In particular, in consideration of a bioremediation approach, the model may be used design scenarios for injection of reagents that will enhance stabilization of U and to demonstrate the permanence of uranium stabilization in groundwater.

The objective was achieved by developing and calibrating the numerical models to include key data that characterize groundwater flow at the site consistent with the CSM-Rev 01 (ENSR, 2006). Specifically, the BA #1 model domain included portions of the uplands at the site, which are underlain by a series of sandstone and mudstone layers, the transition zone, which is characterized by silts and clays underlain by sandstone and mudstone, and the alluvial valley where the geology is predominantly sand with smaller fractions of silt and clay. The BA #1 model was bounded on the south, in part, by the reservoir and on the north by the Cimarron River. The WA model included only the alluvial materials (sands, silts, clay) from the escarpment that forms the northern edge of the uplands to the Cimarron River. In the WA area, the alluvial materials are underlain by sandstone. Upgradient sandstones in both models are assumed to contribute groundwater to the alluvial soils and overlying sandstone and mudstone units. The Cimarron River is a discharge boundary to which all modeled groundwater flows.

Calibration targets included measured groundwater elevations, flow budgets, and flow path data. The flow models achieved good calibration to the observed groundwater elevation data, to the estimated water budgets, and to observed flow path trajectories. Discrepancies between observed and predicted elevations were reasonable. The simulated water table configuration for each model was consistent with flow paths suggested by observations of U concentrations. Overall hydrogeological concepts as presented in the Conceptual Site Model, Rev 01 (ENSR, 2006) were captured by the numerical models. A sensitivity evaluation established that the model simulations will be most sensitive to boundary conditions, especially the recharge from upgradient sandstone units. Uncertainties, especially associated with boundary conditions, are important when interpreting and using model predictions in remedial designs.

Ultimately, the resulting numerical models have captured key hydrologic and geologic features that shape the groundwater flow directions, patterns, and rates, thus satisfying the objective to provide useful tools to consider remediation design options. For instance, groundwater extraction can be simulated to create capture zones that include areas of high U concentration. Injection scenarios can also be simulated to ensure adequate distribution of reagents. Even the calibrated model itself can yield valuable information about groundwater flow directions and rates. For instance, the design of the bioremediation system requires estimates of groundwater flux to the plume area, which can be extracted from the model. The calibrated BA #1 model indicates that there are 19 gpm to the plume area. The calibrated WA area model indicates that there are 31 gpm to the impacted area. ARCADIS will use the model further to help design the bioremediation effort; their uses of the model will be documented in their work plan.



## 6.0 REFERENCES

Adams, G.P. and D.L. Bergman. 1995. Geohydrology of Alluvium and Terrace Deposits, Cimarron River from Freedom to Guthrie, Oklahoma. USGS WRI 95-4066.

Cimarron Corporation, 2003. Burial Area #1 Groundwater Assessment Report for Cimarron Corporation's Former Nuclear Fuel Fabrication Facility, January.

Freeze, R.A. and J. A. Cherry. 1979. Groundwater. Englewood Cliffs, NJ: Prentice-Hall.

Harbaugh, Arlen W., 1990. A computer program for calculating subregional water budgets using results from the U.S. Geological Survey modular three-dimensional ground-water flow model: U.S. Geological Survey Open-File Report 90-392, 46 p.

MacDonald, Michael G. and Arlen, W. Harbaugh. 1988. A Modular Three-Dimensional Finite-Difference Ground-Water Flow Model. U.S. Geological Survey Open File Report 83-875.

Pollock, David W. 1994. User's Guide for MODPATH/MODPATH-PLOT, Version 3: A particle tracking post-processing package for MODFLOW, the U. S. Geological Survey finite-difference ground-water flow model. U. S. Geological Survey Open-File Report 94-464.

Weaver, J.C., 1998. Low-Flow Characteristics and Discharge Profiles for Selected Streams in the Cimarron River Basin, Oklahoma. U.S. Geological Survey Water-Resources Investigations Report 98-4135.

## Tables

**Table 1**  
**Summary of Slug and Aquifer Test Results**  
**Cimarron Corporation**  
**Crescent, Oklahoma**

		Hydraulic Conductivity (cm/s)									
		Analysis Methodology									
Geology	Well	Slug Test Bouwer & Rice	Slug Test Hvorslev	Sieve Analysis	Pumping Test - Jacob Straight Line	Pumping Test - t/t'	Pumping Test - distance- drawdown	Butler and Garnett	Cooper- Bredehoeft- Papadopolus	Geometric Mean (cm/s)	Geometric Mean (ft/day)
Alluvium	TMW-09***	6.01E-03	1.20E-03							2.69E-03	7.61
	TMW-13	6.99E-02	6.20E-02							6.58E-02	186.61
	02W2*	1.92E-05								1.92E-05	0.05
	02W10*	3.36E-04	2.80E-04							3.07E-04	0.87
	02W11***	3.24E-03	4.00E-03	1.70E-03						2.80E-03	7.95
	02W15	1.09E-02	1.80E-02	1.00E-02						1.25E-02	35.49
	02W16	3.66E-02	3.90E-02	1.10E-02						2.50E-02	70.98
	02W17	3.25E-02	6.00E-02	6.00E-03						2.27E-02	64.35
	02W22				8.90E-02					8.90E-02	252.28
	02W33	1.30E-02	1.90E-02	1.70E-03						7.49E-03	21.23
	02W46*	3.56E-05	1.37E-05							2.21E-05	0.06
	02W56**	4.20E-02	7.10E-02	1.70E-02	8.30E-02	8.30E-02	8.60E-02			5.58E-02	158.04
	02W58				9.60E-02	8.60E-02				9.09E-02	257.56
	02W59	1.40E-02	3.30E-02		9.60E-02	8.00E-02				4.34E-02	123.03
	02W60				1.10E-01	8.60E-02				9.73E-02	275.70
	02W61	2.20E-02	2.30E-02		1.10E-01	8.90E-02				4.72E-02	133.73
	02W62							2.80E-02		2.80E-02	79.37
		TMW-24						4.13E-02		4.13E-02	117.07
Sandstone B	TMW-01	6.35E-05	2.70E-05							4.14E-05	0.12
	TMW-20	9.97E-04	4.10E-04							6.39E-04	1.81
	02W40								5.50E-04	5.50E-04	1.56
	02W51	7.10E-05	2.39E-05							4.12E-05	0.12
Sandstone C	02W48		7.85E-05							7.85E-05	0.22

**Notes:**

All data presented is summarized from the Burial Area #1 Groundwater Assessment Report (Cimarron Corporation, 2003).

\* Clay present at or near this well; data excluded from calculating ranges, mean.

\*\* Pumping Well

\*\*\* Some clays/silts present in well screen; data excluded from calculating ranges, means.

**Table 2**  
**Summary of Groundwater Elevation Data used for Calibration**  
**Cimarron Corporation**  
**Crescent, Oklahoma**

Summary ID	9/16/03 Water Level (feet)	12/16/03 Water Level (feet)	Aug/Sep 04 Water Level (feet)	5/24/05 Water Level (feet)	Avg WL Elevation (feet)
**1206				n/a-SEEP	-----
**1206				n/a-SEEP	-----
**1208				n/a-SEEP	-----
**1208				n/a-SEEP	-----
1311	965.48	964.83	966.02	962.70	964.76
1312	962.66	963.64	964.48	964.66	963.86
1312				964.66	964.66
1313	963.60	963.19	964.04	963.97	963.70
1314	944.02	943.67	944.14	944.57	944.10
1315R	932.31	934.73	935.46	936.45	934.74
1315R				936.45	936.45
1316R	931.57	932.89	936.84	936.12	934.35
1319 A-1	969.86	969.63	970.37	969.88	969.93
1319 A-2	969.74	969.49	-	969.79	969.68
1319 A-3	968.46	968.56	968.45	968.35	968.45
1319 B-1	946.73	947.13	948.35	pumping	947.40
1319 B-1				pumping	-----
1319 B-2	947.73	948.25	949.44	950.06	948.87
1319 B-3	946.67	947.12	948.37	949.02	947.79
1319 B-4	946.18	946.52	947.84	948.54	947.27
1319 B-5	945.61	944.87	946.24	947.37	946.02
1319 C-1	942.27	943.81	946.01	pumping	944.03
1319 C-1				pumping	-----
1319 C-2	939.80	940.69	941.94	941.50	940.98
1319 C-3	939.06	939.78	941.07	940.85	940.19
1320	967.04	966.58	968.34	968.20	967.54
1321	935.97	936.45	937.74	938.07	937.06
1322	967.97	966.43	967.95	968.48	967.71
1323	941.84	942.49	943.29	944.19	942.95
1324	968.10	967.45	969.20	969.28	968.51
1325	971.25	970.62	972.44	972.31	971.66
1326	970.85	970.49	971.45	971.54	971.08
1327	966.02	965.95		966.62	966.19
1327B	966.05	965.55	966.01	966.63	966.06
1328	948.85	950.79	950.71	?	950.12
1329	968.26	967.97	968.00	968.62	968.21
1330	967.97	967.72	969.37	970.07	968.78
1331	965.80	965.30	967.02	966.63	966.19
1332	940.00	940.47	941.75	942.43	941.16
1333	967.92	967.16	968.48	969.03	968.15
1334	966.51	966.58	968.20	967.72	967.25
1335A	969.81	969.07	970.78	970.45	970.03
1336A	959.65	959.57	960.53	960.08	959.96
1337	965.90	965.48		966.95	966.11

**Table 2**  
**Summary of Groundwater Elevation Data used for Calibration**  
**Cimarron Corporation**  
**Crescent, Oklahoma**

Summary ID	9/16/03 Water Level (feet)	12/16/03 Water Level (feet)	Aug/Sep 04 Water Level (feet)	5/24/05 Water Level (feet)	Avg WL Elevation (feet)
1338	943.71	943.62	945.25	939.32	942.98
1339	951.68	952.74	938.46	955.13	949.50
1340	961.49	961.42		962.42	961.78
1341	936.75	936.75		939.39	937.63
1342	929.95	930.13		930.40	930.16
1343	928.37	928.57		929.40	928.78
1344	925.84	926.22		928.62	926.89
1345	933.74	933.63	935.32	936.30	934.74
1346	937.60	937.31	938.81	939.22	938.23
1347	965.13	964.47		965.96	965.18
1348	975.27	975.26	977.96	977.50	976.49
1348			977.96	977.50	977.73
1349	971.74	971.23	973.71	973.83	972.63
1349			973.71		973.71
1350	974.98	974.69	977.08	980.01	976.69
1350			977.08		977.08
1351	969.93	969.78	971.33	970.80	970.46
1351			971.33		971.33
1352	966.49	966.06	967.89	967.50	966.99
1352			967.89	967.50	967.70
1352			967.89		967.89
1353	985.70	988.00	988.31	988.04	987.52
1353			988.31		988.31
1354	965.51	965.24	967.00	966.46	966.05
1354			967.00		967.00
1355	967.64	967.01	968.71	968.85	968.05
1355			968.71		968.71
1356	968.83	968.24	969.38	969.57	969.00
1356			969.38	969.57	969.47
1357	969.51	968.88	970.72	970.47	969.89
1357			970.72		970.72
1358	971.26	970.53	972.67	972.49	971.74
1358			972.67	972.74	972.71
1359			972.79		972.79
1359			972.79	974.82	973.80
1360			974.88		974.88
1360			974.88		974.88
02W01	930.56	932.92	934.49	934.51	933.12
02W02	928.87	930.72	932.30	932.25	931.03
02W03	926.43	927.99	930.33	930.40	928.79
02W04	927.64	928.09	929.64	929.81	928.79
02W04				929.81	929.81
02W05	927.43	927.86	929.56	929.77	928.65
02W06	927.37	927.77	929.56	929.78	928.62



**Table 2**  
**Summary of Groundwater Elevation Data used for Calibration**  
**Cimarron Corporation**  
**Crescent, Oklahoma**

Summary ID	9/16/03 Water Level (feet)	12/16/03 Water Level (feet)	Aug/Sep 04 Water Level (feet)	5/24/05 Water Level (feet)	Avg WL Elevation (feet)
02W07	927.53	927.98	929.53	929.76	928.70
02W07				929.76	929.76
02W08	927.57	928.02	929.57	929.80	928.74
02W08				929.80	929.80
02W09	933.09	935.51	936.32	936.57	935.37
02W10	931.73	934.39	935.54	935.62	934.32
02W11	927.27	927.85	929.57	929.73	928.61
02W12	927.29	927.83	929.69	929.71	928.63
02W13	927.41	927.91	929.71	929.89	928.73
02W14	927.27	927.77	929.50	929.70	928.56
02W15	927.34	927.81	929.60	929.80	928.64
02W16	927.37	927.81	929.50	929.77	928.61
02W17	914.25	927.87	929.55	929.80	925.37
02W18	927.30	927.75	929.47	929.69	928.55
02W19	927.56	927.95	929.47	929.41	928.59
02W19				929.41	929.41
02W20	936.42	937.88	938.04	937.99	937.58
02W21	927.43	927.84	929.46	929.74	928.62
02W22	927.42	927.85	929.50	929.72	928.62
02W23	927.42	927.74	929.56	929.79	928.63
02W23				929.79	929.79
02W24	927.32	927.75	929.53	929.75	928.59
02W25	940.60	941.84	947.51	946.01	943.99
02W26	934.13	936.34	937.00	937.14	936.15
02W27	930.37	931.97	934.48	933.97	932.70
02W28	931.52	934.17	935.30	935.41	934.10
02W29	932.59	935.12	936.19	936.65	935.14
02W30	932.19	934.13	937.03	937.17	935.13
02W31	931.19	933.83	934.97	935.02	933.75
02W32	927.31	927.84	929.61	931.65	929.10
02W33	927.44	927.85	929.52	929.77	928.65
02W33				929.77	929.77
02W34	927.44	927.71	929.39	929.66	928.55
02W35	938.70	927.92	929.36	929.60	931.39
02W36	927.42	927.83	929.46	929.71	928.60
02W37	934.00	934.40	935.82	936.03	935.06
02W38	926.67	927.10	929.47	929.64	928.22
02W39	933.00	935.46	936.43	936.90	935.45
02W40	938.36	939.05	940.18	940.18	939.44
02W41	936.42	937.80	938.62	938.66	937.88
02W42	934.42	936.09	941.05	940.34	937.98
02W43	927.35	927.91	929.29	929.53	928.52
02W43				929.53	929.53
02W44	929.23	927.77	929.35	929.55	928.97

**Table 2**  
**Summary of Groundwater Elevation Data used for Calibration**  
**Cimarron Corporation**  
**Crescent, Oklahoma**

Summary ID	9/16/03 Water Level (feet)	12/16/03 Water Level (feet)	Aug/Sep 04 Water Level (feet)	5/24/05 Water Level (feet)	Avg WL Elevation (feet)
02W45	927.55	927.86	929.32	929.56	928.58
02W46	927.97	929.10	930.88	930.73	929.67
02W47	937.87	939.46	941.28	???	939.54
02W48	925.58	926.13		929.09	926.93
02W50	939.89	940.20	941.60	941.70	940.85
02W51	949.20	949.84	952.77	952.03	950.96
02W52	938.96	939.45	940.74	940.97	940.03
02W53	930.40	932.03	934.70	934.13	932.81
02W62	927.68	928.02	929.44	929.69	928.71
02W62				929.69	929.69
T-51	929.26	929.25		930.45	929.66
T-52	929.07	929.14		930.42	929.55
T-53	929.09	929.16		930.57	929.61
T-54	929.65	929.88	930.94	931.61	930.52
T-55	929.30	929.58		931.25	930.04
T-56	929.21	929.54		931.27	930.01
T-57	929.83	929.90	930.94	931.85	930.63
T-58	929.87	929.83	930.77	931.87	930.58
T-59	928.94	929.04		930.60	929.53
T-60	928.89	969.49		930.89	943.09
T-61	928.65	928.65		930.79	929.36
T-62	930.14	930.14	930.82	932.15	930.81
T-63			931.48	932.01	931.75
T-63	930.02	930.02	931.48	932.01	930.88
T-63			931.48		931.48
T-64	930.31	930.31	931.57	932.43	931.15
T-65	930.06	929.93	930.90	932.05	930.74
T-65				932.05	932.05
T-66			931.71		931.71
T-67			931.17		931.17
T-67			931.17		931.17
T-67			931.17		931.17
T-67			931.17		931.17
T-68			930.81		930.81
T-69			930.93		930.93
T-70					-----
T-70R			931.24		931.24
T-71					-----
T-72			930.96		930.96
T-73			931.02		931.02
T-74			931.20		931.20
T-75			930.88		930.88
T-76			931.04		931.04
T-77			930.82		930.82

**Table 2**  
**Summary of Groundwater Elevation Data used for Calibration**  
**Cimarron Corporation**  
**Crescent, Oklahoma**

Summary ID	9/16/03 Water Level (feet)	12/16/03 Water Level (feet)	Aug/Sep 04 Water Level (feet)	5/24/05 Water Level (feet)	Avg WL Elevation (feet)
T-77			930.82		930.82
T-77			930.82		930.82
T-78			930.87		930.87
T-79			930.53		930.53
T-81			930.80		930.80
T-82			930.35		930.35
TMW-01	939.36	940.23	942.38	943.82	941.45
TMW-02	940.65	940.99	941.29	941.62	941.14
TMW-05	930.74	933.29	934.56	934.02	933.15
TMW-06	932.81	935.77	936.02	936.05	935.16
TMW-07	930.17	932.54	933.41	933.05	932.29
TMW-08	933.75	935.89	936.50	936.99	935.78
TMW-09	931.68	934.32	935.02	935.28	934.08
TMW-09				935.28	935.28
TMW-13	927.66	928.18	929.36	929.77	928.74
TMW-13				929.77	929.77
TMW-17	932.23	933.08	933.97	934.11	933.35
TMW-17			933.97		933.97
TMW-18	927.30	927.76	930.18	930.05	928.82
TMW-19	dry	dry		n/a	----
TMW-20	938.43	939.35		939.91	939.23
TMW-21	936.45	937.09	944.33	942.49	940.09
TMW-23	928.33	928.87	929.94	930.37	929.38
TMW-24	927.71	928.05	928.73	929.19	928.42
TMW-25	936.83	938.41	938.42	938.32	937.99

**Table 3**  
**BA #1 Summary of Model Inputs**  
**Cimarron Corporation**  
**Crescent, Oklahoma**

Burial Area (BA#1)				
Subsurface Units:		Value	Units	Reference
Fill	K <sub>H</sub>	3.30E+00	ft/day	Average of Silt, Sand, & Clay
	K <sub>V</sub>	3.30E-01	ft/day	10% of K <sub>H</sub>
	Horizontal Anisotropy	1.0	----	No horizontal anisotropy
	Vertical Anisotropy (K <sub>H</sub> /K <sub>V</sub> )	1.0	----	No vertical anisotropy
	Specific Storage	NA	----	Not required for steady-state simulation
	Specific Yield	NA	----	Not required for steady-state simulation
	Long. Disp.	NA	----	Not required for flow model
	Porosity	30	%	Freeze & Cherry, 1979 Table 2.4
Silt	K <sub>H</sub>	2.83E-01	ft/day	ENSR CSM Sec-3.2.1
	K <sub>V</sub>	2.83E-02	ft/day	10% of K <sub>H</sub>
	Horizontal Anisotropy	1.0	----	No horizontal anisotropy
	Vertical Anisotropy (K <sub>H</sub> /K <sub>V</sub> )	1.0	----	No vertical anisotropy
	Specific Storage	NA	----	Not required for steady-state simulation
	Specific Yield	NA	----	Not required for steady-state simulation
	Long. Disp.	NA	----	Not required for flow model
	Porosity	20	%	Freeze & Cherry, 1979 Table 2.4
Sand	K <sub>H</sub>	2.53E+02	ft/day	Average of pumping tests in alluvial wells
	K <sub>V</sub>	2.53E+01	ft/day	10% of K <sub>H</sub>
	Horizontal Anisotropy	1.0	----	No horizontal anisotropy
	Vertical Anisotropy (K <sub>H</sub> /K <sub>V</sub> )	1.0	----	No vertical anisotropy
	Specific Storage	NA	----	Not required for steady-state simulation
	Specific Yield	NA	----	Not required for steady-state simulation
	Long. Disp.	NA	----	Not required for flow model
	Porosity	30	%	Freeze & Cherry, 1979 Table 2.4
Clay	K <sub>H</sub>	5.00E-01	ft/day	Artificially high to improve model stability
	K <sub>V</sub>	5.00E-02	ft/day	10% of K <sub>H</sub>
	Horizontal Anisotropy	1.0	----	No horizontal anisotropy
	Vertical Anisotropy (K <sub>H</sub> /K <sub>V</sub> )	1.0	----	No vertical anisotropy
	Specific Storage	NA	----	Not required for steady-state simulation
	Specific Yield	NA	----	Not required for steady-state simulation
	Long. Disp.	NA	----	Not required for flow model
	Porosity	20	%	Freeze & Cherry, 1979 Table 2.4
Sandstone-A	K <sub>H</sub>	4.00E+01	ft/day	Calibrated to high end of range in ENSR CSM Sec-3.2.1
	K <sub>V</sub>	2.00E+00	ft/day	5% of K <sub>H</sub>
	Horizontal Anisotropy	1.0	----	No horizontal anisotropy
	Vertical Anisotropy (K <sub>H</sub> /K <sub>V</sub> )	1.0	----	No vertical anisotropy
	Specific Storage	NA	----	Not required for steady-state simulation
	Specific Yield	NA	----	Not required for steady-state simulation
	Long. Disp.	NA	----	Not required for flow model
	Porosity	5	%	Freeze & Cherry, 1979 Table 2.4

**Table 3**  
**BA #1 Summary of Model Inputs**  
**Cimarron Corporation**  
**Crescent, Oklahoma**

Burial Area (BA#1)				
Subsurface Units:		Value	Units	Reference
Siltstone	K <sub>H</sub>	8.43E+00	ft/day	
	K <sub>V</sub>	4.22E-01	ft/day	5% of K <sub>H</sub>
	Horizontal Anisotropy	1.0	----	No horizontal anisotropy
	Vertical Anisotropy (K <sub>H</sub> /K <sub>V</sub> )	1.0	----	No vertical anisotropy
	Specific Storage	NA	----	Not required for steady-state simulation
	Specific Yield	NA	----	Not required for steady-state simulation
	Long. Disp.	NA	----	Not required for flow model
	Porosity	1	%	Freeze & Cherry, 1979 Table 2.4
Sandstone-B	K <sub>H</sub>	5.00E+00	ft/day	Calibrated to high end of range in ENSR CSM Sec-3.2.1
	K <sub>V</sub>	2.50E-01	ft/day	5% of K <sub>H</sub>
	Horizontal Anisotropy	1.0	----	No horizontal anisotropy
	Vertical Anisotropy (K <sub>H</sub> /K <sub>V</sub> )	1.0	----	No vertical anisotropy
	Specific Storage	NA	----	Not required for steady-state simulation
	Specific Yield	NA	----	Not required for steady-state simulation
	Long. Disp.	NA	----	Not required for flow model
	Porosity	5	%	Freeze & Cherry, 1979 Table 2.4
Sandstone-C	K <sub>H</sub>	3.00E+00	ft/day	Slug test results at well 02W48
	K <sub>V</sub>	1.50E-01	ft/day	5% of K <sub>H</sub>
	Horizontal Anisotropy	1.0	----	No horizontal anisotropy
	Vertical Anisotropy (K <sub>H</sub> /K <sub>V</sub> )	1.0	----	No vertical anisotropy
	Specific Storage	NA	----	Not required for steady-state simulation
	Specific Yield	NA	----	Not required for steady-state simulation
	Long. Disp.	NA	----	Not required for flow model
	Porosity	5	%	Freeze & Cherry, 1979 Table 2.4

Cimarron River:		Value	Units	Reference
Upstream Elevation		924.8	feet	Based on Dover and Guthrie gage datums
Downstream Elevation		924.8	feet	Based on Dover and Guthrie gage datums
Conductance		10,000	(ft <sup>2</sup> /day)/ft	Estimate to for high river/aquifer connectivity

Areal Boundaries:		Value	Units	Reference
Recharge		5.48E-04	ft/day	ENSR CSM Sec-3.1.1 & 3.1.4



**Table 4**  
**WA Summary of Model Inputs**  
**Cimarron Corporation**  
**Crescent, Oklahoma**

<b>Western Alluvial Area (WA)</b>				
<b>Subsurface Units:</b>		<b>Value</b>	<b>Units</b>	<b>Reference</b>
<b>Clay</b>	$K_H$	5.00E-01	ft/day	ENSR CSM Sec-3.2.1
	$K_V$	5.00E-02	ft/day	10% of $K_H$
	Horizontal Anisotropy	1.0	----	No horizontal anisotropy
	Vertical Anisotropy ( $K_H/K_V$ )	1.0	----	No vertical anisotropy
	Specific Storage	0.001	----	Default
	Specific Yield	0.001	----	Default
	Long. Disp.	10	----	Default
	Porosity	20	%	Freeze & Cherry, 1979 Table 2.4
<b>Sand</b>	$K_H$	2.35E+02	ft/day	Average of pumping tests in alluvial wells
	$K_V$	2.35E+01	ft/day	10% of $K_H$
	Horizontal Anisotropy	1.0	----	No horizontal anisotropy
	Vertical Anisotropy ( $K_H/K_V$ )	1.0	----	No vertical anisotropy
	Specific Storage	0.001	----	Default
	Specific Yield	0.001	----	Default
	Long. Disp.	10	----	Default
	Porosity	30	%	Freeze & Cherry, 1979 Table 2.4
<b>Sandstone-C</b>	$K_H$	3.00E+00	ft/day	Slug test results at well 02W48
	$K_V$	1.50E-01	ft/day	5% of $K_H$
	Horizontal Anisotropy	1.0	----	No horizontal anisotropy
	Vertical Anisotropy ( $K_H/K_V$ )	1.0	----	No vertical anisotropy
	Specific Storage	0.001	----	Default
	Specific Yield	0.001	----	Default
	Long. Disp.	10	----	Default
	Porosity	5	%	Freeze & Cherry, 1979 Table 2.4

<b>Cimarron River:</b>		<b>Value</b>	<b>Units</b>	<b>Reference</b>
Upstream Elevation		924.8	feet	Based on Dover and Guthrie gage datums
Downstream Elevation		924.8	feet	Based on Dover and Guthrie gage datums
Conductance		20,000	(ft <sup>2</sup> /day)/ft	Medium estimate based on prior experience

<b>Areal Boundaries:</b>		<b>Value</b>	<b>Units</b>	<b>Reference</b>
Recharge		5.48E-04	ft/day	ENSR CSM Sec-3.1.1 & 3.1.4

## Figures



A horizontal scale bar with a black background and white markings. The bar is divided into three equal segments by two vertical white lines. Below the bar, the text "SCALE IN FEET" is centered. Above the bar, the numbers "0", "800", and "1600" are positioned at the left, middle, and right ends respectively.

DESIGNED BY:	REVISIONS				
	NO.:	DESCRIPTION:	DATE:	BY:	
	1.		4/01/05	JAS	
	2.		6/17/05	JAS	
DRAWN BY:	3.		6/8/05	JAS	
CHECKED BY:					
D>JF					
APPROVED BY:					
D>JF					

ENSR AECOM

**ENSR CORPORATION**  
4888 LOOP CENTRAL DRIVE, SUITE 600  
HOUSTON, TEXAS 77081-2214  
PHONE: (713) 520-9900  
FAX: (713) 520-6802  
WEB: [HTTP://WWW.ENSRAECOM.COM](http://www.ensr.aecom.com)

FIGURE 1  
SITE LOCATION MAP  
CIMARRON CORPORATION  
CRESCENT, OKLAHOMA

SCALE:	DATE:	PROJECT NUMBER:
1" = 800'	9/22/06	04020-044-327

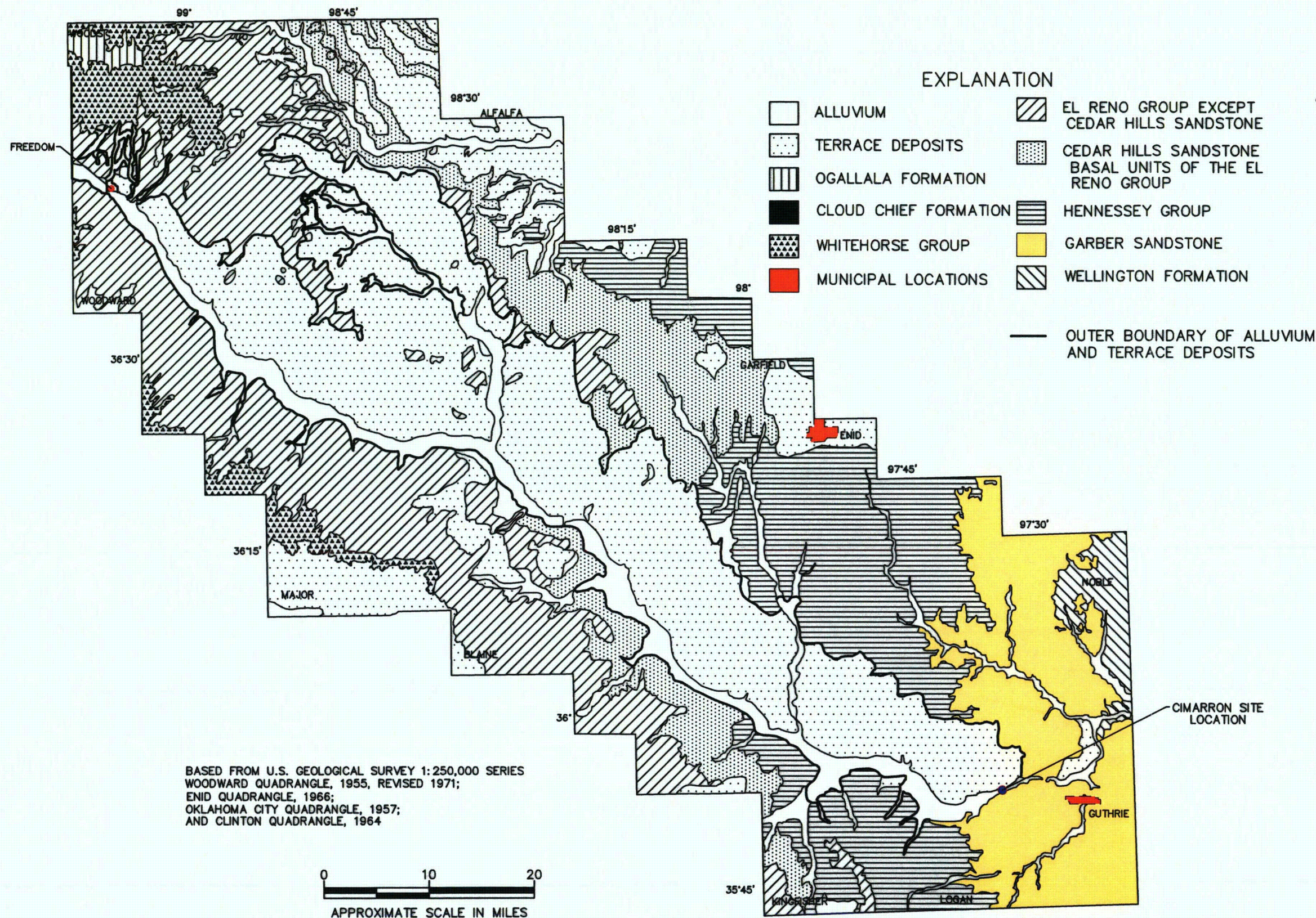
FIGURE NUMBER:

1

SHEET NUMBER:

1





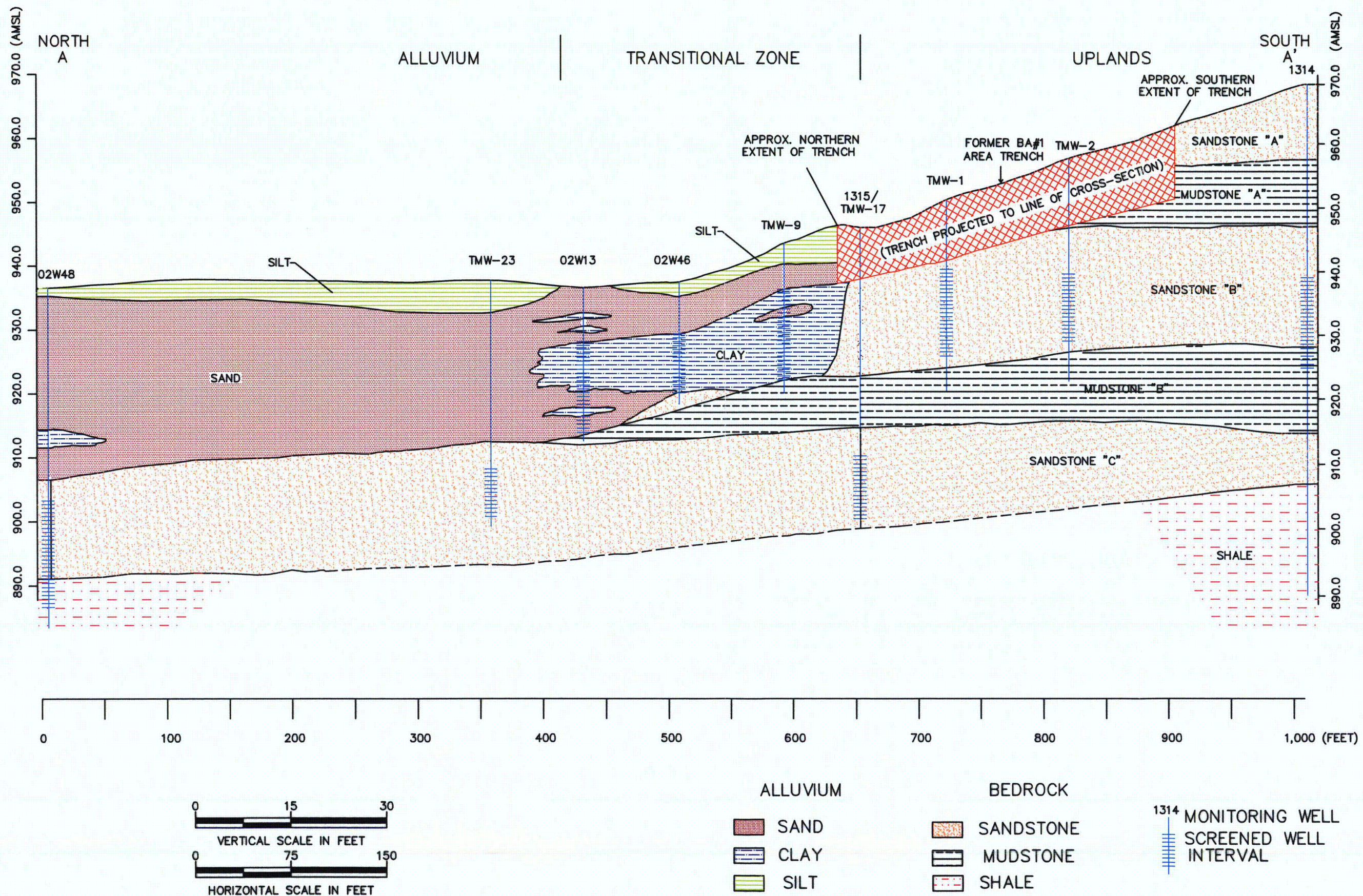
DESIGNED BY:		REVISIONS	
NO.	DESCRIPTION	DATE	BY
1.		4/10/05	JAS
2.		6/17/05	JAS
DRAWN BY:		CHECKED BY:	
JAS		DJF	
APPROVED BY:		DJF	

ENSR | AECOM

ENSR CORPORATION  
4888 LOOP CENTRAL DRIVE, SUITE 600  
HOUSTON, TEXAS 77081-2214  
PHONE: (713) 520-9900  
FAX: (713) 520-6802  
WEB: HTTP://WWW.ENSRAECOM.COM

FIGURE NUMBER:		SHEET NUMBER:	
2		1	





DESIGNED BY:	NO.:	DESCRIPTION:	DATE:	BY:
JAS	1.		4/01/05	JAS
DJF	2.		6/17/05	JAS
DJF				
DJF				

ENSR CORPORATION	AECOM
4888 LOOP CENTRAL DRIVE, SUITE 600	
HOUSTON, TEXAS 77081-2214	
PHONE: (713) 520-9900	
FAX: (713) 520-6802	
WEB: HTTP://WWW.ENSRAECOM.COM	

FIGURE 3	DATE:	PROJECT NUMBER:
BA #1 AREA	9/22/06	04020-044-327
REPRESENTATIVE GEOLOGICAL CROSS-SECTION		
CIMARRON CORPORATION		
CRESCENT, OKLAHOMA		

FIGURE NUMBER:
3
SHEET NUMBER:
1



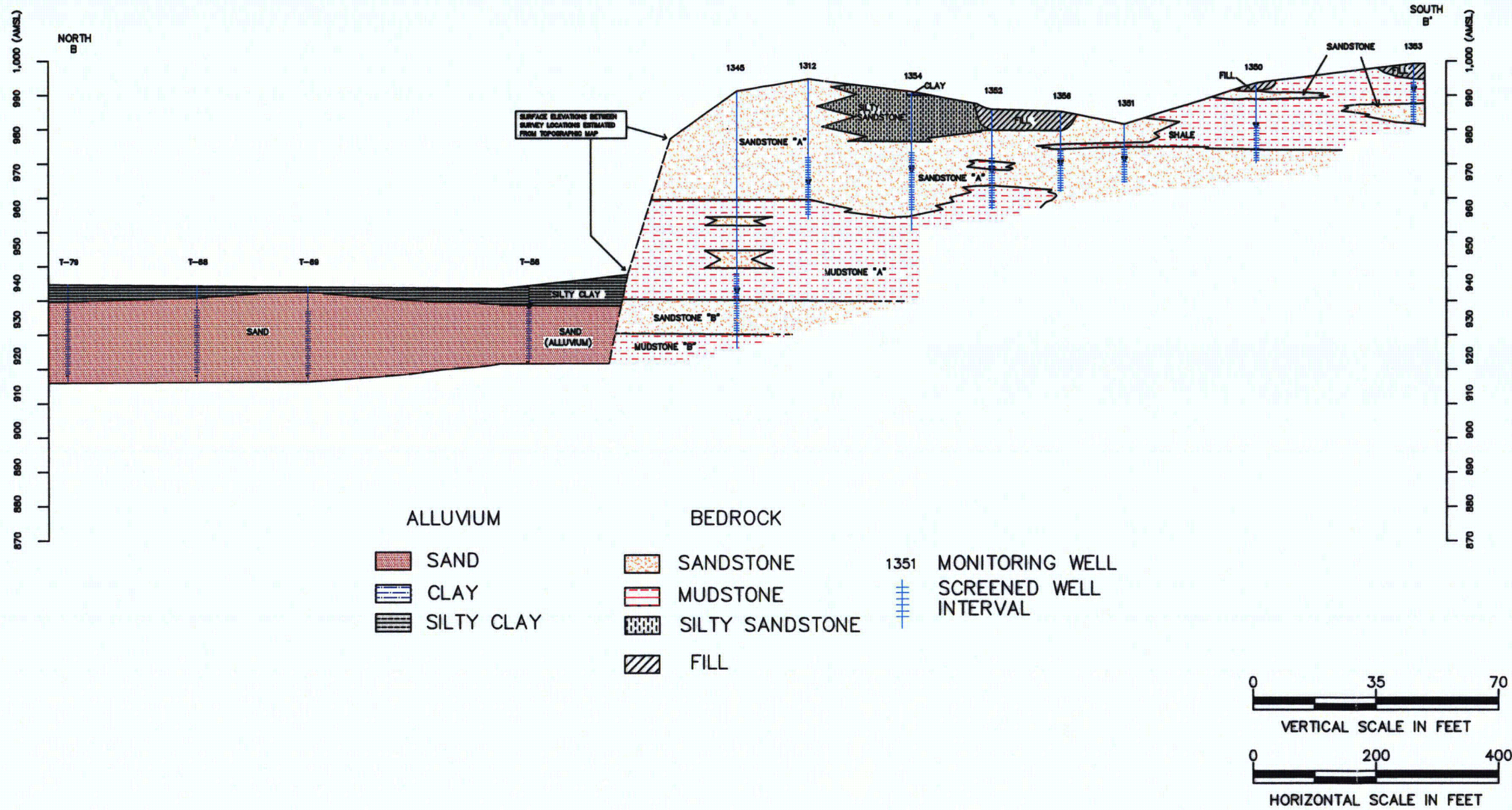


FIGURE 4  
REPRESENTATIVE GEOLOGICAL CROSS-SECTION  
WESTERN UPLAND AND ALLUVIAL AREAS  
CIMARRON CORPORATION  
CRESCENT, OKLAHOMA

ENSR | AECOM

**ENSR CORPORATION**  
4888 LOOP CENTRAL DRIVE, SUITE 600  
HOUSTON, TEXAS 77081-2214  
PHONE: (713) 520-9900  
FAX: (713) 520-6802  
WEB: [HTTP://WWW.ENSR.AECOM.COM](http://www.ensr.aecom.com)

DESIGNED BY:		REVISIONS		
NO.:	DESCRIPTION:	DATE:	BY:	
1.		4/01/05	JAS	
2.		6/17/05	JAS	
DRAWN BY:				
JAS				
CHECKED BY:				
DJF				
APPROVED BY:				
DJF				





BA #1 Boundary

NOT TO SCALE

BA #1 Model Domain  
Cimarron Corporation  
Crescent, Oklahoma

ENSR | AECOM

Figure  
**5**

DATE



October 2006

PROJECT

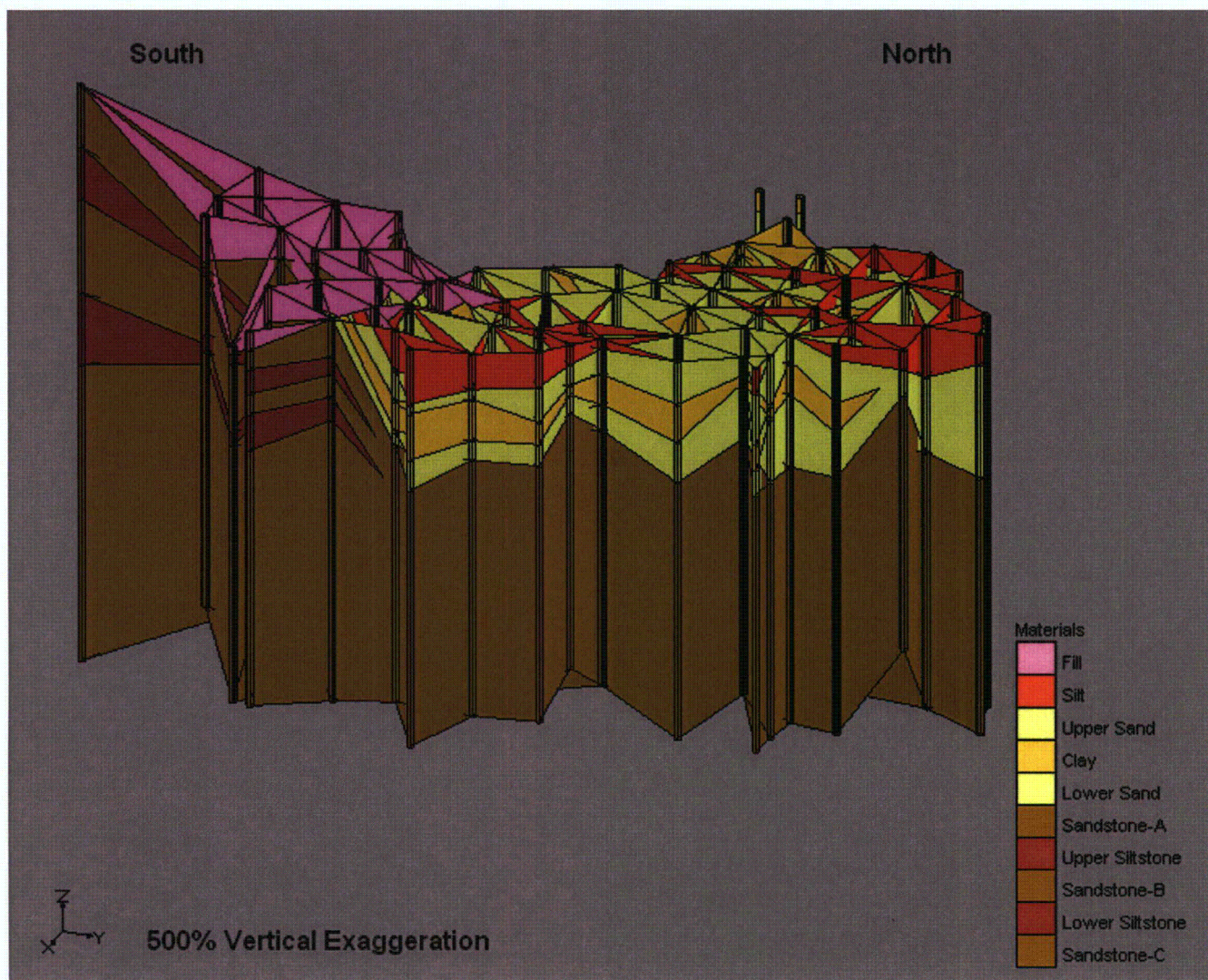
04020-044-300





  WA Area Boundary	WA Area Model Domain Cimarron Corporation Crescent, Oklahoma		ENSR   AECOM
	NOT TO SCALE	DATE October 2006	
		PROJECT 04020-044-300	Figure <b>6</b>





BA #1 Boreholes and Cross-sections  
Cimarron Corporation  
Crescent, Oklahoma

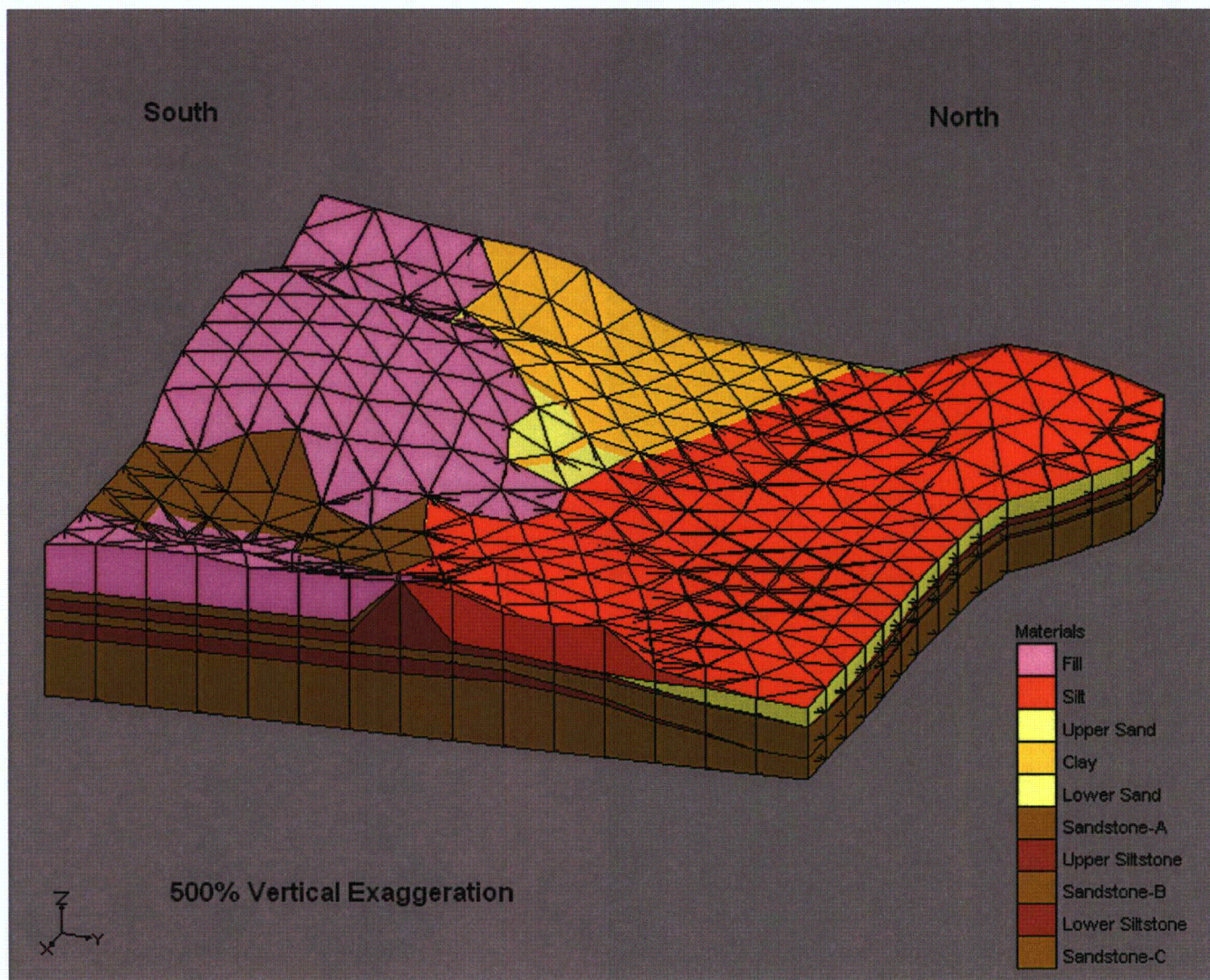
ENSR | AECOM

Figure  
7

DATE  
October 2006

PROJECT  
04020-044-300





BA #1 Solids Developed  
from Borehole Data  
Cimarron Corporation  
Crescent, Oklahoma

ENSR | AECOM

Figure  
8

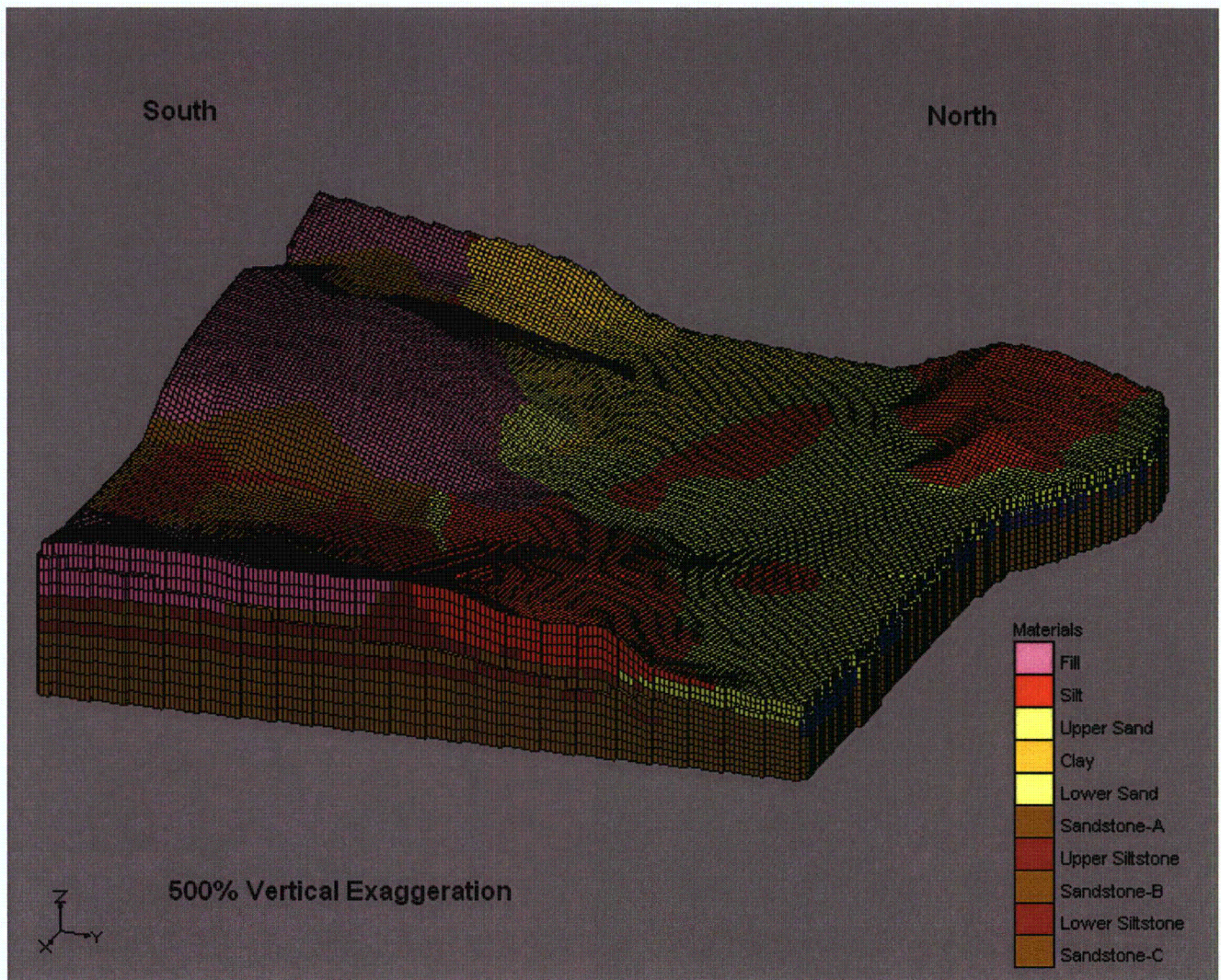
DATE

October 2006

PROJECT

04020-044-300





BA #1 3D Grid Incorporating  
Geologic Information  
Cimarron Corporation  
Crescent, Oklahoma

ENSR | AECOM

Figure  
9

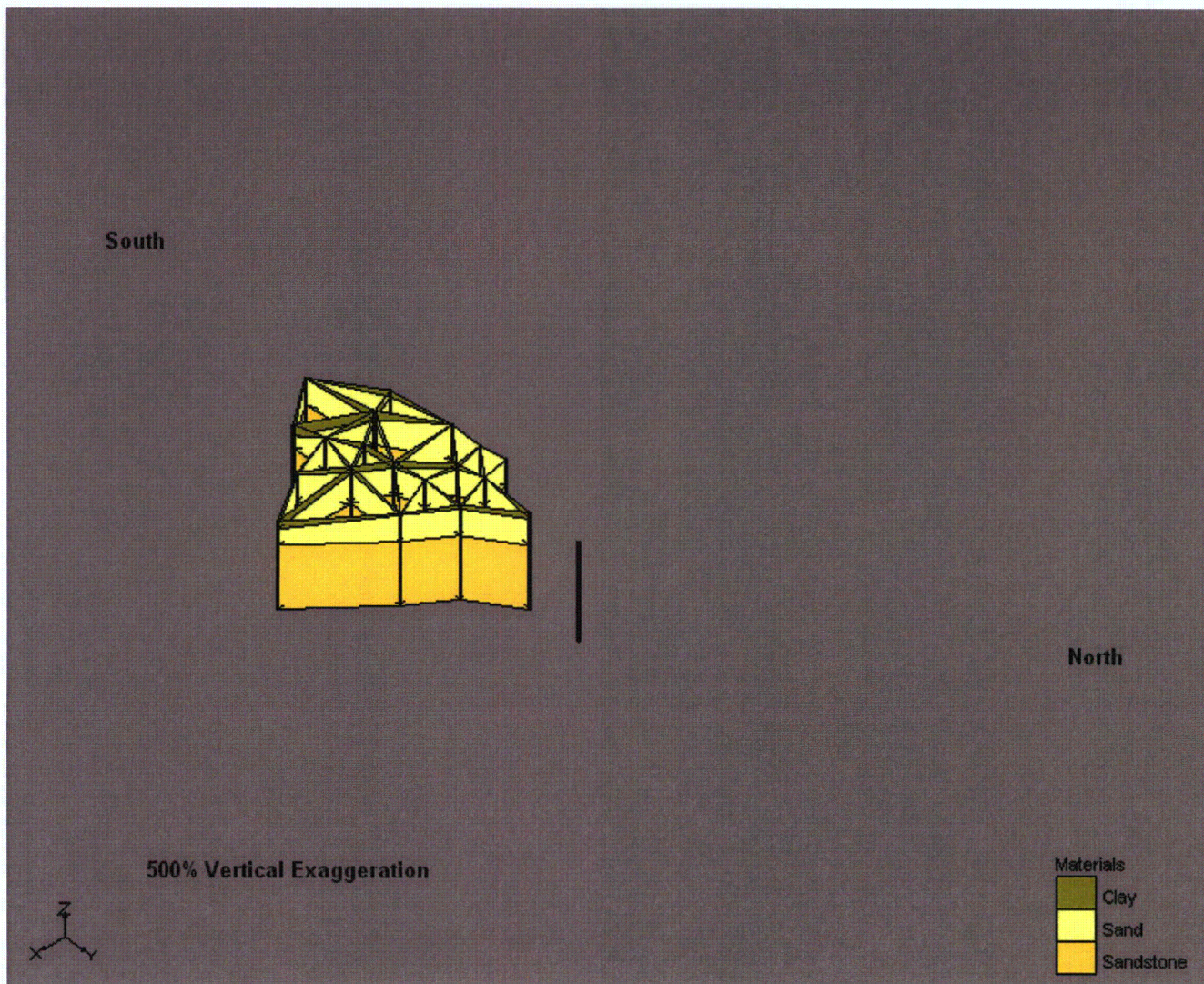
DATE

October 2006

PROJECT

04020-044-300





**Note:**  
Shows extent of borings  
and cross-sections.  
Figure 11 shows extrapolation  
of geology to model domain.

WA Area Boreholes and Cross-sections  
Cimarron Corporation  
Crescent, Oklahoma

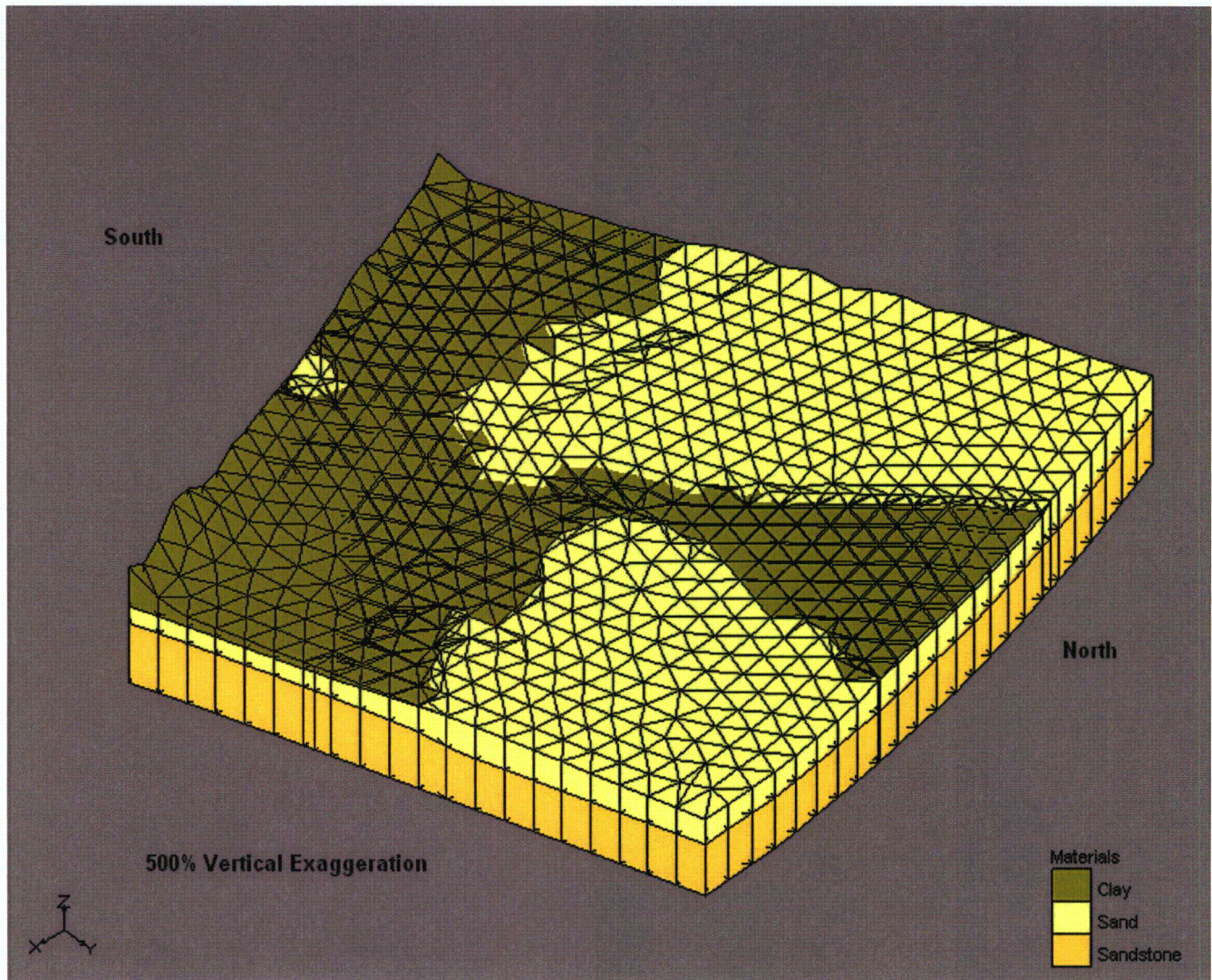
ENSR | AECOM

DATE  
October 2006

PROJECT  
04020-044-300

Figure  
10





WA Area Solids Developed  
from Borehole Data  
Cimarron Corporation  
Crescent, Oklahoma

ENSR | AECOM

Figure  
11

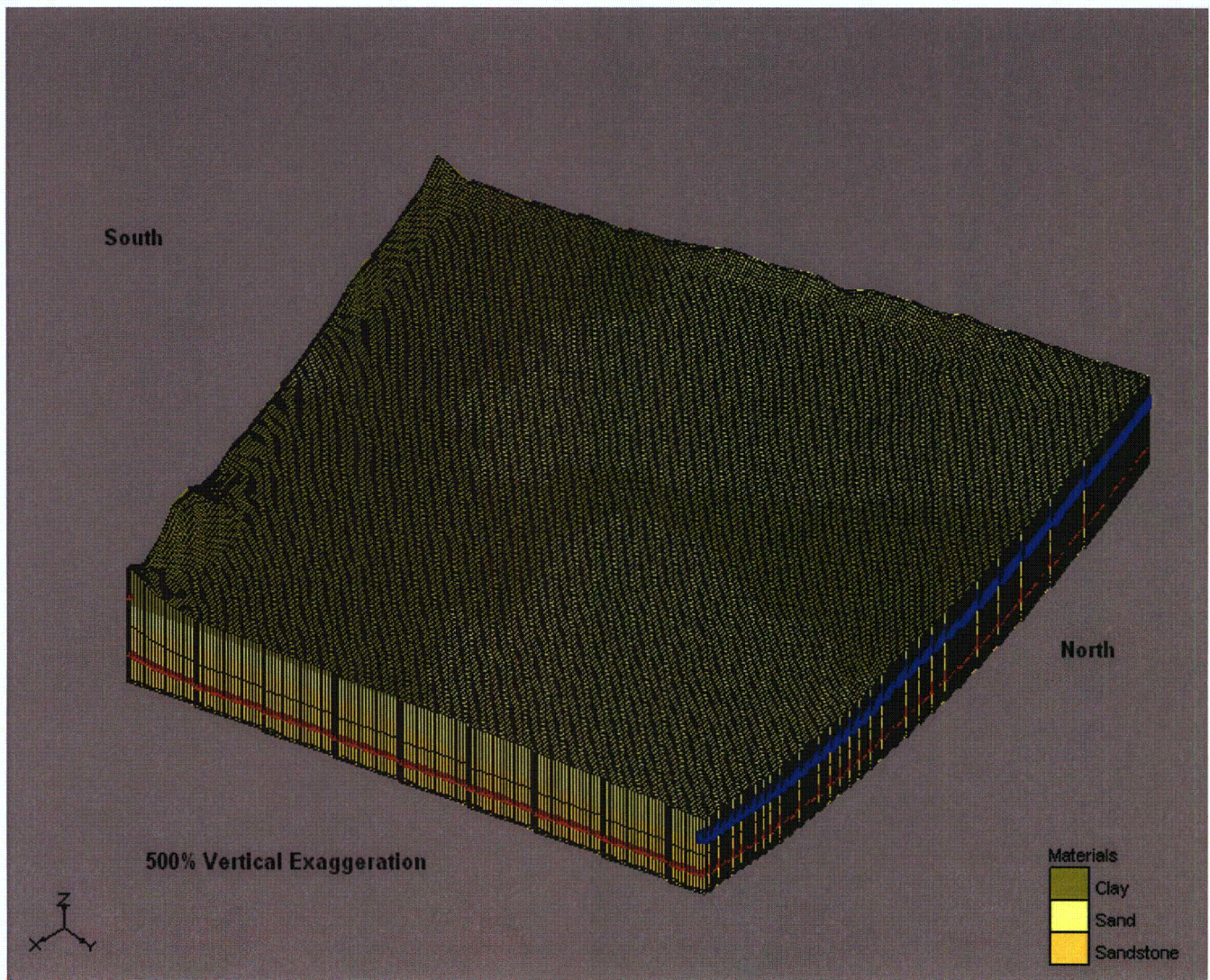
DATE

October 2006

PROJECT

04020-044-300





WA Area 3D Grid Incorporating  
Geologic Information  
Cimarron Corporation  
Crescent, Oklahoma

ENSR | AECOM

Figure  
12

DATE

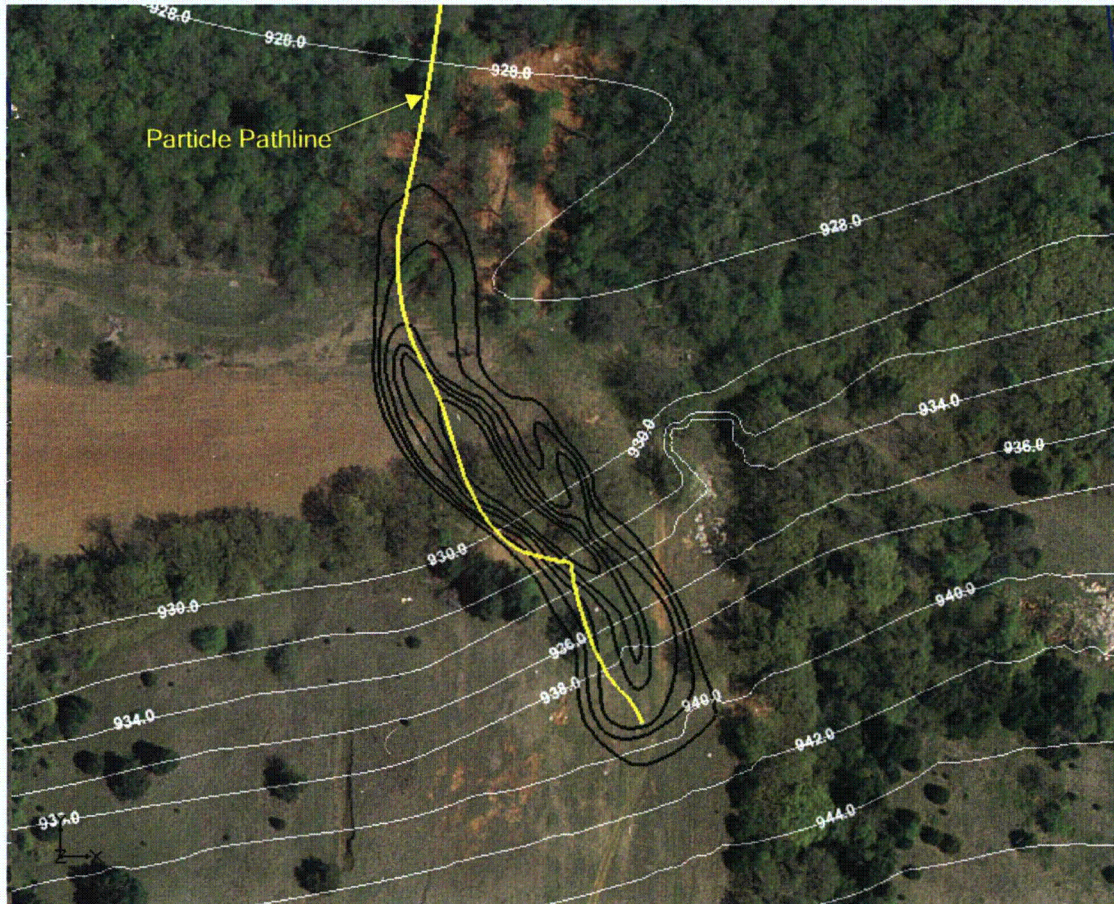
October 2006

PROJECT

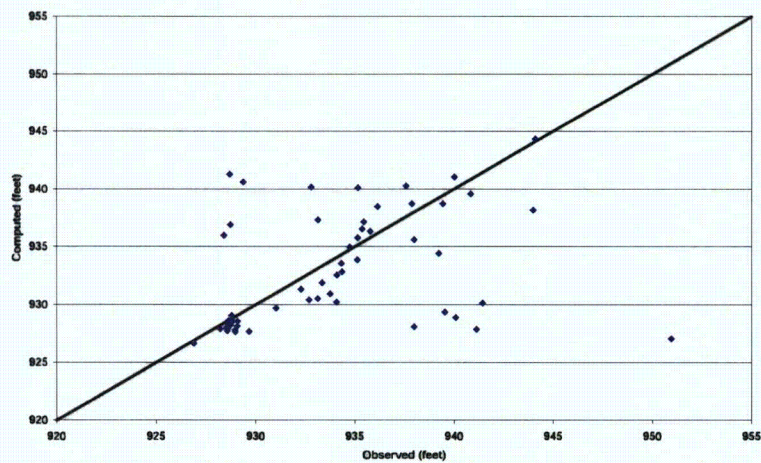
04020-044-300



# Predicted Groundwater Contours and Particle Pathlines



MODFLOW Computed vs Observed Groundwater Levels



NOT TO SCALE

Results of Burial Area #1 Model Calibration:  
Predicted Groundwater Contours with Pathline  
and Measured vs Predicted Water Levels

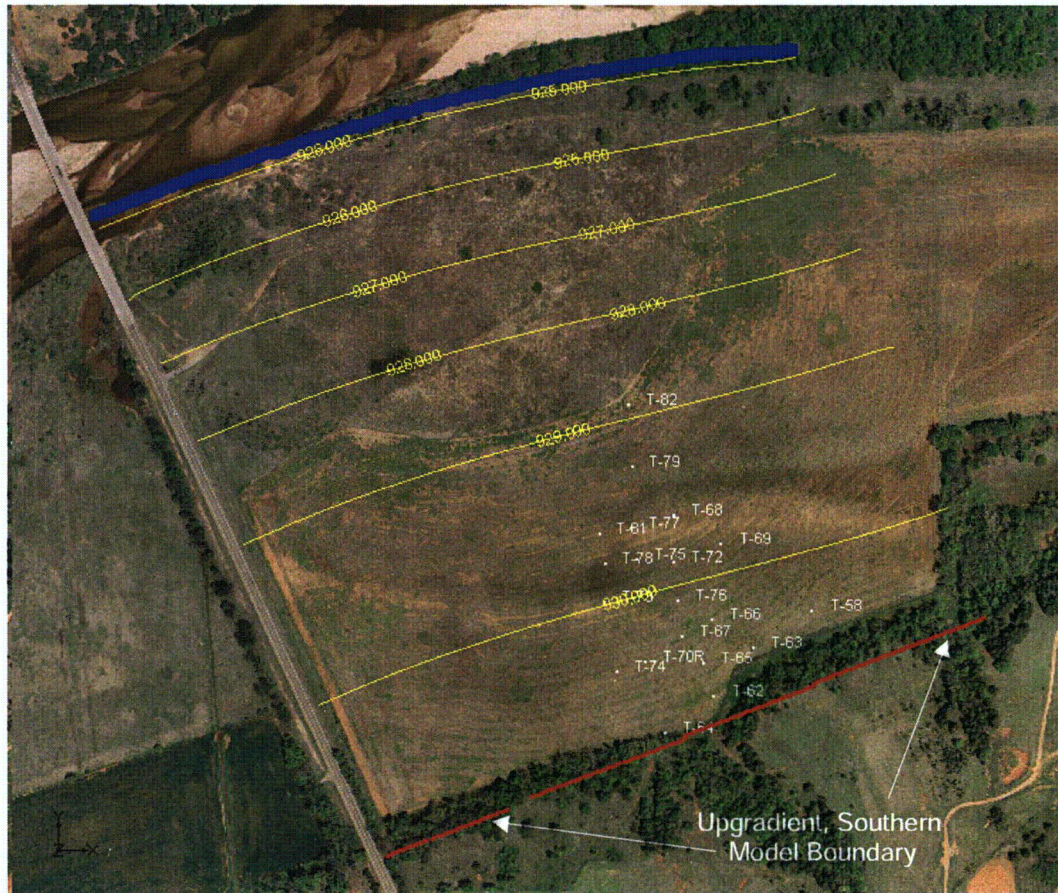
October 2006

ENSR | AECOM

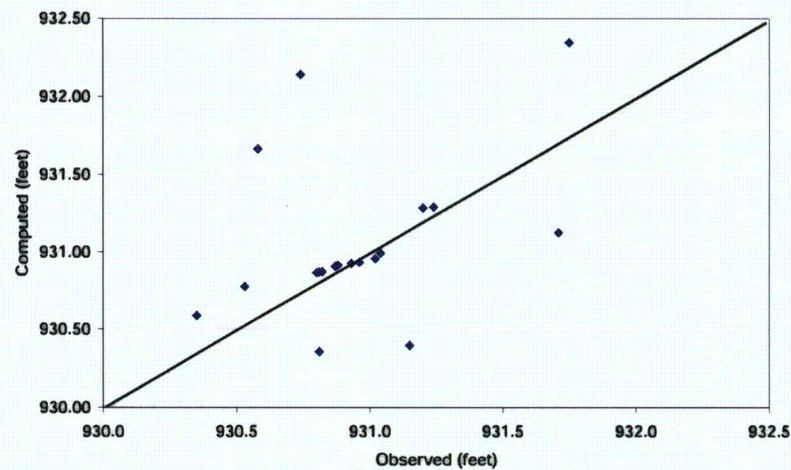
Figure  
13



## Predicted Groundwater Contours



## MODFLOW Computed vs Observed Groundwater Levels



NOT TO SCALE

Results of Western Alluvial Area Model Calibration:  
Predicted Groundwater Contours and  
Measured vs Predicted Water Levels

October 2006

ENSR | AECOM

Figure  
14